

Aus dem Max von Pettenkofer-Institut
für Hygiene und Medizinische Mikrobiologie
Lehrstuhl: Bakteriologie
der Ludwig-Maximilians-Universität München

komm. Vorstand: Prof. Dr. Rainer Haas
vormals Vorstand: Prof. Dr. Dr. Jürgen Heesemann

**The *Legionella longbeachae* Icm/Dot substrate SidC
binds to the LCV through PtdIns(4)P
and facilitates the interaction with the ER**

Dissertation zum Erwerb des Doktorgrades der Naturwissenschaften
an der Medizinischen Fakultät der Ludwig-Maximilians-Universität München

vorgelegt von
Stephanie Dolinsky
aus Meerbusch

2014

Gedruckt mit Genehmigung der Medizinischen Fakultät
der Ludwig-Maximilians-Universität München

Betreuer:

Prof. Dr. Hubert Hilbi

Zweitgutachterin: Priv. Doz. Dr. Alla Skapenko

Dekan:

Prof. Dr. med. Dr. h.c. Maximilian Reiser, FACR, FRCR

Tag der mündlichen Prüfung: 02.12.2014

Eidesstattliche Versicherung

Ich, Stephanie Dolinsky, erkläre hiermit an Eides statt, dass ich die vorliegende Dissertation mit dem Thema

The *Legionella longbeachae* Icm/Dot substrate SidC binds to the LCV through PtdIns(4)*P* and facilitates the interaction with the ER

selbständig verfasst, mich außer der angegebenen keiner weiteren Hilfsmittel bedient und alle Erkenntnisse, die aus dem Schrifttum ganz oder annähernd übernommen sind, als solche kenntlich gemacht und nach ihrer Herkunft unter Bezeichnung der Fundstelle einzeln nachgewiesen habe.

Ich erkläre des Weiteren, dass die hier vorgelegte Dissertation nicht in gleicher oder in ähnlicher Form bei einer anderen Stelle zur Erlangung eines akademischen Grades eingereicht wurde.

Ort, Datum

Unterschrift Doktorandin

Index

Eidesstattliche Versicherung.....iii

Index.....iv

List of publications.....vii

Summary.....viii

Zusammenfassung.....x

1. General introduction.....1

 1.1 *Legionella* spp.....1

 1.2 Clinical diagnostic and therapy of Legionnaires‘ disease.....1

 1.3 The accidental transfer of *Legionella* to a human.....2

 1.4 The infection cycle of *Legionella*.....3

 1.5 Type II and type IV secretion systems.....5

 1.5.1 The Lsp type II secretion system (T2SS).....6

 1.5.2 The Icm/Dot type IVB secretion system (T4BSS).....6

 1.6 Phosphoinositide-binding *Legionella* effector proteins.....7

 1.6.1 SidC and SdcA.....9

 1.6.2 SidM (*alias* DrrA) of *L. pneumophila*.....12

 1.7 Aims of the Ph.D. thesis.....15

2. Materials and methods.....16

 2.1 Materials.....16

 2.1.1 Bacterial strains.....16

 2.1.2 Eukaryotic cell lines.....16

 2.1.3 Plasmids.....17

 2.1.4 Oligonucleotides.....18

 2.1.5 Lab equipment.....19

 2.1.6 Software and data bases.....21

Index

2.2 Methods.....	22
2.2.1 <i>Legionella</i> spp.....	22
2.2.2 <i>Escherichia coli</i>	25
2.2.3 <i>Dictyostelium discoideum</i>	27
2.2.4 <i>Acanthamoeba castellanii</i>	28
2.2.5 RAW 264.7 macrophages.....	29
2.2.6 Cell counting.....	30
2.2.7 Cloning.....	31
2.2.8 Protein analysis.....	32
2.2.9 Protein purification.....	37
2.2.10 Production of a SidC _{L10} antibody.....	40
2.2.11 Phosphoinositide-pulldown.....	40
2.2.12 Protein lipid overlay assay with PIP-strips and PIP-arrays.....	41
2.2.13 Infection of phagocytes.....	41
2.2.14 Immunofluorescence.....	42
2.2.15 Detection of PtdIns(4) <i>P</i> on the LCV.....	43
2.2.16 Intracellular replication assay.....	44
2.2.17 Amoebae competition assay.....	45
2.2.18 Translocation assay.....	46
2.2.19 LCV purification.....	46
2.2.20 Cytotoxicity assay.....	48
3. Results.....	49
3.1 The <i>L. longbeachae</i> Icm/Dot substrate SidC.....	49
3.1.1 The <i>L. longbeachae</i> effector SidC _{L10} is the major PtdIns(4) <i>P</i> binding protein...49	
3.1.2 SidC _{L10} is binding through a P4C domain to PtdIns(4) <i>P</i>	51
3.1.3 The Icm/Dot substrate SidC _{L10} localizes to LCVs.....	55

Index

3.1.4 The $\Delta sidC_{L10}$ and $\Delta sidC-sdcA_{Lpn}$ deletion mutants are outcompeted by the wild-type strains in competition assays.....	58
3.1.5 SidC _{L10} and SidC _{Lpn} promote ER recruitment to the LCV.....	59
3.1.6 SidC _{L10_P4C} and SidC _{Lpn_P4C} are binding to PtdIns(4)P on the LCV.....	66
3.2. Purification of LCVs from <i>L. longbeachae</i>	67
3.2.1 Purification of <i>L. longbeachae</i> -containing vacuoles from <i>D. discoideum</i> with an anti-SidC _{Lpn} antibody.....	68
3.2.2 Purification of <i>L. longbeachae</i> -containing vacuoles from RAW 264.7 macrophages.....	71
4. Discussions.....	75
4.1 The <i>L. longbeachae</i> Icm/Dot substrate SidC.....	75
4.2 Purification of LCVs from <i>L. longbeachae</i>	79
5. General conclusions and outlook.....	81
6. List of abbreviations.....	83
7. Index of figures.....	86
8. Index of tables.....	88
9. Acknowledgement.....	90
10. References.....	91

List of publications

- Weber, S., Dolinsky, S., and H. Hilbi, *Interactions of Legionella effector proteins with host phosphoinositide lipids*. *Methods Mol Biol*, 2013. **954**: p. 367-80.
- Dolinsky, S., Haneburger, I., Cichy, A., Hannemann, M, Itzen, I., and Hilbi, H, *The Legionella longbeachae Icm/Dot substrate SidC selectively binds PtdIns(4)P with nanomolar affinity and promotes pathogen vacuole-ER interactions*. *Infect Immun*, 2014 (in revision).

Summary

The genus *Legionella* consists of environmental bacteria which are the causative agents of the severe pneumonia Legionnaires' disease. *L. longbeachae* and *L. pneumophila* are able to replicate intracellularly in human alveolar macrophages and aquatic or soil amoebae. In order to replicate within host cells the bacteria establish a compartment derived from the endoplasmic reticulum (ER) which is called "*Legionella*-containing vacuole" (LCV). A bacterial intracellular multiplication/defective in organelle transport (Icm/Dot) type IV secretion system (T4SS) is essential for the formation of this LCV. The Icm/Dot T4SS enables translocation of effector proteins into the host cell. More than 100 effector proteins are presumably translocated during an *L. longbeachae* infection whereas around 300 translocated effector proteins are known for *L. pneumophila*. During maturation the LCV communicates with vesicles from the endocytic vesicle trafficking pathway, avoids fusion with lysosomes and instead fuses with the ER. Phosphoinositides (PI) such as phosphatidylinositol-4-phosphate (PtdIns(4)P) are enriched on the LCV which mediate the binding of Icm/Dot translocated effector proteins like SidC_{Lpn} (substrate of Icm/Dot transporter) as well as its paralogous protein SdcA_{Lpn}.

The 73 kDa effector SidM but not the 106 kDa SidC_{Lpn} was found in a previous phosphoinositide pulldown assay with *L. pneumophila* lysate to be the major PtdIns(4)P binding protein. Using *L. longbeachae* lysate we showed binding of the 111 kDa SidC_{Llo} to PtdIns(4)P in a phosphoinositide pulldown. This result was confirmed by protein-lipid overlay assays using "PIP-strips". In further analysis the P4C (PtdIns(4)P-binding of SidC) domain was identified as a 19 kDa domain of SidC_{Llo} located in the amino acid region 609 to 782. This P4C domain was located in the same region as the 20 kDa SidC_{Lpn_P4C} domain of *L. pneumophila*. Both P4C domains can be used as LCV markers. This was shown with GST-tagged proteins binding to LCVs in a cell homogenate. The two P4C domains show a sequence identity of only 45% and the full-length protein of 40%. Circular dichroism measurements revealed that the secondary structure of the two proteins is similar. Moreover, isothermal titration calorimetric measurements indicated a 3.4 higher affinity of SidC_{Llo} towards PtdIns(4)P compared with SidC_{Lpn}.

In RAW 264.7 macrophages infected with *L. longbeachae* we showed that endogenous SidC_{Llo} as well as heterologously produced SidC_{Lpn} is translocated to the LCV in an

Summary

Icm/Dot-dependent manner. The deletion of the *sidC_{Llo}* gene led to a reduced recruitment of calnexin to the LCV in infected *Dictyostelium discoideum*. This effect was complemented by adding plasmid-encoded SidC_{Llo}, SidC_{Lpn} or SdcA_{Lpn}. The same recruitment defect for a *L. pneumophila* strain lacking the *sidC_{Lpn}* and *sdca_{Lpn}* genes was complemented by the production of SidC_{Llo} and SidC_{Lpn} as published before. Therefore, these effectors play a role for pathogen-host interactions by promoting the recruitment of ER to the LCV. *L. longbeachae* or *L. pneumophila* wild-type strains outcompeted their *sidC* deletion mutant in a competition assay in *Acanthamoeba castellanii*. However neither of the deletion mutants were impaired in their growth in single strain replication experiments. In summary despite of the small sequence identity and the higher binding affinity to PtdIns(4)*P* of SidC_{Llo} compared to SidC_{Lpn} both effector proteins seem to have similar functions during an infection of *Legionella*.

For the characterization of *L. longbeachae*-containing vacuoles through proteomic analysis, LCVs had to be isolated from infected *D. discoideum* or RAW 264.7 macrophages. Endogenous SidC_{Llo} or heterologously produced SidC_{Lpn} were used as LCV markers for the isolation. Pathogen vacuoles harbouring *L. longbeachae* were isolated by immuno-affinity purification using antibodies specifically recognizing SidC_{Llo} or SidC_{Lpn}. Future investigations aim at optimizing the LCV purification protocol for *L. longbeachae* to determine the proteome composition of the *L. longbeachae*-containing vacuole.

Zusammenfassung

Die Gattung *Legionella* besteht aus opportunistischen Pathogenen, die Auslöser für die schwere Lungenentzündung Legionärskrankheit sind. Die *Legionella*-Spezies *L. longbeachae* sowie *L. pneumophila* vermehren sich intrazellulär in humanen alveolaren Makrophagen sowie in aquatischen oder im Boden lebenden Amöben. Ein vom endoplasmatischen Retikulum (ER) abstammendes Kompartiment ist notwendig für die intrazelluläre Replikation. Diese Nische wird als „*Legionella*-containing vacuole“ (LCV) bezeichnet. Die Bildung der LCV benötigt ein „intracellular multiplication/defective in organelle transport“ (Icm/Dot) Typ IV Sekretionssystem (T4SS), das Effektorproteine in die Wirtszelle transportiert. Zurzeit sind über 100 vermutete Effektorproteine für *L. longbeachae* und etwa 300 Effektorproteine für *L. pneumophila* beschrieben. Im Verlauf eines Reifungsprozesses kommuniziert die LCV mit endosomalen Vesikeln, verhindert eine Fusion mit den Lysosomen und fusioniert mit dem ER. Phosphoinositide wie das PtdIns(4)*P* wurden auf der LCV gefunden. Diese dienen als Bindestellen für die durch das Icm/Dot translozierten Effektorproteine wie das SidC_{Lpn} und sein paraloges Protein SdcA_{Lpn}.

In einer früheren Studie wurde in einem Phosphoinositid-Pulldown Experiment das 73 kDa Effektorprotein SidM aber nicht das 106 kDa Protein SidC_{Lpn} als Bindepartner von PtdIns(4)*P* nachgewiesen. Wir konnten in einem Phosphoinositid-Pulldown Experiment mit *L. longbeachae* Lysat zeigen, dass das 111 kDa homologe Protein von SidC_{Lpn} SidC_{Llo} der Bindepartner von *L. longbeachae* für PtdIns(4)*P* ist. Ein 19 kDa großes SidC_{Llo}-Fragment im Bereich der Aminosäuren 609 bis 782 konnte identifiziert werden, das für die Bindung von SidC_{Llo} an PtdIns(4)*P* notwendig ist. Interessanterweise liegt die früher beschriebene 20 kDa große P4C Domäne von SidC_{Lpn} in der gleichen Region. Durch Inkubation von GST-gekoppelten SidC_{Llo_P4C}-Proteinen mit *L. pneumophila* Zellhomogenat konnten wir zeigen, dass SidC_{Llo_P4C} die Vakuole von *L. pneumophila* homogen dekoriert. Daher kann SidC_{Llo_P4C} genauso wie das SidC_{Lpn_P4C} als LCV Marker benutzt werden. Die P4C Domänen besitzen eine Sequenzhomologie von 45% und SidC_{Llo} und SidC_{Lpn} zeigen eine Sequenzhomologie von 40%. Mittels zirkularer Dichroismus Messung konnte gezeigt werden, dass die beiden Proteine ähnliche Sekundärstrukturen

Zusammenfassung

besitzen. Mittels isothermer Titrationskalorimetrie konnten wir zeigen, dass SidC_{L10} eine 3.4-fach höhere Bindeaffinität zu PtdIns(4)P besitzt als SidC_{Lpn}.

In infizierten RAW 264.7 Makrophagen konnte wir zeigen, dass *L. longbeachae* nicht nur sein eigenes endogen produziertes SidC_{L10} sondern auch ein heterolog exprimiertes SidC_{Lpn} in einer Icm/Dot abhängigen Art und Weise auf die LCV transloziert. Frühere Studien zeigten, dass in einer *sidC-sdcA_{Lpn}* Deletionsmutante die ER Rekrutierung zu der LCV in infizierten *D. discoideum* Zellen beeinträchtigt ist. Wir konnten zeigen, dass die heterologe Produktion von SidC_{L10} diesen Rekrutierungsfehler komplementieren kann, ebenso wie Plasmid-kodiertes SidC_{Lpn} oder SdcA_{Lpn}. Die Deletion vom Gen *sidC_{L10}* in *L. longbeachae* führt ebenfalls zu einer verminderten Rekrutierung von ER-Markern zur LCV in infizierten *D. discoideum*. Dieser Effekt konnte durch eine Produktion von SidC_{L10}, SidC_{Lpn} und SdcA_{Lpn} komplementiert werden. Die SidC Deletionsstämme von *L. longbeachae* oder *L. pneumophila* replizierten in *Acanthamoeba castellanii* wie die entsprechenden Wildtyp-Stämme, aber in direkter Konkurrenz wurden die Deletionsmutanten von den Wildtyp-Stämmen verdrängt. Insgesamt scheinen trotz der geringen Sequenzidentität und der höheren Bindeaffinität von SidC_{L10} im Vergleich zu SidC_{Lpn} zu PtdIns(4)P beide Effektorproteine ähnliche Funktionen im Infektionsweg von *Legionella* wahr zu nehmen.

Für die Charakterisierung von *L. longbeachae*-enthaltenden Vakuolen in einer Proteomanalyse müssen LCVs aus *D. discoideum* oder RAW 264.7 Makrophagen isoliert werden. Endogenes SidC_{L10} oder heterolog produziertes SidC_{Lpn} wurden als Vakuolen-Marker für die Isolation von *L. longbeachae*-enthaltenden Vakuolen verwendet. *L. longbeachae*-enthaltene Vakuolen wurden in einer Immunaффinitätsaufreinigung mit Hilfe spezifischer Antikörper gegen SidC_{L10} oder SidC_{Lpn} isoliert. Weitere Studien zielen auf die Verbesserung der Vakuolen-Isolation von *L. longbeachae*, um das Proteom dieser LCV zu charakterisieren.

1. General introduction

1.1 *Legionella* spp.

Legionella spp. are Gram-negative, obligate aerobe bacteria which live in a broad range of natural or man-made aquatic systems [4] or in potting soil [5, 6]. Two major *Legionella* species are *L. longbeachae* and *L. pneumophila* which both cause the severe pneumonia Legionnaires' disease through inhalation of aerosols [7, 8]. The first and largest outbreak in the US history was in 1976 where American Legion members were infected by *L. pneumophila* [5]. After this outbreak the genus was termed "*Legionella*" [5]. *L. longbeachae* serogroup 1 (Sg 1) was isolated for the first time from a patient with pneumonia in Long Beach, California, USA in 1981 [9]. In the same year the serogroup 2 of *L. longbeachae* was discovered [10].

1.2 Clinical diagnostic and therapy of Legionnaires' disease

Legionellosis is divided into two clinical diseases, Legionnaires' disease, a severe pneumonia, and Pontiac fever [5]. Pontiac fever is a flue-like illness which is self-limiting. Legionellosis is causing a broad range of symptoms like myalgia, dyspnea, non-productive cough, headache, fever, rigors, delirium and diarrhea [11]. However Legionellosis cases are known where a person had no symptoms at all [5, 12]. It is not possible to distinguish between Legionnaires' disease and other forms of pneumonia based on the symptoms only [5]. Even chest radiographic pictures look identical [13]. Cases are reported where Pontiac fever and Legionnaires' disease were occurring during the same outbreak of Legionellosis [14].

From more than 50 known *Legionella* species *L. pneumophila* is causing around 90% and *L. longbeachae* less than 5% of the Legionellosis cases worldwide. *L. longbeachae* is mainly found in Australia and New Zealand where it accounts for 30% of the Legionellosis cases whereas *L. pneumophila* accounts only for 46% [15]. The diagnosis is based on a screen for *L. pneumophila* and therefore biases the statistic [5]. 15 different serogroups for *L. pneumophila* [5] and two serogroups for *L. longbeachae* are known. However, the serogroup 1 of *L. pneumophila* and *L. longbeachae* is mainly found in human infections [8, 15].

1. General introduction

L. pneumophila was first cultured on Mueller-Hinton agar which was supplemented with haemoglobin and IsoVitaleX (a supplemental mixture consisting primarily of sugars and cysteine). Later IsoVitaleX and haemoglobin were replaced by L-cysteine hydrochloride and soluble ferric pyrophosphate respectively [16]. Last the medium was replaced by a charcoal yeast extract (CYE) agar [17]. Lung tissue, blood and respiratory secretions like sputum and stool can be used to isolate *Legionella* [5]. *Legionella* can be detected by microscopic examination through a direct fluorescent antibody (DFA) but the specificity and sensitivity of this method is not optimal [14, 18]. Also a species-specific antigen for *L. pneumophila* is available which detects the serogroups 1 - 8 [19] but a cross-reaction with *Bacillus cereus* spores is possible [20]. The antigen used in an urine antigen detection assay is only detecting the serogroup 1 of *L. pneumophila* [5].

Erythromycin is the major drug used to cure Legionnaires' disease [5]. Moreover, azithromycin and levofloxacin are licenced through the Food and Drug Administration to cure this disease [5].

1.3 The accidental transfer of *Legionella* to a human

L. pneumophila is mainly found in biofilms in water systems like cooling towers [21-25], shower heads and in natural sources like rivers and lakes [5, 25]. In 1989 a direct link between *L. longbeachae* and potting soil was found [5, 6] but no cases are known in which a person was infected with *L. longbeachae* through inhalation of aerosols from a water system. A human-to-human transmission was not observed for *Legionella* [23].

A recently performed genome analysis of *L. longbeachae* revealed its environmental habitats [26]. Several genes for enzymes were found which are associated with plants like cellobiohydrolases, β -glucosidases, glucanases, pectin lyases, endo-1,4-xylanase and chitinases. These enzymes could be used for the degradation of cellulose to use it as a carbon source. Furthermore, a putative cyanophycin synthase and a putative cyanophycinase, which are normally present in cyanobacteria, were found in the genome of *L. longbeachae*. Cyanophycin can be used as a storage compound for carbon, energy and nitrogen. *L. pneumophila*, on the other hand, possesses only genes for one putative β -glucosidase, an endo-1,4-glucanase, endo-1,4-xylanase and chitinase. The genomic

1. General introduction

analysis also indicated a putative capsule-like structure for *L. longbeachae* NSW150, which was validated by electron microscopy and is not present in *L. pneumophila* [26].

1.4 The infection cycle of *Legionella*

In 1980 a *L. pneumophila* infection of *A. castellanii* and human monocytes under lab conditions was first reported [22, 27]. *Legionella* spp. are also able to infect and replicate in protozoan hosts like *D. discoideum* [3, 28, 29] and human and murine macrophages [3, 30-32]. *L. longbeachae* can also replicate in *A. castellanii* [26]. Contrary to *L. pneumophila*, *L. longbeachae* can also replicate in C57BL/6 mice [33]. The cytosolic flagellin of *L. pneumophila*, which triggers the activation of Naip5-dependent caspase-1 followed by a proinflammatory cell death through pyroptosis, seems to be the reason of this failure [34-38]. *L. longbeachae* does not trigger caspase-1 activation in C57BL/6 mice macrophages and does not possess flagellar biosynthesis genes [26].

L. pneumophila undergoes a biphasic life cycle in which it switches from a transmissive, virulent to a replicative, non-virulent phase [26]. In the post-exponential growth phase of a liquid over night culture *L. pneumophila* is virulent [30, 39]. *L. pneumophila* is using the flagella to reach host cells and is attaching through self-produced adhesins to the cell surface [24]. The uptake is an Icm/Dot-dependent [40, 41] process which can take place as “coiling phagocytosis” [41-43] or macropinocytosis [40, 44] (Figure 1.1). Non-motile *L. longbeachae* does not possess such a pronounced biphasic life cycle, but a chemotactic system was found in a genome analysis which is missing for *L. pneumophila* [26]. No invasion strategies are known for *L. longbeachae*. Amoebae are a suitable model to study the intracellular life cycle of *Legionella* since the creation of a LCV and the intracellular replication in protozoa and mammalian phagocytes are similar.

After entering the cell the bacteria is remodelling the phagosome and a LCV is formed. The *L. pneumophila*-containing vacuole acquires components from the mitochondria, fuses with vesicles from the ER and communicates with vesicles from the early and late endosomal vesicle trafficking pathway (e.g. EEA1 (early endosomal antigen 1)) [45, 46] whereas fusion with the lysosome is avoided [43, 45, 47-51] (Figure 1.1). During maturation the shape of a *L. pneumophila*-containing vacuole changes from a tight to a spacious vacuole. Only the bacterial poles stay attached to the LCV [52, 53]. 1150 host cell

1. General introduction

proteins were found on the LCV purified from macrophages [1] and 566 host proteins for *D. discoideum* [54] in a recent proteomics analysis. Only few details are known for the host factor composition of the *L. longbeachae*-containing vacuole. Acquisition of the early endosomal marker EEA1 and the late endosomal marker LAMP-2 was observed in U937 macrophages. Also co-localization with the rough endoplasmatic reticulum (rER) was reported. An acquisition of the lysosomal marker Cathepsin D and the lysosomal tracer Texas red Ovalbumin (TROV) was not observed for *L. longbeachae* wild-type but for the *dotA* deletion mutant [30].

L. pneumophila is switching from the transmissive, virulent to the replicative, non-virulent phase [26]. During this process the expression of almost half of the genome expression is altered upon infection of *A. castellanii* [55]. *L. pneumophila* produces over 300 different effector proteins which are translocated by the Icm/Dot T4SS into the host cell [56-58]. These effector proteins play a role in vesicle trafficking pathways and communication with host cell compartments. A modulation of the host cell response is initiated [59]. *L. longbeachae* possesses over 110 putative effector proteins [58] and replicates intracellularly irrespective of the bacterial growth phase [30] in a vacuole which recruits vesicles from the endoplasmatic reticulum [26, 30].

L. pneumophila upregulates genes during the replicative phase, which are predicted to be necessary for the transmission to a new host cell. This includes genes for invasion and virulence such as the Icm/Dot T4SS system. The bacteria are preparing themselves for the next infection [55]. At the end of the intracellular replication phase the LCV in infected amoebae or macrophages is disrupted, a process which is independent of a bacterial pore-forming activity in macrophages and the bacteria are released in the cytosol of the cell [60, 61] (Figure 1.1). The pore-forming activity of the bacteria allows the cytolysis of the host cell [61-64]. *L. pneumophila* can also escape from infected *A. castellanii* in expelled vesicles and can survive in this vesicles for months [65]. *L. longbeachae* seems to escape from the cell like *L. pneumophila* within 24 hours. However, a pore-forming activity is missing [30, 66].

1. General introduction

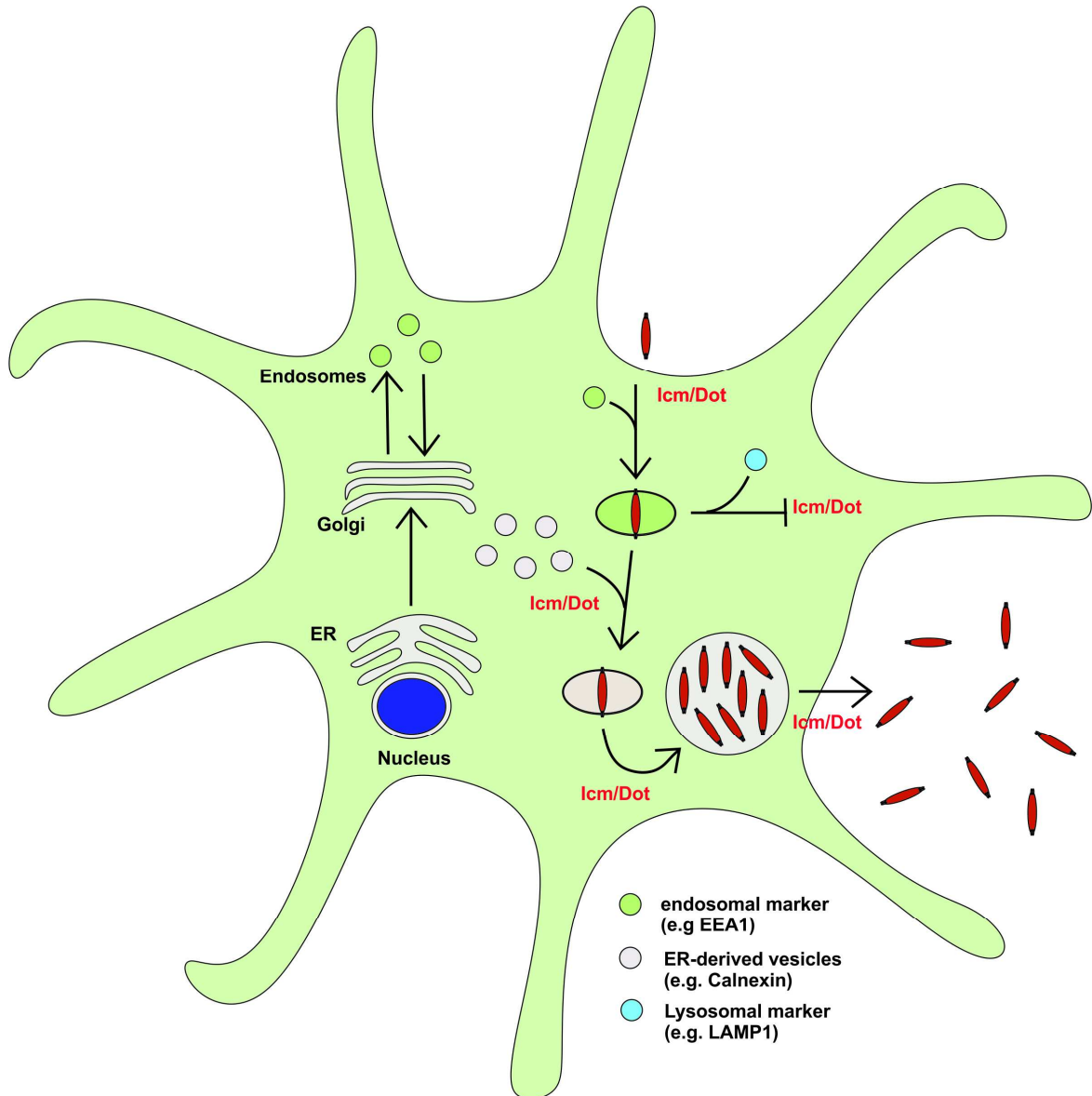


Figure 1.1. *L. pneumophila* replicates in phagocytes. The bacteria invade phagocytes in an Icm/Dot-dependent way. A phagosome is built which fuses with endosomes [45, 46], ER-derived vesicles [47, 51] but avoids to fuse with lysosomes [67, 68]. The bacteria are replicating in the LCV. After replication the bacteria destroy the LCV and the plasma membrane of the cell [61-64]. The figure is based on a scheme published in [69].

1.5 Type II and type IV secretion systems

L. pneumophila and *L. longbeachae* both possess a large number of secretion systems. The two major secretion systems are called Lsp type II secretion system (T2SS) and the Icm/Dot type IVB secretion system (T4BSS). Both secretion systems are necessary for the infection [8, 70]. Also, three type IVA secretion systems are present in the genome of *L. longbeachae* but the Lvh T4ASS of *L. pneumophila* was not found in the genome [26].

1. General introduction

1.5.1 The Lsp type II secretion system (T2SS)

A functional Lsp type II secretion system was found in the genome of *L. pneumophila* and *L. longbeachae* [8, 26]. Between 25 and 60 type II secreted proteins are known for *L. pneumophila* [71]. 45% of the type II secreted substrates of *L. pneumophila* were missing in the genome of *L. longbeachae* [26].

1.5.2 The Icm/Dot type IVB secretion system (T4BSS)

Many Gram-negative bacteria like *Legionella* use the type IV secretion system (T4SS) to transfer DNA substrates and proteins to the recipient cell [72]. A T4SS type A (T4ASS) and B are known. The Icm/Dot T4SS of *Legionella* spp. is part of the T4BSS which is independent of the T4ASS [72]. The secretion system is necessary for the efficient formation of a LCV and for the translocation of effector proteins into the host cell [50]. The protein identities and organization of the genes is 47% to 92% similar between *L. longbeachae* and *L. pneumophila* [8].

The Icm/Dot T4BSS system of *Legionella* comprises 27 proteins. Five proteins were found to be located in the cytoplasm and 16 proteins are connected with the inner membrane of the LCV. Additionally four outer membrane proteins and one periplasmic protein were identified. The type 4B secretion system contains nearly twice as many proteins as the VirB/D4 type 4A system of *Agrobacterium tumefaciens* which consists 11 VirB proteins and a putative ATPase, VirD4 [72].

L. pneumophila genes called *icm* or *dot* code for proteins which form a membrane spanning transport complex. This complex is necessary for substrate translocation [73] and for intracellular replication [74-78]. Similarly organized genes were found to code for proteins which are related to Icm/Dot components. These DNA elements were located in the IncI plasmid *colI-P9* and R64 and were necessary for conjugation. It seems as if the Dot/Icm system was adapted from a plasmid-encoded conjugal transfer system [79].

The Icm/Dot T4SS system translocates effector proteins at different time points into the host cell. SidC_{Lpn} is translocated in an Icm/Dot-dependent way and localizes to the LCV at early time points of the infection [3, 80, 81]. The effector proteins LepA and LepB, which are important for the evasion of the bacteria from *D. discoideum*, are probably produced

1. General introduction

and translocated during the later phases of the infection cycle [73, 82]. Effector proteins like LidA seem to be expressed and translocated during all growth phases [83].

1.6 Phosphoinositide-binding *Legionella* effector proteins

Today over 110 putative effector proteins are known for *L. longbeachae* [58]. 300 effector proteins are characterized for *L. pneumophila* [56, 58] which is equal to 10% of the total amount of proteins known [8]. Some effector proteins might be functionally redundant. After deletion of a single gene only few deletions lead to an intracellular growth defect of *L. pneumophila* [84-86]. The diversity of the Icm/Dot effector proteins might reflect the potential to infect different host cells [86]. After translocation of the effector proteins into the host cell the proteins decorate the LCV or target organelles or host factors in the host cell [50]. *L. longbeachae* lacks around 66% of the Icm/Dot substrates of *L. pneumophila* but possesses 51 novel putative Icm/Dot substrates [26].

The first Icm/Dot substrate identified through bioinformatics analysis was RalF (Recruitment of Arf to *Legionella* phagosome) [73]. RalF recruits a member of the small GTPase family named ARF (ADP ribosylation factor) to the LCV and catalyzes a GDP-GTP nucleotide exchange [87]. It was shown for RalF and LidA (Lowered viability in the presence of *dotA*) that the C-terminus of these effector proteins is necessary for the translocation of the protein by the Icm/Dot T4SS [84, 88]. A current assumption is that the secretion signal in general does not possess distinct amino acids at specific positions. Instead it is expected that the physicochemical properties of the amino acids at the last 35 amino acids of the C-terminus are important [58].

Several of these effector proteins of *L. pneumophila* have been mechanistically characterized. The effector protein SidK inhibits the vacuolar H⁺-ATPase [89], the autophagy machinery is modified by an effector protein called RavZ [90] and the retromer complex [91] or phosphoinositide (PI) lipids are also targeted [50, 92].

Many intracellular bacteria target the PI metabolism in order to be able to survive and replicate within the host cell [69, 93, 94]. PI lipids play an important role in the vesicle trafficking and signal transduction of eukaryotes [95] but the amount of PIs in the cell is low. Only around 10% of the total cellular phospholipids are PIs [96]. PI lipids are derivatives of phosphatidylinositol (PtdIns) composed of a diacylglycerol (DAG) backbone

1. General introduction

and one *D-myo*-inositol 1-phosphate head group. The head group is oriented to the cytosol and can be phosphorylated by PI-kinases and dephosphorylated by PI-phosphatases at the 3', 4' or 5' position [50]. PtdIns(3)*P*, PtdIns(4)*P*, PtdIns(5)*P*, PtdIns(3,4)*P*₂, PtdIns(3,5)*P*₂ and PtdIns(3,4,5)*P*₃ can be formed [45, 96].

The distribution and function of the different PIs in the cell varies. Specific PIs together with small GTPases are responsible for the transport between subcellular compartments [97]. PI-metabolizing enzymes interconvert these lipids. PIs have specific localisations within the cell and thus serve as organelle markers. PtdIns(3)*P* is mainly found on phagosomes, multivesicular bodies (MVBs) as well as on early endosomes [95-97]. PtdIns(4)*P* has a broad distribution. It is found on the plasma membrane, on secretory vesicles, the Golgi apparatus and the ER [95, 97, 98]. In an immunofluorescence analysis the localisation of PtdIns(4)*P* on the LCV was shown by an anti-PtdIns(4)*P* antibody. PtdIns(3,5)*P*₂ is found in the later steps of the endosomal pathway [95]. PtdIns(4,5)*P*₂ is enriched at the plasma membrane and together with PtdIns(3,4,5)*P*₃ is located at sites of phagocytosis [96]. Proteins interact with PIs through specific PI lipid-binding domains like the pleckstrin homology (PH) domain which is known to bind to PtdIns(4)*P* [96, 99], PtdIns(3,4)*P*₂ and PtdIns(3,4,5)*P*₃ [100]. Therefore, a purified eukaryotic PH_{FAPP1} domain coupled to GST can be used as a probe for PtdIns(4)*P* [80]. A number of effector proteins are known which modify PI lipids. LpnE might be important for binding of inositol polyphosphate 5-phosphatase OCRL1 (oculocerebrorenal syndrome of *Lowe* 1) to the LCV [50, 101] and SidF is a known PtdIns(3)-phosphatase [102].

Many T4SS effector proteins of *L. pneumophila* are characterized to bind to PtdIns(3)*P* or PtdIns(4)*P* on the LCV. PtdIns(4)*P*-binding effector proteins are for example SidC_{Lpn}, its homolog SdcA_{Lpn} [80, 92, 94, 103] and the GEF (guanine nucleotide exchange factor)/AMPylase (adenosine mono-phosphorylase) SidM (also known as DrrA) [45, 56, 81, 104]. LidA is an example for a PtdIns(3)*P*-binding effector protein [83, 94]. *L. pneumophila* is interacting with the host cell regulation of PIs to form a replication-permissive niche. Finally, also *Legionella* spp. are avoiding the lysosomal or autophagosomal pathway through imitating the lipid composition of the host cell organelles. This strategy is called "identity theft" [97].

1. General introduction

1.6.1 SidC and SdcA

1.6.1.1 SidC_{Lpn} and SdcA_{Lpn} of *L. pneumophila*

The 106 kDa protein SidC_{Lpn} (substrate of Icm/Dot transporter) and its paralog SdcA_{Lpn} are known Icm/Dot-dependent effector proteins of *L. pneumophila* which bind through PtdIns(4)*P* homogenously to the cytoplasmic side of the LCV [80, 84, 101, 103] (Figure 1.2). SidC_{Lpn} and SdcA_{Lpn} have an identity of 72% [3]. Both effector proteins also bind with a much smaller affinity to PtdIns(3)*P* [103]. The results were confirmed for SidC_{Lpn} by protein lipid overlay assays [3, 80]. A 20 kDa PtdIns(4)*P*-binding domain, termed SidC_{Lpn_P4C} (PtdIns(4)*P*-binding of SidC), was found to be the binding region for PtdIns(4)*P*. This P4C domain binds with higher affinity to PtdIns(4)*P* than the full length SidC_{Lpn} [3, 81]. The P4C domain is unique for prokaryotes and does not show any homology to eukaryotic PI domains [103]. A glutamate cluster called E-block in the C-Terminus is important for the efficient translocation of SidC_{Lpn} [105].

Until now little is known about how PtdIns(4)*P* accumulates on the LCV and effector proteins like SidC_{Lpn} can bind to it [101]. The amoeba PtdIns(4, 5)*P*₂ 5-phosphatase Dd5P4 (*Dictyostelium discoideum* 5-phosphatase 4) as well as its human homologue OCRL1, which hydrolyses PtdIns(4,5)*P*₂ to produce PtdIns(4)*P* [50, 106], are found on the LCV and could be responsible for the production of PtdIns(4)*P* [101]. In a *D. discoideum* Dd5P4 mutant less SidC_{Lpn} was found on the LCV. It is known that more SidC_{Lpn} binds to the LCV in infected *D. discoideum* if phosphatidylinositol 3-kinase (PI3K) is depleted because PI3K converts PtdIns(4)*P* to PtdIns(3,4)*P*₂ and PtdIns(3,4,5)*P*₃ [80]. In a RNA interference assay in *Drosophila melanogaster* Kc167 phagocytes the depletion of PtdIns 4-kinase IIIβ (PI4KIIIβ), which produces PtdIns(4)*P*, lowered the amounts of SidC_{Lpn} on the LCV. A depletion of the isoenzyme PI4KIIIα or PI4KIIα did not affect the SidC_{Lpn} binding to the LCV [81].

SidC_{Lpn} is competing with SidM for the PtdIns(4)*P* binding site on the LCV. In a phosphoinositide-pulldown assay with PI-coated agarose beads only SidM but not SidC_{Lpn} was found to bind to PtdIns(4)*P*. Even in the absence of SidM no SidC_{Lpn} was detected [81]. Proteolysis of SidC was ruled out and it was found that the affinity of SidM and SidC_{Lpn} towards PtdIns(4)*P* is nearly the same. A masking “in *cis*” by a domain of SidC_{Lpn} could be the reason for the lack of binding in agreement with the finding that the P4C

1. General introduction

domain is binding with a higher affinity to PtdIns(4)*P* than the full length SidC_{Lpn}. Alternatively, a complexation of SidC_{Lpn} with other *L. pneumophila* proteins could prevent the binding of SidC_{Lpn} [81]. Putative chaperones like IcmS and IcmW could be interactors for SidC_{Lpn} [81, 107, 108]. It was shown in an immunofluorescence analysis that in the absence of SidM more SidC_{Lpn} is binding to the LCV [81].

SidC_{Lpn} localizes to tight and spacious LCVs [80]. The deletion of the genes *sidC_{Lpn}* and *sdcA_{Lpn}* in *L. pneumophila* does not lead to a decreased intracellular replication of the bacteria in *D. discoideum*, *A. castellanii* or macrophages. However, a slower and less pronounced interaction with the ER and a failure of the LCVs to develop from tight to spacious LCVs were results of this deletion [80, 103, 106, 109]. Also, the establishment of a replication-permissive LCV was delayed [109]. The deletion is causing a reduction of the ER markers HDEL and calnexin to the LCV, up to 20% for calnexin. The calnexin recruitment defect was complemented by plasmid-encoded SidC_{Lpn} or SdcA_{Lpn} but not by plasmid-encoded SidC_{Lpn_P4C}. The LCVs of *D. discoideum* or RAW 264.7 macrophages infected with a *sidC-sdcA_{Lpn}* deletion mutant were harbouring endosomal but not lysosomal markers [103]. The 70 kDa N-terminal domain of SidC_{Lpn} was binding ER and ER-derived vesicles like the full length SidC. Therefore SidC_{Lpn} and SdcA_{Lpn} facilitate the acquisition of ER and ER-derived vesicles (Figure 1.2) through a N-terminal domain to the LCV [103]. It was postulated that the amino acids 225 to 323 are important for the interaction of SidC_{Lpn} with ER-derived vesicles over a host factor [109].

The genes *sidC_{Lpn}* and *sdcA_{Lpn}* are important for the early recruitment of LCV markers like ubiquitin and Arf1. The effect was only visible for Arf1 if both effector proteins were depleted indicating that the two effector proteins have redundant functions [109]. RalF recruits Arf1 to the LCV and RalF is a GEF for Arf1 [87, 110]. SidC_{Lpn}/SdcA_{Lpn} did not affect the function of RalF, and therefore, their effect on the Arf1 recruitment seems to be indirect [109] (Figure 1.2).

The absence of the effector proteins SidC_{Lpn} and SdcA_{Lpn} did not result in a decreased recruitment of Rab1 to a LCV [103], but the deletion mutant caused a loss of the monoubiquitination of Rab1A (Figure 1.2). SidC_{Lpn} and SdcA_{Lpn} had again a redundant function and the amino acids 222 to 315 were necessary for the ubiquitination. In liquid chromatography-mass spectrometry (LCMS) analysis the ubiquitin was found at lysine 187. A temporary ubiquitination in the early steps of the infection was shown. Recently, a

1. General introduction

structural analysis of the N-terminal fragment of SidC (amino acids 1 to 608) was published. The length of SidC_{Lpn} (around 220 Å) is comparable with other tethering proteins. No structural homolog was found [109].

Finally, in biochemical and biological assays the P4C domain can be used as a probe for PtdIns(4)*P* on the LCV [3, 103]. The full-length SidC_{Lpn} can be used in an immuno-affinity separation of LCVs from infected amoebae or macrophages [2, 54].

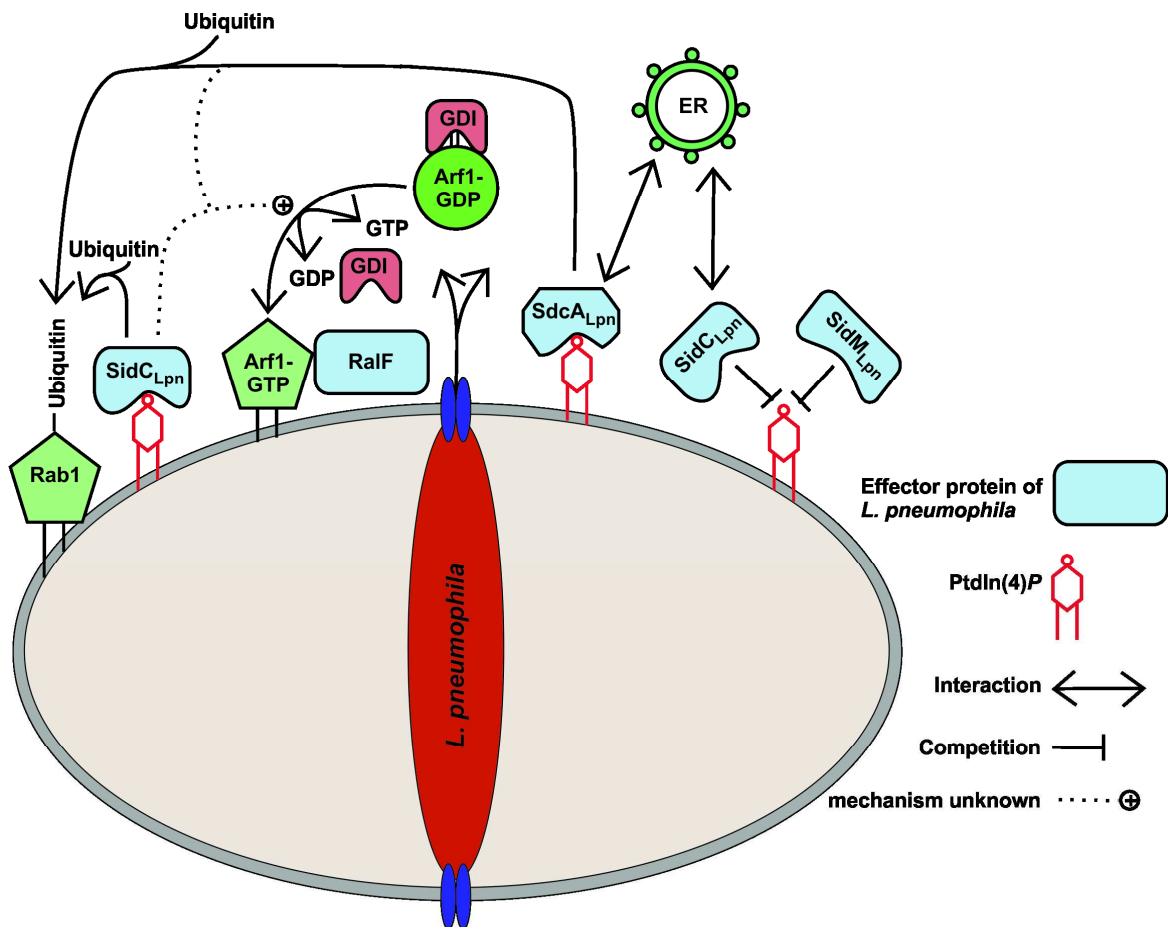


Figure 1.2. The role of SidC_{Lpn} and SdcA_{Lpn} on a *L. pneumophila*-containing vacuole. SidC_{Lpn} and SdcA_{Lpn} are binding through PtdIns(4)*P* to the *L. pneumophila*-containing vacuole. Both effector proteins interact with the ER [80, 103, 106]. SidC_{Lpn} is competing with SidM_{Lpn} for PtdIns(4)*P* [81]. SidC_{Lpn} and SdcA_{Lpn} promote the activation of Arf1, which is recruited to the LCV through RalF [87, 109, 110]. Rab1 is ubiquitinated by SidC_{Lpn} and SdcA_{Lpn} [109].

1.6.1.2 SidC_{Llo} of *L. longbeachae*

A 111 kDa homolog to SidC_{Lpn} was found in the genome of *L. longbeachae* and was named also SidC (SidC_{Llo}). SidC_{Llo} is a putative substrate of the Icm/Dot type IV secretion

1. General introduction

system [26] (Figure 1.3). No *sdca* gene was found in the genome of *L. longbeachae* [26] (Figure 1.3).

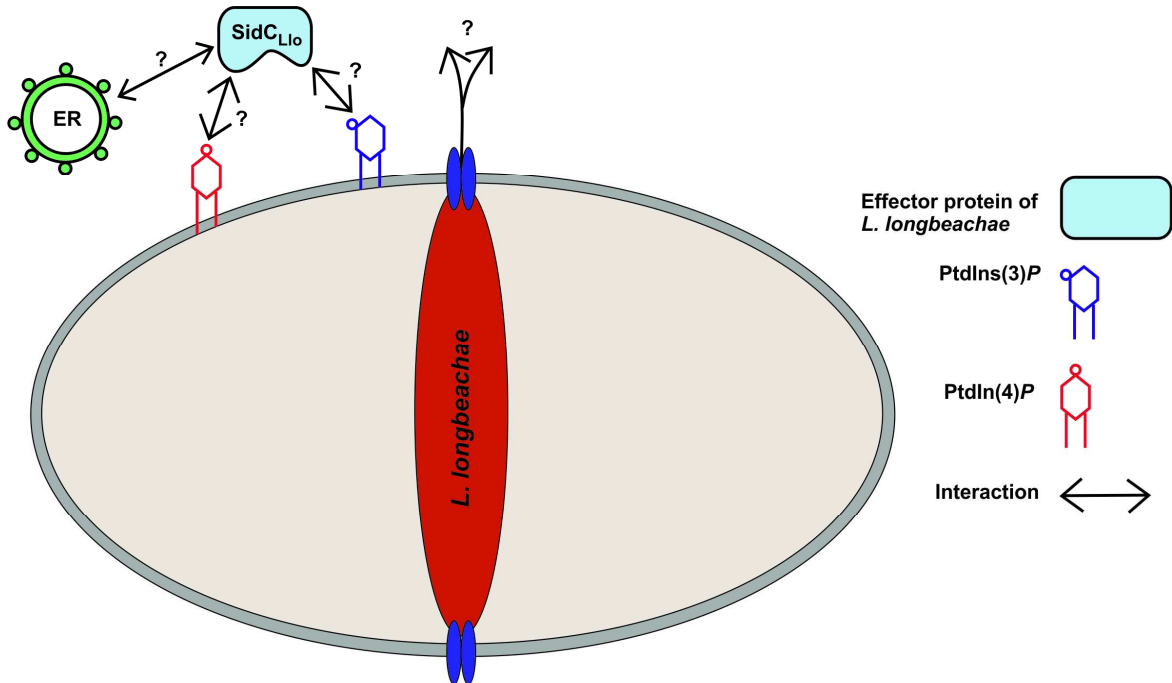


Figure 1.3. The role of SidC_{Lio} on a *L. longbeachae*-containing vacuole. It is not known if SidC_{Lio} is translocated through the Icm/Dot T4SS into the cytosol of the host cell. It is possible that a translocated SidC_{Lio} is binding through PtdIns(3)P, PtdIns(4)P or other PI lipids to the LCV. SidC_{Lio} could also be located in the cytosol of the host cell. SidM and SdcA are missing in the genome of *L. longbeachae* [26].

1.6.2 SidM (alias DrrA) of *L. pneumophila*

SidM is a 73 kDa Icm/Dot substrate of *L. pneumophila* which is translocated through a C-terminal translocation signal. The effector protein binds through a 12 kDa PtdIns(4)P binding domain called P4M (PtdIns(4)P-binding of SidM/DrrA; amino acids 544 to 647) to PtdIns(4)P on the LCV during the early stage of infection [81, 111]. The binding affinity of the P4M domain for PtdIns(4)P is reduced compared to the full length SidM [81]. The structure of a SidM fragment including the P4M domain was analysed. A novel fold of the effector protein was found. This SidM fragment possesses a high affinity to PtdIns(4)P with a dissociation equilibrium constant (K_D) of 30 nM [104]. The P4M binding domain has no similarity with the P4C domain of *L. pneumophila* or the PtdIns(4)P-binding PH domain of the adaptor protein phosphatidylinositol (4) phosphate adaptor protein 1 (FAPP1) of eukaryotic cells. SidM is competing with SidC_{Lpn} for binding to PtdIns(4)P on the LCV. SidM also weakly binds to the phosphate in position 4 of PtdIns(3,4)P₂,

1. General introduction

PtdIns(4,5) P_2 and PtdIns(3,4,5) P_3 as well as to PtdIns(3) P [81]. The *sidM* gene is not found in the genome of *L. longbeachae* [26].

SidM is a known GEF and GDF (GDI displacement factor) for the small GTPases Rab1, Rab8 and Rab14 of the Rho subfamily [54, 59, 81, 112, 113]. Two activation states of Rho GTPases are known. GTPases are inactive if they have bound a guanine nucleotide dissociation inhibitor (GDI) and GDP. In the active state the GDP is exchanged by a GTP through a GEF and the GDI is removed. In this state the GTPases interacts with downstream effector proteins such as adaptor proteins, lipid kinases and proteins. GTPases of the Rho subfamily play a role in regulation of the actin cytoskeleton and in signal transduction pathways of eukaryotes [114].

SidM binds through its P4M domain [81] to PtdIns(4) P located on the LCV. SidM activates Rab1 through its GDF activity [111, 115, 116] and catalyses a GDP-GTP exchange [104, 111, 112, 115-118] through its GEF activity in the central part [119]. Finally, SidM is bound to Rab1-GTP [45] (Figure 1.4). Rab1 is necessary for the vesicle transport from the ER to the Golgi [81].

The N-terminal part of SidM possesses also an “AMPylation” (adenosine monophosphorylation) activity for the switch II region of Rab1. This switch II region of Rab1 is involved in the interaction with GEF, GDI and GAP [109, 119, 120]. The “AMPylation” is important for the retention of Rab1 on the LCV [116]. The Icm/Dot-dependent effector protein LidA was found to be an Icm/Dot substrate which decorates the LCV [83, 121]. LidA is binding to PtdIns(3) P and with lower affinity to PtdIns(4) P [81]. LidA is binding to GDI-free Rab1 and therefore facilitates the recruitment of early secretory vesicles to the LCV [112, 113, 115, 121]. Through the binding to Rab1 LidA supports the GEF activity of SidM [113]. LidA can interact with Rab1 modified by different covalent modifications like AMPylation and phosphocholination. It is also able to prohibit the dephosphocholination through the effector protein Lem3 or the de-AMPylation of Rab1 through the effector protein SidD [122]. Also, an interaction of LidA with small Rab GTPases like Rab6 and Rab8 was described (Figure 1.4).

The effector protein SidD deampylates Rab1-GTP [123, 124]. LepB dephosphorylates the GTP of Rab1 and binds to the LCV and Rab1-GDP. Thus, Rab1 is inactivated [116]. Therefore LepB is the antagonist of SidM [111]. A GDI binds to Rab1-GDP, removes it

1. General introduction

from the surface of the LCV and the cycle starts again with the activation of GDI bound Rab1-GDP through SidM [104, 111, 112, 115, 117, 118] (Figure 1.4).

Rab1-GTP bound SidM can also be phosphocholinated by AnkX. This is not required for the retention of Rab1 to the LCV [116]. AnkX is inhibiting the formation of a Rab1-GDP:GDI complex [125]. Lem3 dephosphorylates Rab1, and consequently Rab1 is accessible for the effector protein LepB [126].

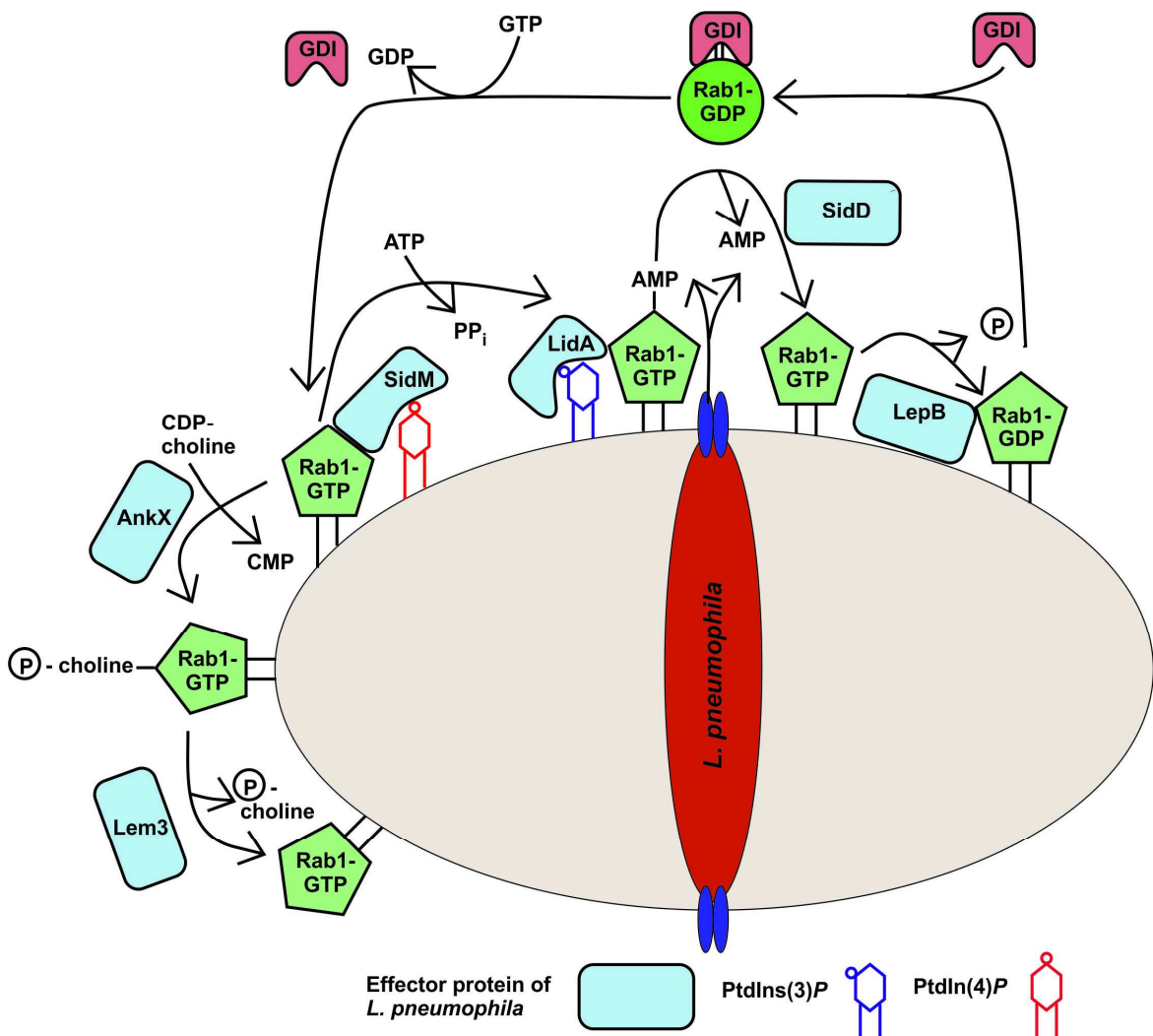


Figure 1.4. Effector proteins compete with SidM for Rab1 on the *L. pneumophila*-containing vacuole. An Icm/Dot T4SS system is necessary for the translocation of effector proteins into the host cell. Some of the effector proteins bind through PI lipids (PtdIns(3)P and PtdIns(4)P) to the LCV. These effector proteins can modify the small GTPase Rab1 and possess different activities like a GEF and GDF activity (SidM), GAP activity (LepB), de-phosphocholinase (Lem3), phosphocholinase (AnkX) or deampylase (SidD). The figure is based on the scheme published in [45].

1. General introduction

1.7 Aims of the Ph.D. thesis

At the onset of this thesis not a single *L. longbeachae* effector (among more than 100 candidates) was biochemically characterized. Using PI lipids covalently coupled to agarose beads, we thought to identify PI-binding *L. longbeachae* proteins in an unbiased screen. Thus, we identified the *L. pneumophila* homologue of *L. pneumophila* SidC as a PI-binding protein. The genome of *L. longbeachae* NSW150 was published in the first half of 2010. A homolog of SidC_{Lpn} was identified and the protein corresponding to the gene *llo3098* was termed SidC_{Llo} [26]. Therefore, we characterized SidC_{Llo} and compared it to SidC_{Lpn} using genetic, biochemical and cell-biological approaches. Since the available SidC_{Lpn} antibody did not recognize SidC_{Llo} in a Western blot or in an immunofluorescence analysis, a SidC_{Llo} antibody was produced.

Another aim of the thesis was to isolate and purify intact LCVs harbouring *L. longbeachae*. To this end, a protocol based on immuno-affinity purification, previously established for *L. pneumophila*, was used. The goal was to perform a proteomic analysis of the *L. longbeachae*-containing vacuole. LCV purifications were tried with infected *D. discoideum* as well as with infected RAW 264.7 macrophages.

Taken together, this thesis aimed at a better understanding of LCV formation and intracellular replication of *L. longbeachae*.

2. Materials and methods

2.1 Materials

2.1.1 Bacterial strains

The bacterial strains listed in table 2.1 were used (Table 2.1).

Table 2.1. Bacterial strains*.

Strain	Property	Reference
<i>E. coli</i>		
TOP10	---	Invitrogen
BL21 (DE3)	---	Novagen
<i>L. longbeachae</i>		
NSW150	<i>L. longbeachae</i> Serogroup 1	[26]
$\Delta dotA$	NSW150 <i>dotA</i> ::Kan ^R ($\Delta dotA$)	[26]
IH02	NSW150 <i>sidC</i> _{L10} ::Kan ^R ($\Delta sidC$ _{L10})	[3]
<i>L. pneumophila</i>		
JR23	<i>L. pneumophila</i> Philadelphia strain 1	[127]
GS3011	JR32 <i>icmT3011</i> ::Kan ^R ($\Delta icmT$)	[128]
LELA3118	JR32 <i>dotA3118</i> ::Kan ^R ($\Delta dotA$)	[127]
CR001	JR32 <i>sidC-sdcA</i> ::Kan ^R ($\Delta sidC-sdcA$ _{Lpn})	[103]

*Abbreviation: kanamycin (Kan)

2.1.2 Eukaryotic cell lines

The eukaryotic cell lines listed in table 2.2 were used (Table 2.2).

2. Materials and methods

Table 2.2. Eukaryotic cell lines*.

Cell line	Property	Reference
<i>Acanthamoeba castellanii</i>	---	ATCC 30234
RAW 264.7 macrophages	---	ATCC TIB-71
<i>D. discoideum</i>		
AX3/pCaln-GFP	P_{act15} , calnexinA-RSSSKLK-GFP (S65T), G418	[129]

*Abbreviation: geneticin sulphate (G418)

2.1.3 Plasmids

The plasmids listed in table 2.3 were used (Table 2.3).

Table 2.3. Plasmids*.

Plasmid	Property	Reference
pCetLI1	pZT- <i>llo0105-cyaA-C</i> (P_7)	[58]
pCR02	pGEX4T-1, <i>GST-sidC_{Lpn}</i> (P_{tac})	[80]
pCR34	pMMB207-C, <i>M45-sidC_{Lpn}</i> (P_{tac})	[80]
pCR77	pMMB207-C, <i>dsred</i> (P_{tac})	[91]
pCR80	pMMB207-C, <i>dsred</i> (P_{tac}), <i>sidC_{Lpn}</i> (P_{tac})	[91]
pET28a(+)	N-terminal <i>His₆</i> -fusion, Kan ^R (P_{T7})	Novagen
pGEX4T-1	N-terminal <i>GST</i> -fusion, Amp ^R (P_{tac})	Amersham
pGEX-PH_FAPP1	pGEX4T-1, <i>GST-PH_FAPP1</i> (P_{tac})	[130, 131]
pHP056	pGEX4T-1, <i>GST-sidC_{Lpn_609-776}</i> (P_{tac})	[103]
pIH031	pMMB207-C- <i>cyaA-sidC_{Llo}</i> (P_7)	unpublished
pIH047	pMMB207-C-RBS- <i>dsredexpress</i> -RBS- <i>sdca</i> (P_{tac})	[3]

2. Materials and methods

pIH060	pGEX4T-1, <i>SidC</i> _{Lpn_1-608-Llo_609-969} (P _{tac})	[3]
pMH01	pGEX4T-1, <i>sidC</i> _{Llo_1-608-Lpn_609-917} (P _{tac})	[3]
pMMB207-C-M45	pMMB207-C, Δ <i>mobC</i> , <i>M45</i> -(Gly) ₅ , Cam ^R (P _{tac})	[80]
pSD01	pET28a(+); <i>His</i> ₆ - <i>sidC</i> _{Llo} (P ₇)	[3]
pSD02	pET28a(+); <i>His</i> ₆ - <i>sidC</i> _{Llo} (P ₇); deletion of <i>Bam</i> HI and <i>Sall</i> in <i>sidC</i> _{Llo}	[3]
pSD03	pGEX4T-1, <i>GST-sidC</i> _{Llo_609-782} (P _{tac})	[3]
pSD04	pGEX4T-1, <i>GST-sidC</i> _{Llo_1-340} (P _{tac})	[3]
pSD05	pGEX4T-1, <i>GST-sidC</i> _{Llo_341-608} (P _{tac})	[3]
pSD06	pGEX4T-1, <i>GST-sidC</i> _{Llo_783-969} (P _{tac})	[3]
pSD07	pGEX4T-1, <i>GST-sidC</i> _{Llo} (P _{tac})	[3]
pSD13	pMMB207-C, <i>M45-sidC</i> _{Llo} (P _{tac})	[3]
pSD14	pMMB207-C, <i>dsred</i> (P _{tac}), <i>sidC</i> _{Llo} (P _{tac})	[3]
pSH097	pMMB207-C- <i>cyaA</i> (P _{tac})	[91]
pSH098	pMMB207-C- <i>cyaA-sidC</i> (P _{tac})	[91]
pSW001	pMMB207-C, Δ <i>lacI</i> ^q , constitutive <i>dsred</i> (P _{tac})	[132]

*Abbreviations: ampicillin (Amp); chloramphenicol (Cam); kanamycin (Kan)

2.1.4 Oligonucleotides

The oligonucleotides listed in table 2.4 were used (Table 2.4).

Table 2.4. Oligonucleotides [3].

Oligo	Sequence (5' - 3') *	Comment
oSD07	TTTT <u>CATATG</u> ATGAGAGTCACTAAAATGCCT AAAGAC	5' flanking sequence of <i>sidC</i> _{Llo} (fo)
oSD08	TTTTT <u>GCTAGC</u> TTAAGTACGTGAATTAAAAGT ACGTCC	3' flanking sequence of <i>sidC</i> _{Llo} (re)

2. Materials and methods

oSD16	TTTTG <u>GGATCC</u> ATG AGA GTC ACT AAA ATG CCT AAA GAC	5' of <i>sidC_{Llo}</i>
oSD17	TTTTT <u>GTCGACT</u> CATCCAGTGATTTTTCTAC GTC	3' of <i>sidC_{Llo_1-340}</i> (re)
oSD18	TTTTG <u>GGATCC</u> GCTGCTGTTATTCCTGGG	5' of <i>sidC_{Llo_609-782}</i> (fo)
oSD19	TTTTT <u>GTCGACT</u> CATTCATTGAAAAAGTTAAG CGCTG	3' of <i>sidC_{Llo_609-782}</i> (re)
oSD22	GAAAATAATATCAAGGCATGGTCCACTGATC TTGAAGCAATCG	Quick Change of <i>sidC_{Llo}</i> (<i>SalI</i>) (fo)
oSD23	CGATTGCTTCAAGATCAGTGGACCATGCCTT GATATTATTTTC	Quick Change of <i>sidC_{Llo}</i> (<i>SalI</i>) (re)
oSD24	AAACGCG <u>GATCC</u> GATGAATCACAGCAAAG GAAGC	5' of <i>sidC_{Llo_341-608}</i> (fo)
oSD25	AAACGCG <u>TCTCGACT</u> CAATTTTCTCTATTCACGT TTGCTGGAG	3' of <i>sidC_{Llo_341-608}</i> (re)
oSD26	AAACGCG <u>GATCCT</u> TGTCTTTACATGAGGTGC TTAAAGTAGC	5' of <i>sidC_{Llo_783-970}</i> (fo)
oSD27	AAACGCG <u>TCTCGACT</u> TAAGTACGTGAATTA GTACGTCC	3' of <i>sidC_{Llo_783-970}</i> (re)
oSD28	GATGAGTTCTTTTTGATGGACCCAATAGAA AAGG	Quick Change of <i>sidC_{Llo}</i> (<i>BamHI</i>) (fo)
oSD29	CCTTTTCTATTGGGGTCCATCAAAAAGAACT CATC	Quick Change of <i>sidC_{Llo}</i> (<i>BamHI</i>) (re)

*The restriction sites are underlined.

2.1.5 Lab equipment

The lab equipments listed in table 2.5 were used (Table 2.5).

2. Materials and methods

Table 2.5. Lab equipments.

Application	Name of the lab equipment	Supplier
autoclave	STERIMAQUET	MAQUET
Bunsen burner	FIREBOY plus	INTEGRA Biosciences
cell culture centrifuge	Megafuge 40R	Thermo Scientific
cell homogenizer	---	Isobiotech
centrifuge	3-30K	Sigma
centrifuge	Centrifuge 5415R	Eppendorf
centrifuge	Sorvall [®] RC-5B	Du Pont
colony counter	Countermat Flash	IUL
confocal fluorescence microscope	Leica Sp5 TCS	Leica
culture microscope	Primo Vert	Zeiss
diaphragm vacuum pump	MZ 2C	Vacuubrand
electrophoresis chamber	Mini-Subcell GT/ Subcell GT/ Mini-Protean 3	Bio-Rad
electroporation device	GenePulser XCell [™]	Bio-Rad
FACS machine	FACS Canto [™] II	BD Bioscience
French Press	SIM-AMINCO	Spectronic
gel imaging system	ChemiDoc MP System	Bio-Rad
hot plate magnetic stirrer	RCT basic	IKA
ice cube machine	AF30	Scotsman
incubation cabinet	Orbital shaker, Forma	Thermo Scientific
incubator	Heraeus BR6000/ Heraeus Function Line	Thermo Scientific
incubator	IPP400/ IPP500	Memmert

2. Materials and methods

magnetic separator	MACS multistand	Miltenyi Biotec
medical film processor	FPM-100A	FUJIFILM
mixer	Vortex-Genie 2	IKA
pH-meter	Level 1	inoLab
pipettes	pipetman	Gilson
pipettor	pipetus	Hirschmann
plate reader	FLUO star OPTIMA	BMG Labtech GmbH
power supply	PAC100	Bio-Rad
precision balance	BP61-S	Sartorius
precision balance	PG2002-S	Mettler-Toledo
protein transfer device	MAXI-Semi-Dry-Blotter	Roth
rocking platform	Duomax 1030	Heidolph
spectrophotometer	NanoDrop ND-1000	PeqLab
spectrophotometer	Libra S12	Biochrom
thermocycler	T3	Biometra
thermomixer	Thermomixer Comfort	Eppendorf
ultracentrifuge	OPTIMA™ TL	Beckham
UV transilluminator	---	Bachofer
water bath	Wasserbad 1005	GFL
wheel for cups and falcons	KABE Mischgerät BM 92	KABE Labortechnik

2.1.6 Software and data bases

The figures were created with “Microsoft Excel” (Microsoft) and “Corel Draw” (Corel). The amino acid alignment was made by “ClustalOmega” alignment (EMBL-EBI homepage).

2.2 Methods

2.2.1 *Legionella* spp.

2.2.1.1 General growth conditions

L. longbeachae and *L. pneumophila* were frozen in glycerol stocks (section 2.2.1.2). This stocks were used to inoculate charcoal yeast extract agar (CYE) plates (Table 2.6) [17]. The bacteria were grown at 37°C for 3 days and diluted in ACES yeast extract medium (AYE) (Table 2.7) [48] to an optical density at 600 nm (OD₆₀₀) of 0.1. 2×10^9 bacteria ml⁻¹ correlate to an OD₆₀₀ of 3.0. The overnight cultures were cultivated for 18 till 21 hours on a rotating wheel at 37°C until the culture reached the stationary growth phase. A brown colour of the bacterial solution indicated this growth phase. 10 µg ml⁻¹ (*L. longbeachae*) or 5 µg ml⁻¹ chloramphenicol (Cam) (*L. pneumophila*) were added to the overnight culture in which the bacteria harboured a plasmid with a Cam resistance. 0.5 mM isopropyl-β-D-thiogalactopyranoside (IPTG) (Roth) was added to the medium if a gene under the control of a P_{tac}-promotor was to be induced.

Table 2.6. Charcoal yeast extract agar (CYE) [17]*.

Component	Per liter agar	Supplier
ACES	10 g	AppliChem
Bacto yeast extract	10 g	BD Biosciences
activated charcoal	2 g	Fluka
agar	15 g	Serva
L-cysteine	0.4 g in 10 ml dH ₂ O	Sigma
FeN ₃ O ₉ x 9H ₂ O	0.25 g in 10 ml dH ₂ O	Sigma

*The ACES and Bacto yeast extract were dissolved in dH₂O and adjusted to a pH of 6.9. 10 M KOH (Merck) was used for the adjustment. The solution was added to the activated charcoal and agar. A stir bar was added. The agar was autoclaved and cooled down to 50°C. Filter sterilized (Filter Glass Microfiber Filter, WhatmanTM) L-cysteine solution was slowly added to the medium followed by the filter sterilized iron solution. An antibiotic was added if needed (5 µg ml⁻¹ of chloramphenicol for *L. pneumophila*, 10 µg ml⁻¹ of chloramphenicol for *L. longbeachae*, 50 µg ml⁻¹ kanamycin).

2. Materials and methods

Table 2.7. ACES yeast extract medium (AYE) [17]*.

Component	Per liter medium	Supplier
ACES	10 g	AppliChem
Bacto yeast extract	10 g	BD Biosciences
L-cysteine	0.4 g in 10 ml dH ₂ O	Sigma
FeN ₃ O ₉ x 9H ₂ O	0.25 g in 10 ml dH ₂ O	Sigma

*ACES and the Bacto yeast extract were dissolved in dH₂O. The dissolved L-cysteine was slowly added to the medium followed by the iron solution. The pH was adjusted with 10 M KOH to 6.9. The medium was filtered six to eight times through a glass fiber filter followed by a filtration step with a filter with a smaller pore size (500 ml Rapid-Flow Bottle Top Filter, A. Hartenstein). The medium was stored at 4°C.

2.2.1.2 Glycerol stock

A single colony was used to inoculate 3 ml AYE in a test tube (section 2.2.1.1). The culture was cultured for 18 till 21 hours on a rotating wheel at 37°C until it reached the stationary phase. The culture was mixed with glycerol (Roth) to a final glycerol concentration of 25%. The mixture was frozen in liquid nitrogen in a cryovial (Thermo Scientific) and stored at -80°C.

2.2.1.3. Production of electrocompetent *Legionella* spp.

2.2.1.3.1 *L. longbeachae*

L. longbeachae were streaked out from a glycerol stock densely on a CYE plate (section 2.2.1.2). The bacteria lawn was harvest with an inoculating loop and resuspended in sterile ice cold dH₂O. The suspension was diluted to an OD₆₀₀ of 2.0. The bacterial mixture was washed two times with 10 ml ice cold sterile dH₂O (3.350 x g, 10 minutes, 4°C) and one time with 10 ml ice cold sterile 10% glycerol. 250 µl of ice cold sterile 10% glycerol were used to resuspend the bacterial pellet. This bacterial suspension was used immediately for a transformation [133].

2. Materials and methods

2.2.1.3.2 *L. pneumophila*

L. pneumophila was grown in an overnight culture to pre-stationary phase (section 2.2.1.1). 1 ml of the overnight culture was added to 30 ml AYE. The culture was grown at 37°C on a rotating wheel to an OD₆₀₀ of 0.3 till 0.5 and cooled down. The bacteria were washed three times (5.000 x g, 5 minutes, 4°C) with 10 ml sterile, ice cold 10% glycerol. After the last washing step the bacterial pellet was resuspended in 160 µl sterile, ice cold 10% glycerol and aliquoted in portions of 25 µl. The aliquots were frozen in liquid nitrogen and stored at -80°C.

2.2.1.4 Transformation of electrocompetent *Legionella*

2.2.1.4.1 *L. longbeachae*

50 µl of the electrocompetent bacteria (section 2.2.1.3.1) were mixed with three to five µg of DNA on ice and transferred in a precooled cuvette with a 2 mm electrode gap (Gene Pulser Cuvette, Bio-Rad). The cell suspension was electroporated in a GenePulser XCell™ Electroporation Systems (Bio-Rad) (2.4 kV, 200 Ω, 0.25 µF). 1 ml AYE medium was added to the cell suspension and the bacterial solution was transferred in a test tube. The culture was incubated for five hours at 37°C on a rotating wheel. The bacterial solution was plated onto CYE plates with the necessary antibiotics. Colonies appeared after four till five days [133].

2.2.1.4.2 *L. pneumophila*

One aliquot of the electrocompetent bacteria (section 2.2.1.3.2) were mixed with 100 ng of DNA on ice. The bacteria/DNA mixture was transferred to a precooled cuvette with an 2 mm electrode gap. The bacteria/DNA mixture was electroporated (2.5 kV, 200 Ω, 25 µF). The solution was mixed with 450 µl AYE medium and transferred to a test tube. The culture was incubated for five hours at 37°C on a rotating wheel. The bacterial solution was plated onto a CYE plate with an appropriate antibiotic.

2. Materials and methods

2.2.2 *Escherichia coli*

2.2.2.1 General growth conditions

Escherichia coli was streaked out from a glycerol stock (section 2.2.2.2) with an inoculating loop on a Luria-Bertani (LB) agar plate (Invitrogen) and cultivated over night at 37°C. An overnight culture was inoculated with one *E. coli* colony. The culture was grown in LB broth base (Invitrogen) over night at 37°C on a shaker. Antibiotic was added to the LB agar plates and LB broth if necessary (Table 2.8). A gene under P_{tac}-control was induced by adding 0.5 mM IPTG to the LB broth.

Table 2.8. Antibiotics.

Component	MW [g/mol]	Final concentration	Supplier
ampicillin (Amp)	371.39 g mol ⁻¹	100 µg ml ⁻¹	Roth
chloramphenicol (Cam)	323.13 g mol ⁻¹	30 µg ml ⁻¹	AppliChem
kanamycin (Kan)	582.58 g mol ⁻¹	50 µg ml ⁻¹	Sigma

2.2.2.2 Glycerol stock

An *E. coli* overnight culture (section 2.2.2.1) was diluted with glycerol to a final concentration of 25%. The mixture was transferred into a cryovial tube, frozen in liquid nitrogen and stored at -80°C.

2.2.2.3. Production of chemical competent *E. coli*

A small overnight culture of *E. coli* was inoculated in LB broth medium and cultivated at 37°C on a shaker (section 2.2.2.1). 100 ml of a fresh LB broth base culture was inoculated with 1 ml of the overnight culture. The culture was incubated until the OD₆₀₀ reached 0.5. The following steps were performed on ice. The culture was transferred in a 50 ml test tube, cooled down for 15 minutes and washed once with 40 ml ice cold TFB1 (Table 2.9) (3.350 x g, 15 minutes, 4°C) and once with 4 ml ice cold TFB2 (Table 2.10). The bacterial solution was incubated for 15 minutes on ice. 50 µl aliquots were aliquoted, frozen in liquid nitrogen and stored at -80°C.

2. Materials and methods

Table 2.9. TFB1*, **.

Component	Concentration	Gram	Supplier
KAc	30 mM	1.41 g	Roth
KCl	100 mM	3.73 g	Merck
CaCl ₂ x 2H ₂ O	10 mM	0.74 g	Merck
MnCl ₂	50 mM	3.15 g	Fluka
glycerol	15%	150 ml	Roth

*Distilled H₂O was added to reach a final volume of one liter.

**The pH of the solution was adjusted to 5.8 with 0.2 N acetic acid (Roth). The solution was filter sterilized and stored in aliquots of 40 ml at -20°C.

Table 2.10. TFB2 *, **.

Component	Concentration	Gram	Supplier
MOPS (3-(N-morpholino) propanesulfonic acid)	10 mM	0.105 g	Sigma
CaCl ₂ x 2H ₂ O	75 mM	0.552 g	Merck
KCl	10 mM	0.037 g	Merck
glycerol	15%	15 ml	Roth

*Distilled H₂O was added to reach a final volume of 50 ml.

**The pH of the solution was adjusted to 6.5 with KOH (Merck), filter sterilized and stored in aliquots of 4 ml at -20°C.

2.2.2.4 Transformation of chemical competent *E. coli*

The chemical competent bacteria were thawed on ice (section 2.2.2.3). 100 ng of DNA were added to the bacteria. The bacteria were incubated on ice for 30 minutes. A heat shock was performed at 42°C for one minute. The bacteria were cooled on ice for two minutes and transferred with 1 ml LB broth medium in a test tube. The culture was incubated at 37°C on a shaker for one hour. The culture was plated onto LB agar plates with the appropriate antibiotic. Colonies appeared after one day at 37°C.

2. Materials and methods

2.2.3 *Dictyostelium discoideum*

2.2.3.1 General growth conditions

Dictyostelium discoideum strain Ax3 was cultivated axenically in HL-5 medium (Table 2.11) at 23°C in a 75 cm² flask (Tissue culture Flask 75, TPP Technic Product Plastics AG) [80, 134]. In case *D. discoideum* harboured a plasmid encoding geneticin sulphate (G418) resistance, 20 µg ml⁻¹ G418 (Roth) was added to the medium.

Table 2.11. HL5-medium [135]*, **.

Component	Gram	Supplier
D(+)-glucose-monohydrate	11 g	Fluka
BBL™Yeast Extract	5 g	BD Biosciences
bacteriological peptone	5 g	BD Biosciences
Na ₂ HPO ₄	0.355 g	Fluka
KH ₂ PO ₄	0.34 g	Oxoid

*Distilled H₂O was added to reach a final volume of one liter.

**The pH of the solution was adjusted to 6.5 with 1 M KOH or 1 M HCl (Roth). The medium was autoclaved and stored at 4°C. Geneticin sulphate was added to the medium (20 µg ml⁻¹) if necessary.

2.2.3.2 Storage of *D. discoideum*

The axenically grown amoebae were cultivated in a 75 cm² flask (section 2.2.3.1). The cells of one confluent flask were centrifuged (500 x g, 10 minutes, room temperature (RT)) and resuspended in 9 ml freezing medium (Table 2.12). 1 ml of the cell suspension was aliquoted into a cryovial. A freezing box (Nalgene™ Cryo 1°C Freezing Container, Nalgene) was filled with isopropanol and precooled at 4°C. The cryovials were transferred into the freezing box and frozen at -80°C over night. The cells were stored permanently in liquid nitrogen.

2. Materials and methods

Table 2.12. Freezing medium.

Component	Percentage [%]	Supplier
HL-5	80%	self made (2.2.3.1)
FCS	10%	Gibco
DMSO	10%	Merck

2.2.3.3 Thawing of *D. discoideum*

One frozen cryovial was thawed on ice (section 2.2.3.2). The cell solution was washed once (500 x g, 5 minutes, RT) with 10 ml HL-5 medium to remove the DMSO. The cells were resuspended in 10 ml HL-5 medium and transferred to a 75 cm² flask.

2.2.4 *Acanthamoeba castellanii*

2.2.4.1 General growth conditions

A. castellanii were cultivated in PYG medium (Table 2.13) at 23°C in a 75 cm² flask.

Table 2.13. PYG medium*, **.

Component	Concentration (stock, in dH₂O)	Gram or ml	Supplier
bacteriological peptone	---	20 g	BD Biosciences
Bacto Yeast extract	---	1 g	BD Biosciences
MgSO ₄ x 7H ₂ O	0.4 M	10 ml	Merck
CaCl ₂	0.05 M	8 ml	Merck
sodium-citrate x 2H ₂ O	1 M	3.4 ml	Roth
Fe(NH ₄) ₂ (SO ₄) ₂ x 6H ₂ O	---	20 mg	Fluka
Na ₂ HPO ₄ x 7H ₂ O	0.25 M	10 ml	Fluka
KH ₂ PO ₄	0.25 M	10 ml	Oxoid

*Distilled H₂O was added to reach a final volume of one liter.

2. Materials and methods

**The pH of the solution was adjusted to 6.5 with HCl. 50 ml of a 2 M glucose dissolved in dH₂O was added to the medium. The medium was filter sterilized twice with a pore size of 0.45 µm and once with a pore size of 0.2 µm.

2.2.4.2 Storage of *A. castellanii*

A. castellanii were grown in a 75 cm² flask (section 2.2.4.1). The cells of one confluent flask were centrifuged (500 x g, 10 minutes, RT) and resuspended in 9 ml freezing medium (Table 2.14). 1 ml of the cell solution was transferred to a cryovial and stored in a freezing box overnight at -80°C. The cryovials were transferred into a liquid nitrogen tank 24 hours later.

Table 2.14. Freezing medium.

Component	Percentage [%]	Supplier
PYG	80%	self made (2.2.4.1)
FCS	10%	Gibco
DMSO	10%	Merck

2.2.4.3 Thawing of *A. castellanii*

One frozen cryovial (section 2.2.4.2) was thawed on ice. The cells were resuspended in 10 ml PYG medium to remove the DMSO from the medium. The cells were transferred with PYG medium in a 75 cm² flask and cultivated at 23°C.

2.2.5 RAW 264.7 macrophages

2.2.5.1 General growth conditions

RAW 264.7 macrophages were cultivated in RPMI 1640 medium (Gibco). 10% fetal calf serum (FCS; Gibco) and 2 mM L-glutamine (Gibco) were added to the medium. The cells were cultivated at 37°C with 5% CO₂. 1% of a penicillin/streptomycin mixture (Omnilab) was added to the medium if needed.

2. Materials and methods

2.2.5.2 Storage of RAW 264.7 macrophages

RAW 264.7 macrophages were grown in RPMI 1640 medium supplemented with L-glutamine and FCS (section 2.2.5.1). The cells of one confluent 75 cm² flask were harvested using a cell scraper. The cells were sedimented (500 x g, 10 minutes, RT) and resuspended in 3 to 4 ml of a freezing medium (Table 2.15). 1 ml of the cell suspension was transferred to a cryovial, frozen over night in a freezing box at -80°C and stored permanently in a liquid nitrogen tank.

Table 2.15. Freezing medium.

Component	Percentage [%]	Supplier
RPMI 1640	45%	Gibco
FCS	45%	Gibco
DMSO	10%	Merck

2.2.5.3 Thawing of RAW 264.7 macrophages

Frozen RAW 264.7 macrophages were thawed on ice (section 2.1.5.2). The DMSO was removed by washing the cells once with 10 ml RPMI 1640 medium supplemented with L-glutamine and FCS (500 x g, 10 minutes, RT). The cells were transferred to a 75 cm² flask and cultivated at 37°C with 5% CO₂.

2.2.6 Cell counting

10 µl of a cell suspension were applied to a “Neubauer counting chamber” (Glaswarenfabrik Karl Hecht). The cells were counted under the microscope. The total amount (N) of cells per ml solution was calculated with the formula:

$$N_{\text{counted cells/quadrant}} \times 10^4 = N_{\text{cells}} \text{ ml}^{-1}.$$

2. Materials and methods

2.2.7 Cloning

The vectors for cloning were bought from Novagen, Amersham or were available in the lab (section 2.1.3). The polymerase, restrictions enzymes, ligase and DNA Ladder were bought from BioLabs, Fermentas and Thermo Scientific.

1% agarose gels were poured with dissolved agarose (Biozym LE Agarose, Biozym) in 1x TAE agarose running buffer (Table 2.16). Ethidium bromide (Sigma) was added. A DNA standard was used (1 kb DNA Ladder, BioLabs). Plasmid purification and agarose gel purification was done using kits from Macherey-Nagel (NucleoSpin® Plasmid, NucleoSpin® Gel and PCR Clean-up). The plasmids were sequenced by GATC Biotech (Konstanz, Germany).

The gene sequence of *sidC_{Llo}* was amplified by PCR from the genome of *L. longbeachae* with the oligonucleotides oSD07 and oSD08 and cut with *NdeI* and *NheI*. The gene was cloned in a pET28(a)+ vector (Novagen) cut with the same enzymes to create a N-terminal *His₆*-fusion. The gene was under the control of a T₇ promotor. The plasmid was called pSD01. This plasmid was used to insert silent mutations in order to remove the restrictions sites *BamHI* and *SalI* from the gene *sidC_{Llo}* (QuickChange®Lightning Site-Directed Mutagenesis Kit, Agilent Technologies) (pSD02) (sections 2.1.3 and 2.1.4).

The gene *sidC_{Llo_609-782}* was amplified by a PCR using pSD02 as a template and oSD18 and oSD19 as the oligonucleotides (sections 2.1.3 and 2.1.4). The gene was cut with *BamHI* and *SalI* and ligated into a pGEX4T-1 (Amersham) vector cut with the same enzymes (pSD03) (section 2.1.3) to create a N-terminal GST-fusion. A P_{tac} promotor controlled the expression of the gene.

The plasmids pSD04 (*GST-sidC_{Llo_1-340}*, oligonucleotides oSD17 and oSD52), pSD05 (*GST-sidC_{Llo_341-608}*, oligonucleotides oSD24 and oSD25), pSD06 (*GST-sidC_{Llo_783-969}*, oligonucleotides oSD26 and oSD27) and pSD07 (*GST-sidC_{Llo}*, oligonucleotides oSD27 and oSD52) were cloned by using the same protocol (sections 2.1.3 and 2.1.4).

The gene *sidC_{Llo}* was cut with *BamHI* and *SalI* from the plasmid pSD07 and ligated into a pMMB207-C-M45 vector [80] cut with the same enzymes (pSD13). The same procedure was used to ligate *sidC_{Llo}* into a pCR77 vector [91] (pSD14) (section 2.1.3).

2. Materials and methods

Table 2.16. 50x TAE buffer*.

Component	Gram	Supplier
TRIS	242 g	MP Biomedical
acetic acid [100%]	57.1 ml	Roth
ethylendiamintetraacetate (EDTA)	100 ml	Roth

*Dissolved dH₂O was used to fill up the buffer to one liter.

2.2.8 Protein analysis

2.2.8.1 Protein separation by sodium dodecyl sulphate polyacrylamide gel electrophoresis (SDS-PAGE)

5x sodium dodecyl sulphate (SDS) sample buffer (Table 2.17) was added to the protein sample. The mixture was boiled for 5 minutes at 95°C. A 10% SDS-polyacrylamide gel (Table 2.18) was poured and fixed in an electrophoresis chamber (Mini-Protean ® 3, Bio-Rad). The chamber was filled with 1x running buffer (Table 2.19). A protein marker (Page Ruler™ Prestained Protein Ladder, Thermo Scientific) were used.

Table 2.17. 5x SDS sample buffer*.

Component	Concentration	Supplier
TRIS (pH 6.8)	0.2 M	MP Biomedical
SDS	4.3 g	Biomol
bromphenolblue	1 µg	Sigma
glycerol	15 ml	Roth
dH ₂ O	45 ml	---
β-mercaptoethanol	8.5 ml	AppliChem

*The SDS sample buffer was frozen in aliquots at -20°C.

2. Materials and methods

Table 2.18. SDS gel.

Component	Concentration for the stacking gel	Concentration for the running gel [10%]	Supplier
acrylamide/bis-solution [40%]	2.5 ml	1.25 ml	Serva
dH ₂ O	5 ml	6.15 ml	---
0.5 M TRIS (pH 6.8)	---	2.5 ml	MP Biomedical
1.5 M TRIS (pH 8.8)	2.5 ml	---	MP Biomedical
20% SDS	50 µl	50 µl	Biomol
10% ammonium persulphate (APS)	30 µl	30 µl	Biomol
N, N, N', N' tetramethylethylenediamin (TEMED)	15 µl	15 µl	Biomol

Table 2.19. 10x running buffer*.

Component	Gram	Supplier
TRIS	30.25 g	MP Biomedical
glycine	144.5 g	MP Biomedical
SDS	10 g	Biomol

*The solution was filled up to one liter with dH₂O.

2.2.8.2 Coomassie staining of a SDS gel

SDS-polyacrylamide gels were stained with a Coomassie staining solution (Table 2.20) to visualize proteins.

2. Materials and methods

Table 2.20. Coomassie staining and destaining solutions*.

Component	Concentration for the Coomassie staining solution	Concentration for the Coomassie destaining solution	Supplier
Coomassie® Brilliant Blue R250	0.25%	---	Fluka
ethanol	40%	40%	Roth
acetic acid	10%	10%	Roth

*Distilled H₂O was used to set the volume of the buffer to one liter.

2.2.8.3 Silver staining of a SDS gel

The SDS-polyacrylamide gel (section 2.2.8.1) was incubated in a fixation solution (one hour till overnight). The SDS gel was washed three times with 50% ethanol for 20 minutes at RT. Between the washing steps the SDS gel was bathed in dH₂O for two to three minutes at RT. The SDS gel was pre-treated with 0.13g l⁻¹ sodium thiosulfate (Merck) (in dH₂O) for one minute at RT and washed three times with dH₂O over 20 seconds at RT. The SDS gel was incubated over 20 to 30 minutes at RT in fresh made impregnating solution (Table 2.21). The gel was washed three times over 20 seconds (RT) in dH₂O. The SDS gel was incubated in a developing solution (RT) (Table 2.22) until brown bands appeared. The SDS gel was washed with 50% methanol (Roth) followed by 50% ethanol for one to two minutes at RT. The gel was dried afterwards.

Table 2.21. Impregnating solution*.

Component	Concentration	Supplier
AgNO ₃	0.1 g	Merck
37% formaldehyde	37.5 µl	Merck

*The buffer was adjusted with distilled H₂O to 50 ml.

2. Materials and methods

Table 2.22. Developing solution*.

Component	Concentration	Supplier
Na ₂ CO ₃	30 g	Merck
sodium thiosulfate	1.25 mg	Merck
37% formaldehyde	0.25 ml	Merck

*Distilled H₂O was used to set the volume of the buffer to 500 ml.

2.2.8.4 Western blot analysis

The SDS gel (section 2.2.8.1) was laid on a nitrocellulose membrane (A. Hartenstein), covered with chromatography paper (A. Hartenstein) from both sides and laid in a protein transfer device (MAXI-Semi-Dry-Blotter, Roth). The protein transfer device was connected to a power supply (PAC100, Bio-Rad) (200 mA, 2 hours). A transfer blotting buffer (Table 2.23) was used to keep the membrane wet.

Table 2.23. 10x transfer blotting buffer.

Component	Concentration (in dH ₂ O)	Supplier
TRIS	250 mM	MP Biomedical
glycine	1.92 M	MP Biomedical
methanol	20%	Roth

2.2.8.5 Immune detection

The nitrocellulose membrane (section 2.2.8.1) was washed with PBS (phosphate buffered saline) (Table 2.24) or TBS (TRIS buffered saline) (Table 2.25) and incubated for one hour at RT with milk-buffer (4% milk powder in PBS or TBS). The primary antibody (Table 2.26) was diluted in the milk-buffer. The nitrocellulose membrane was incubated with this solution over night at 4°C. The membrane was washed with PBS/0.1% Tween ® 20 (Roth) or TBS/1% Tween ® 20 three times for 10 minutes at RT. A horseradish peroxidase conjugated secondary antibody (Table 2.27) was diluted in the milk-buffer and the nitrocellulose membrane was incubated with this solution for one hour at RT. The

2. Materials and methods

nitrocellulose membrane was washed three times for 10 minutes at RT with PBS/0.1% Tween ® 20 or TBS/1% Tween ® 20 and twice with PBS or TBS for five minutes at RT. Signals from the secondary antibody were detected with the Amersham™ ECL™ Western Blotting Analysis System (GE Healthcare Life Sciences). The developing bands were analyzed with a gel imaging system (ChemiDoc MP System, Bio-Rad).

Table 2.24. 10x phosphate buffered saline (PBS)*.

Component	Gram	Supplier
NaCl	80 g	Roth
KCl	2 g	Merck
Na ₂ HPO ₄	14.2 g	Fluka
KH ₂ PO ₄	2.4 g	Oxoid

*Distilled H₂O were used to reach a final volume of one liter.

Table 2.25. 10x TRIS buffered saline (TBS).

Component	Concentration	Supplier
TRIS-HCl (pH 7.4 - 7.6)	500 mM	MP Biomedical
NaCl	1.5 M	Roth

Table 2.26. Primary antibodies.

Primary antibody	Origin	Dilution	Supplier
anti-GST	mouse	1:1.000	Sigma
anti-M45	mouse	1:1.000	Genovac AG
anti-SidC _{Llo}	rabbit	1:2.000	affinity purified [3]
anti-SidC _{Lpn}	rabbit	1:2.000	affinity purified [80]

Table 2.27. Secondary antibodies.

Secondary antibody	Origin	Label	Dilution	Supplier
anti-mouse IgG	goat	HRPO	1:5.000	Sigma
anti-rabbit IgG	goat	HRPO	1:5.000	GE Healthcare

2.2.9 Protein purification

2.2.9.1 Protein production from *E. coli*

A plasmid was transformed into BL21 (DE3) *E. coli* (sections 2.1.1, 2.2.2.3 and 2.2.2.4). LB broth medium harbouring the necessary antibiotic was inoculated with an *E. coli* colony and cultivated over night at 37°C on a shaker. 1 L LB broth medium was inoculated with the preparatory culture (OD₆₀₀ of 0.05). The culture was grown to an OD₆₀₀ of 0.5 to 0.8, 1 mM IPTG was added to the medium and the culture was cultivated at 30°C or 37°C for two to three hours. The cells were harvested (8.000 x g, 15 minutes, 4°C) and washed once with PBS or TBS (3.350 x g, 15 minutes, 4°C). The bacterial pellet was frozen in liquid nitrogen and stored at -80°C.

2.2.9.2 Protein purification of His₆-conjugated proteins

The bacterial pellet of BL21 (DE3) *E. coli* transformed with pSD01 (sections 2.1.1, 2.1.3 and 2.2.9.1) was thawed on ice. 10 ml lysis buffer (Table 2.28) was used to resuspend the bacterial pellet. 1 mg ml⁻¹ lysozyme was added to the solution and incubated for 30 minutes. The bacteria were destroyed by passing through a French Press three times with 1000 pound-force per square inch (psi). The suspension was centrifuged (3.350 x g, 10 minutes, 4°C). 1 ml 50% Ni-NTA-agarose beads (Quiagen) were washed with 10 ml washing buffer (Table 2.29) (600 x g, 5 minutes, 4°C). The beads were incubated for one hour at 4°C on a rotating wheel with 5 ml of the bacterial supernatant. The beads were washed three times with 10 ml washing buffer (600 x g, 5 minutes, 4°C). 0.5 ml of an elution buffer (Table 2.30) was incubated for 30 minutes with the beads on a rotating wheel at 4°C. The beads were centrifuged (600 x g, 5 minutes, 4°C), the supernatant was collected and dialyzed with dialysis buffer (Table 2.31). The protein concentration was measured with a spectrophotometer. The samples were frozen in liquid nitrogen and stored

2. Materials and methods

at -80°C. Samples of the lysate, washing steps and eluate were boiled with SDS sample buffer, separated on a SDS gel and stained with Coomassie Brilliant Blue ® 250 (section 2.2.8.2).

Table 2.28. Lysis buffer*.

Component	Concentration	Supplier
NaH ₂ PO ₄	50 mM	Merck
NaCl	300 mM	Roth
imidazole	10 mM	Biomol

*The pH was adjusted with NaOH (Merck) to 8.0.

Table 2.29. Washing puffer*.

Component	Concentration	Supplier
NaH ₂ PO ₄	50 mM	Merck
NaCl	300 mM	Roth
imidazole	20 mM	Biomol

*The pH was adjusted with NaOH to 8.0.

Table 2.30. Elution buffer*.

Component	Concentration	Supplier
NaH ₂ PO ₄	50 mM	Merck
NaCl	300 mM	Roth
imidazole	250 mM	Biomol

*The pH was adjusted with NaOH to 8.0.

Table 2.31. Dialysis buffer.

Component	Concentration	Supplier
HEPES (pH 7.5)	20 mM	Gibco
NaCl	500 mM	Roth
TRIS(2-carboxyethyl) phosphine (TCEP)	1 mM	Roth

2.2.9.3 Protein purification of GST-tagged proteins

Plasmids expressing GST-SidC_{Llo} (pSD07), GST-SidC_{Llo_1-340} (pSD04), GST-SidC_{Llo_341-608} (pSD05), GST-SidC_{Llo_609-782} (pSD03), GST-SidC_{Llo_783-969} (pSD06), GST-SidC_{Lpn} (pCR02), GST-SidC_{Lpn_P4C} (pHP056), GST-PH_{FAPP1} (pGEX-PH_FAPP1), GST-SidC_{Llo_1-608-Lpn_609-917}, GST-SidC_{Lpn_1-608-Llo_609-969} or GST (pGEX4T-1) (section 2.1.3) were transformed in *E. coli* BL21 (DE3) (section 2.1.1) and protein production was done as described (section 2.2.9.1).

The pellets were thawed on ice, resuspended in 10 ml TBS and incubated with 1 mg ml⁻¹ lysozyme for 30 minutes at 4°C. The bacteria were destroyed using a French Press three times with 1000 psi. The suspension was spun down (3.350 x g, 10 minutes, 4°C). The Glutathione SepharoseTM 4B beads (GE Healthcare) were washed three times with 1 ml TBS to remove the ethanol in the sample (600 x g, 5 minutes, 4°C). 1 ml of the beads were mixed with the bacterial supernatant and incubated on a rotating wheel at 4°C for two hours. The beads were washed three times with TBS. 1 ml elution buffer (Table 2.32) was added to the beads and incubated for 30 minutes on a rotating wheel at 4°C. The beads were spun down (600 x g, 5 minutes, 4°C) and the supernatant was collected. The protein amount was measured with a spectrophotometer. The samples were frozen in liquid nitrogen and stored at -80°C. The purity of the samples were analysed on a Coomassie stained SDS gel (section 2.2.8.2).

2. Materials and methods

Table 2.32. Elution buffer*.

Component	Concentration	Supplier
TRIS (pH 8.0)	700 μ l	MP Biomedical
glutathione	15 mM	Fluka

*The final volume was adjusted with dH₂O to 10 ml.

2.2.10 Production of a SidC_{L10} antibody

His₆-SidC_{L10} was produced (section 2.2.9.2) and lyophilized (Alpha1-4, Christ®). 6 mg protein was sent to the company SeqLab (Goettingen, Germany) and was used to produce an antibody against SidC_{L10} in two rabbits. The final bleeding of the two rabbits was pooled and affinity purified. The antibody was tested in a Western blot and an immunofluorescence assay.

2.2.11 Phosphoinositide-pulldown

Legionella was grown in AYE medium (section 2.2.1.1). A 10 ml overnight culture was inoculated with an OD₆₀₀ of 0.1, grown overnight and used to inoculate a 200 ml overnight culture. The culture was grown overnight and harvested (8.000 x g, 10 minutes, 4°C). The following steps were performed on ice. The bacteria were washed in 10 ml ice cold washing buffer (3.350 x g, 5 minutes, 4°C) and 1 mM phenylmethylsulfonyl fluorid (PMSF) (Sigma) was added. The bacteria were lysed with a French Press three times with 1000 psi. The cell solution was centrifuged with low speed (3.350 x g, 10 minutes, 4°C) and high speed (86.000 x g, 1 hour, 4°C). 1 ml of the supernatant was mixed with 50 μ l of PI-coated agarose beads (PIP-BeadTM Sample Pack, Echelon Biosciences Inc., USA) (10 pM PtdIns μ l⁻¹ slurry) and incubated overnight at 4°C on a rotating wheel in the dark. The beads were washed five times (600 x g, 5 minutes, 4°C) with washing buffer (Table 2.33). The bound proteins were eluted with 20 μ l SDS sample buffer [81]. The protein samples were separated by their size over an SDS gel and stained with Coomassie solution (section 2.2.8.2). After destaining the SDS gel with a Coomassie destaining solution the dominant bands were cut out and send to MALDI-TOF analysis (matrix-assisted laser

2. Materials and methods

desorption/ionization-time of flight). In parallel a SDS gel was stained with silver (section 2.2.8.3).

Table 2.33. Washing solution.

Component	Concentration	Supplier
HEPES (pH 7.4)	10 mM	Gibco
NaCl	150 mM	Roth

2.2.12 Protein lipid overlay assay with PIP-strips and PIP-arrays

“PIP-strips” and “PIP-arrays” (Echelon Biosciences Inc., USA) are nitrocellulose membranes on which different PtdIns, PIs and other lipids are bound at 100 pmol/spot (“PIP-strips”) or at a two-fold serial dilution (1.56–100 pmol/spot) (“PIP-arrays”). A GST-tagged protein was diluted in milk-buffer (120 pmol ml⁻¹ milk-buffer) (4% milk powder (Roth) and 0.1% Tween ® 20 in TBS) and added to the nitrocellulose membrane. The sample was incubated overnight at 4°C on a shaker. The nitrocellulose membrane was washed three times for 30 minutes with milk-buffer and incubated afterwards with the primary monoclonal anti-GST antibody (Sigma) (section 2.2.8.5) diluted in the same buffer. As a secondary antibody a goat anti-mouse peroxidase-labelled antibody (GE Healthcare) was used (section 2.2.8.5). The Western blot analysis was done as described previously (section 2.2.8.4) [80, 81, 103, 136]. Only the washing time was increased from three times 10 minutes to three times 30 minutes to reduce the background signal of the antibody. An ECL detection kit was used to visualize the binding of the GST-tagged proteins to the samples (section 2.2.8.5).

2.2.13 Infection of phagocytes

Amoebae or macrophages were seeded in the adequate medium 24 hours before the infection took place (section 2.2.3, 2.2.4 and 2.2.5). The medium was exchanged prior to the infection in the case the medium contained an antibiotic. The cells were infected with a bacterial overnight culture with a specific multiplicity of infection (MOI) (section 2.2.1.1). To this end, the bacteria were added to the cells and spun down on the cells (3.350 x g,

2. Materials and methods

10 minutes, RT). The cells were incubated at 25°C for *D. discoideum*, 30°C for *A. castellanii* and 37°C with 5% CO₂ for RAW 264.7 macrophages.

2.2.14 Immunofluorescence

Cells were seeded (sections 2.2.3, 2.2.4 and 2.2.5) on coverslips (Menzelglaser) coated with poly-L-lysine (Sigma) and infected with an overnight culture (section 2.2.1.1). All steps were performed at RT except the fixation step. The cells were washed twice with SorC (Sørensen phosphate buffer) (Table 2.34) (*D. dictyostelium*) or PBS (RAW 264.7 macrophages). The cells were fixed with 250 µl 4% paraformaldehyde (PFA) (Sigma) for 15 minutes (*D. discoideum*) or 250 µl methanol for five minutes at -20°C (RAW 264.7 macrophages). The cells were permeabilized with 0.1% Triton X-100 (Merck) in PBS or SorC for 10 minutes. The cells were washed twice with 1% bovine serum albumin (BSA) (Albumin fraction V, Roth) in SorC or PBS. The cells were blocked over 30 minutes with 1% BSA in SorC or PBS and incubated with the primary antibody (Table 2.35) diluted in 50 µl of the same buffer for one hour. The chamber was kept wet with a nitrocellulose membrane bathed in water. The cells were washed three times with 1% BSA in SorC or PBS and blocked with the same buffer for 10 minutes. The secondary antibody (Table 2.36) was diluted in 1% BSA in SorC or PBS and the cells were incubated with the solution for 45 minutes. The cells were washed three times with 1% BSA in SorC or PBS and three times with SorC or PBS alone. The cover slips were mounted upside down on object slides (A. Hartenstein) with 3 µl “Vectashield mounting medium for fluorescence” (Vector Laboratories, Inc.). The cover slips were fixed using nail polish. The object slides were dried and stored at 4°C in the dark. Images were produced using a Leica SP5 TCS confocal laser fluorescence microscope.

Table 2.34. Sørensen phosphate buffer (SorC) [137]*, **.

Component	Concentration	Supplier
Na ₂ HPO ₄	2 mM	Fluka
KH ₂ PO ₄	15 mM	Oxoid
CaCl ₂ x 2H ₂ O	50 µM	Merck

*The final volume was set to one liter with dH₂O.

2. Materials and methods

**The pH was adjusted with 1M KOH or 1M HCl to 6.0. The solution was autoclaved and stored at room temperature.

Table 2.35. Primary antibodies.

Primary antibody	Origin	Dilution	Supplier
anti-GST	mouse	1:100	Sigma
anti-SidC _{Llo}	rabbit	1:100	affinity purified [3]
anti-SidC _{Lpn}	rabbit	1:100	affinity purified [80]

Table 2.36. Secondary antibodies.

Secondary antibody	Origin	Label	Dilution	Supplier
anti-mouse IgG	goat	Cy5	1:200	Jackson
anti-rabbit IgG	goat	Cy5	1:200	Invitrogen

2.2.15 Detection of PtdIns(4)*P* on the LCV

Calnexin-GFP producing *D. discoideum* Ax3 were infected with the indicated MOI for 1 hour with red fluorescent *L. pneumophila* (section 2.1.3) at 25°C. The cells were washed with SorC and homogenized with a ball homogenizer [80, 103]. The samples were spun down (500 x g, 10 minutes, RT) and fixed with 4% PFA on cover slips coated with poly-L-lysine. The samples were incubated with purified GST-SidC_{Llo}_{P4C} (pSD03), GST-SidC_{Lpn}_{P4C} (pHP056), GST-PH_{FAPP1} (pGEX-PH_FAPP1) or GST (pGEX4T-1) (sections 2.1.3 and 2.2.9.3) for 15 minutes at RT. An immunofluorescence staining was performed with an anti-GST antibody (Sigma) (section 2.2.14). As a secondary antibody a Cy5-coupled anti-mouse antibody (Jackson) was used (section 2.2.14). Pictures were acquired using a Leica SP5 TCS confocal laser fluorescence microscope.

2. Materials and methods

2.2.16 Intracellular replication assay

2.2.16.1 *D. discoideum*

The cells were seeded in a 96well plate in SorC with 10^5 cells per well (section 2.2.3). The *Legionella* culture was diluted in MB-medium (Table 2.37) and the cells were infected with a MOI of 0.01 (section 2.2.13). The bacteria were spun down (3.350 x g, 10 minutes, RT) and incubated for 10 minutes at 25°C. Input-controls were plated out in triplicates on CYE plates. 10 minutes, two days, four days and six days post infection the supernatants of the cells were collected, diluted in dH₂O and plated on CYE plates in triplicate. Colonies were counted after three days of incubation at 37°C.

Table 2.37. MB medium [138]*, **.

Component	Gram	Supplier
Bacto yeast extract	7 g	BD Biosciences
bacteriological peptone	14 g	BD Biosciences
MES sodium salt	4.26 g	Sigma

*The final volume of one liter was reached through adding dH₂O.

**The pH was adjusted with 1 M KOH or 1 M HCl to 6.9. The solution was autoclaved and stored at 4°C.

2.2.16.2 *A. castellanii*

A. castellanii were seeded in 96well plates (5×10^4 per well) in PYG medium (section 2.2.4.1) and incubated for one hour at 23°C. The medium was exchanged against Ac buffer (Table 2.38). The *Legionella* overnight culture was diluted in Ac buffer. The cells were infected with an MOI of 0.1. The bacteria were spun down (3.350 x g, 10 minutes, RT) and incubated for 20 minutes at 30°C. Input controls were plated out on CYE plates in triplicate. For the time point zero (20 minutes post infection), one day, two days and three days the supernatants of the cells were collected, diluted in Ac buffer and plated on CYE plates in triplicate. Colonies were counted after three days incubation at 37°C.

2. Materials and methods

Table 2.38. Ac buffer*.

Component	Concentration	Supplier
MgSO ₄ x 7H ₂ O [0.4 M]	1 ml	Merck
CaCl ₂ [0.05 M]	0.8 ml	Merck
sodium citrate x 2H ₂ O [1 M]	0.34 ml	Roth
Fe(NH ₄) ₂ (SO ₄) ₂ x 6H ₂ O	2 mg	Fluka
Na ₂ HPO ₄ x 7H ₂ O [0.25 M]	1 ml	Fluka
KH ₂ PO ₄ [0.25 M]	1 ml	Oxoid
dH ₂ O	95 ml	---

*The pH was adjusted to 6.5 with HCl (Roth). The buffer was autoclaved and stored at 4°C.

2.2.16.3 RAW 264.7 macrophages

RAW 264.7 macrophages (2×10^4 per well) were seeded in RPMI 1640 medium supplemented with 10% FCS and L-glutamine in a 96well plate one day prior to the infection (section 2.2.5.1). The *Legionella* overnight cultures were diluted in RPMI 1640 medium. The cells were infected (MOI of 0.1) and the bacteria were spun down (3.350 x g, 10 minutes, RT) on the cells (section 2.2.13). The cells were incubated at 37°C with 5% CO₂. Input-controls were plated out in triplicate on CYE plates. At time point zero (10 minutes post infection), one day, two days and three days the supernatants of the cells were collected, diluted in dH₂O and plated out in triplicate on CYE plates. Colonies were counted after three days of incubation at 37°C.

2.2.17 Amoebae competition assay

The assay was performed as described before [139]. Briefly, *A. castellanii* were seeded in a 96well plate one hour prior to the experiment and incubated at 30°C. For each bacterium three wells were seeded for each time point. The medium was exchanged against Ac buffer. *Legionella* overnight cultures were diluted in Ac buffer and used to infect the cells (MOI of 0.05) (section 2.2.13). The cells were incubated at 30°C for one hour. The Ac

2. Materials and methods

buffer was exchanged. Input controls were plated out on CYE plates with and without antibiotics in duplicate. Three days after infection the supernatant of the infected cells was collected. The cells were lysed with 0.8% saponin (Sigma) for 10 minutes. The supernatant and the homogenate were mixed. The solution was diluted 1:1.000 in Ac buffer and 50 μ l were used to infect freshly seeded amoebae. The remaining solution was diluted in Ac buffer and plated out in duplicates with and without antibiotics. The colony forming units (cfu) were counted after an incubation time of three days at 37°C.

2.2.18 Translocation assay

2.5×10^5 RAW 264.7 macrophages were seeded in 24well plates one day prior to the experiment (section 2.2.5.1). The cells were infected with a bacterial overnight culture with a MOI of 50 in RPMI 1640 medium supplemented with L-glutamine and FCS (section 2.2.13). The cells were incubated for one hour at 37°C with 5% CO₂. The medium was discarded and the cells were lysed with 110 μ l dH₂O or with the lysis buffer offered by the company (Amersham cAMP Biotrak Enzymeimmunoassay (EIA) System, GE Healthcare Life Sciences). The assay was performed as described in the manual of the detection kit. The final reaction was measured in a plate reader at 450 nm.

2.2.19 LCV purification

The LCV purification from phagocytes has been done as published previously [2, 54, 140, 141]. Briefly, calnexin-GFP producing *D. discoideum* or RAW 264.7 macrophages were grown to approximately 80% confluence in a 75 cm² flask (sections 2.2.3.1 and 2.2.5.1). The cells were infected with an overnight culture of a Dsred expressing bacteria (section 2.2.13). The cells were incubated at 25°C for *D. discoideum* or 37°C with 5% CO₂ for RAW 264.7 macrophages for one hour. For each purification three flasks were needed. The cells were washed three times with SorC for *D. discoideum* or PBS for RAW 264.7 macrophages and were resuspended in 3 ml HB-buffer (Table 2.39) using a cell scraper. The washing step for *D. discoideum* was omitted in later experiments. The cells were homogenized with a ball homogenizer using an exclusion size of 8 μ m. 2% FCS were used to block the cell homogenate for 30 minutes at 4°C on a rocking platform. The cell suspension was incubated with an anti-SidC_{Lpn} or anti-SidC_{Llo} antibody (dilution 1:3.000)

2. Materials and methods

for one hour at 4°C on a rocking platform (“homogenate” sample). The suspension was centrifuged (2.700 x g, 15 minutes, 4°C) and the pellet was resuspended in HB-buffer (“pellet” sample). MACS anti-rabbit antibodies were added to the suspension and incubated with the suspension for 30 minutes at 4°C. A MACS-MS separation column (Miltenyi Biotec) was put on a magnetic separator MACS Multistand (Miltenyi Biotec) and the column was equilibrated with HB-buffer. The sample was applied to the MACS columns (“flow through” sample) and the column was washed three times with HB-buffer. The MACS columns were removed from the magnetic separator MACS Multistand and the probe were eluted with HB-buffer by squirting (“eluate” sample). A density gradient was produced with 5.5 ml of 35% Histodenz (Sigma) (in PBS) coated with 5.5 ml of 10% Histodenz (in PBS) in a 15 ml tube. The tube was carefully laid down for one hour to allow an establishing of the gradient. The sample from the column was added slowly to the gradient. The gradient was centrifuged (3.350 x g, 1 hour, 4°C). Eight 1.5 ml fractions were taken with a long Pasteur pipette beginning from the bottom (“fraction 1”). The fractions were pipetted on a cover slide coated with poly-L-lysine and were centrifuged (3.350 x g, 10 minutes, 4°C). The samples were fixed and analyzed by immunofluorescence labeling with an anti-SidC_{L10} or anti-SidC_{Lpn} primary antibody (section 2.2.14).

Table 2.39. HB buffer*.

Component	Concentration	Supplier
HEPES	20 mM	Gibco
sucrose	250 mM	Sigma
ethylenglycol-bis(aminoethylether)-N, N, N', N'-tetra acetic acid (EGTA)	0.5 mM	AppliChem

*The pH was set to 7.2 with 1 M NaOH or 1 M HCl. The buffer was sterile filtered and stored at 4°C.

2. Materials and methods

2.2.20 Cytotoxicity assay

D. discoideum Ax3 were seeded in a 24well plate (2×10^5 cells per well) one day prior to the infection (section 2.2.3.1). The cells were infected with a bacterial overnight culture and incubated for 1 hour at 25°C (section 2.2.13). The cells were detached with pipetting up and down with a blue tip of a pipette for 10 times. The cell suspension was centrifuged (500 x g, 3 minutes, RT) and the supernatant was discarded. The cells were resuspended in SorC and $2.5 \mu\text{g ml}^{-1}$ propidium iodide was added. The propidium iodide staining was measured with a FACS machine.

3. Results

3.1 The *L. longbeachae* Icm/Dot substrate SidC_{Llo}

The putative Icm/Dot substrate SidC_{Llo} was identified in the genome of *L. longbeachae* NSW150 as one of the 44% of Icm/Dot substrates which *L. longbeachae* shares with *L. pneumophila* [26]. This study aimed at investigating the role of SidC_{Llo} in the infection of *L. longbeachae*.

SidC_{Lpn} is an Icm/Dot-dependent effector protein and binds with a P4C domain to PtdIns(4)*P* and to a lower extent to PtdIns(3)*P* [80, 84, 101]. Other effector proteins like SidM compete with SidC_{Lpn} for binding to PtdIns(4)*P* [81]. SidC_{Lpn} has a paralog called SdcA_{Lpn} which shares a sequence identity with SidC_{Lpn} of 72% [50]. SidC_{Lpn} and SdcA_{Lpn} are necessary for the acquisition of ER-derived vesicles [103]. No gene for *sdcA* was found in the genome of *L. longbeachae* [26].

3.1.1 The *L. longbeachae* effector SidC_{Llo} is the major PtdIns(4)*P* binding protein

In a previous study *L. pneumophila* lysate was incubated with agarose beads coupled to different PIs. Only the Icm/Dot-dependent effector SidM but not SidC_{Lpn} was found to bind to PtdIns(4)*P* [81]. To identify a putative *L. longbeachae* protein which binds to PtdIns or a PI lipid, the phosphoinositide-pulldown assay (section 2.2.11) was adopted. In the phosphoinositide-pulldown five dominant protein bands appeared in a Coomassie stained gel (Figure 3.1C) and were cut out. The samples were analysed by MALDI TOF mass spectrometry (MS). As a control experiment *L. pneumophila* lysate was incubated with PtdIns- or PtdIns(4)*P*-coupled beads. A band at the size of SidM was detected (Figure 3.B and D).

MALDI TOF analysis revealed that SidC_{Llo} was the major PtdIns(4)*P* binding protein of *L. longbeachae* (Figure 3.1A and C, marked with * or 2). SidM was not found in the phosphoinositide-pulldown with *L. longbeachae* (Figure 3.1A and C), in agreement with the finding that SidM is missing in the genome of *L. longbeachae* [26]. Also two acyl CoA carboxylases were found which bind to the beads and PtdIns(3,4,5)*P*₃ (Figure 3.1C, marked with 1, 5). A heat shock protein 90 and an elongation factor Tu were pulled down with PtdIns(4,5)*P*₂ (Figure 3.1C, marked with 3 and 4). In the control experiment a protein

3. Results

of the size of SidM was pulled down with *L. pneumophila* lysate (Figure 3.1B and D, marked with * or 6).

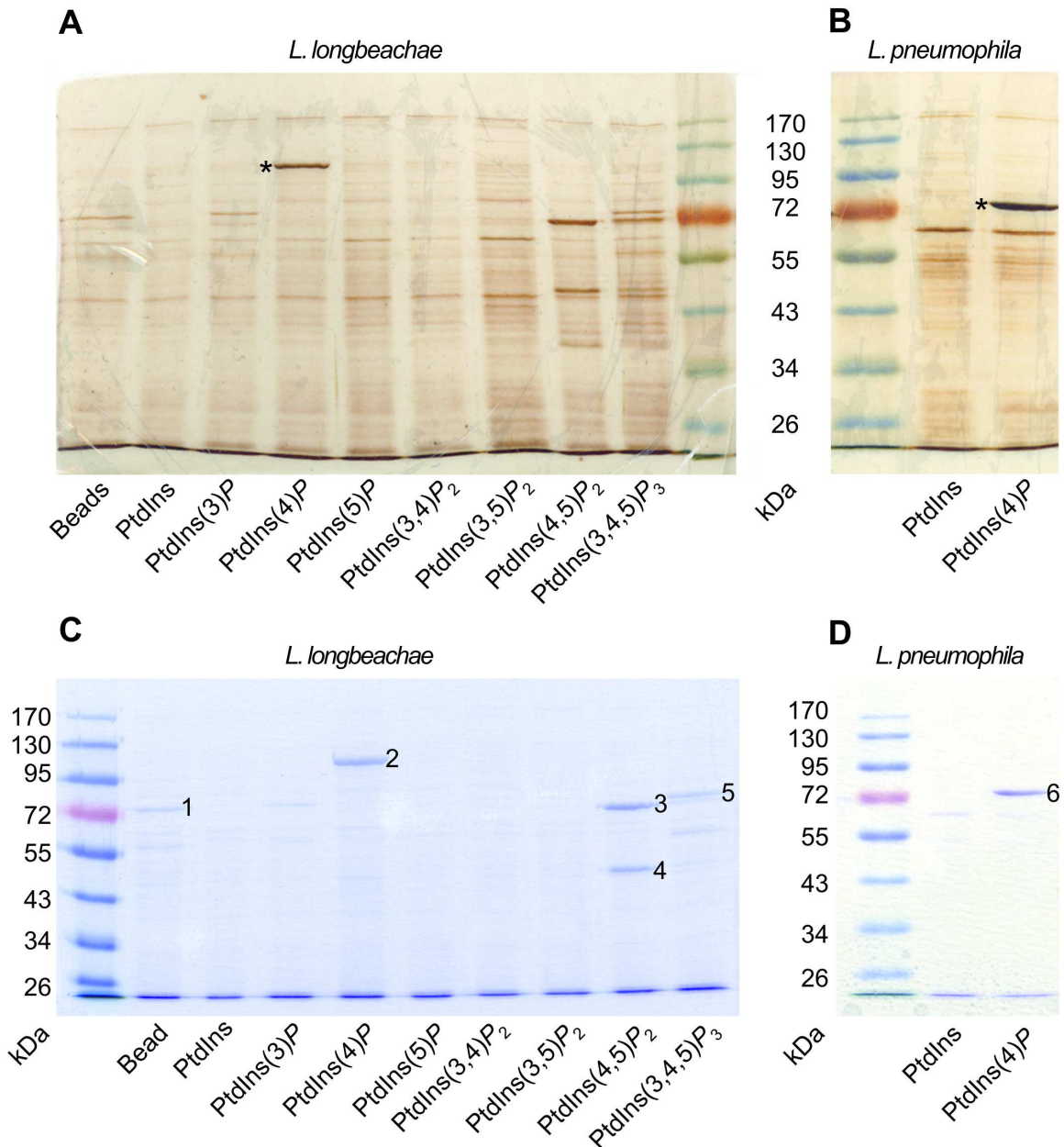


Figure 3.1. SidC_{L10} is the major PtdIns(4)P binding protein of *L. longbeachae*. Bacterial lysate from *L. longbeachae* (A, C) and *L. pneumophila* (B, D) wild-type strains were incubated with agarose beads coated with PtdIns or various PIs. The beads were washed and the proteins were separated by SDS-PAGE. The SDS gels were stained with silver (A, B) or Coomassie (C, D). In a mass spectrometry analysis the 111 kDa *L. longbeachae* SidC_{L10} was identified to bind to PtdIns(4)P (*, 2). Acyl CoA carboxylase (1, 5), heat shock protein 90 (3) and elongation factor Tu (4) were also identified. In the control experiment with *L. pneumophila* lysate a band in the size of 73 kDa appeared. This could be SidM (*, 6). The experiment has been done in triplicate [3].

3. Results

3.1.2 SidC_{Llo} is binding through a P4C domain to PtdIns(4)*P*

In the next step we analysed the binding domain of SidC_{Llo}. To this end, GST was coupled to the N-terminus of SidC_{Llo}, SidC_{Llo_1-340}, SidC_{Llo_341-608}, SidC_{Llo_609-782} and SidC_{Llo_783-969} (Figure 3.2A). The proteins were produced in *E. coli*, purified and incubated with commercially available “PIP-strips” as described previously [80, 81, 103, 136] (Figure 3.2B) (section 2.2.12). “PIP-strips” are nitrocellulose membranes on which PtdIns, PIs or other lipids are bound (100 pmol/spot). The full-length GST-SidC_{Llo} and the GST-SidC_{Llo_609-782} fragment bound to PtdIns(4)*P* (Figure 3.2B). Thus, the PtdIns(4)*P* binding domain of SidC_{Llo} was narrowed down to the amino acids 609 to 782. The previously found PtdIns(4)*P*-binding domain of SidC_{Lpn_P4C} is located in the amino acid region of 609 to 776 [103]. Therefore, we termed the PtdIns(4)*P*-binding domain of SidC_{Llo} SidC_{Llo_P4C}.

In the next step the binding affinity of SidC_{Llo}, SidC_{Llo_P4C}, SidC_{Lpn} and SidC_{Lpn_P4C} were compared in an assay using “PIP-arrays” in which PtdIns or PIs are spotted in two-fold serial dilution on a nitrocellulose membrane. SidC_{Llo} as well as SidC_{Llo_P4C} bound strongly to PtdIns(4)*P* and weakly to PtdIns(3)*P*. The binding affinity of SidC_{Llo_P4C} to PtdIns(4)*P* appeared higher than the binding affinity of the full length SidC_{Llo} (Figure 3.2C). In contrast, SidC_{Lpn} bound only weakly to PtdIns(4)*P*. In previously published experiments SidC_{Lpn} bound to PtdIns(4)*P* and to a lower extent also to PtdIns(3)*P* [80, 103]. In this assay we used harsher washing conditions to reduce the background signal. This reduced the amount of SidC_{Lpn} bound to PtdIns(4)*P* and PtdIns(3)*P*. SidC_{Lpn_P4C} bound with seemingly higher affinity to PtdIns(4)*P* than SidC_{Llo_P4C}. The P4C domain of SidC_{Lpn} also bound weakly to PtdIns(3)*P* (Figure 3.2C).

Afterwards the influence of the first 608 amino acids on the binding affinity of the P4C domains of *L. longbeachae* and *L. pneumophila* were tested. To this end chimera proteins consisting of the first 608 amino acids of *L. longbeachae* and the amino acids 609 to 917 of *L. pneumophila* were purified (SidC_{Llo_N-Lpn_C}). Also chimera proteins consisting of the first 608 amino acids of *L. pneumophila* fused to the amino acids 609 to 969 of *L. longbeachae* were purified (SidC_{Lpn_N-Llo_C}). The two chimera proteins were compared with SidC_{Llo} and SidC_{Lpn} using PIP-strips (Figure 3.2D) and PIP-arrays (Figure 3.2E). The SidC_{Llo_N-Lpn_C} chimera protein and SidC_{Llo} bound equally with high affinity to PtdIns(4)*P*. The binding affinity of SidC_{Lpn_N-Llo_C} to PtdIns(4)*P* was slightly lower compared to SidC_{Llo_N-Lpn_C} and SidC_{Llo} (Figures 3.2D and E). Both chimera proteins and SidC_{Llo} bound

3. Results

with low affinity to PtdIns(3)*P*. A binding of SidC_{Lpn} to PtdIns(3)*P* or PtdIns(4)*P* was not detected (Figures 3.2C and D).

In summary, SidC_{Llo} was identified as the first PtdIns(4)*P*-binding protein of *L. longbeachae*. The P4C domain of this protein is located in a similar C-terminal region as SidC_{Lpn_P4C} [3].

An alignment of SidC_{Llo}, SidC_{Lpn} and its paralogous protein SdcA_{Lpn} was made (Figure 3.3) to analyse if the amino acid composition could be the reason for the different apparent binding affinities of SidC_{Llo} and SidC_{Lpn} to PtdIns(4)*P*. SidC_{Lpn} and SdcA_{Lpn} showed a sequence identity of 72%. SidC_{Lpn} as well as SdcA_{Lpn} showed a sequence identity of only 40% to SidC_{Llo}. The P4C domains of SidC_{Llo} and SidC_{Lpn} are located nearly in the same amino acid region but the sequence identity of these two P4C domains was only 45%. Therefore, the difference in the amino acid composition could be the reason for the differences in the binding affinity of SidC_{Llo} and SidC_{Lpn} to PtdIns(4)*P*.

Despite of a sequence identity of 40% (Figure 3.3) between SidC_{Llo} and SidC_{Lpn}, we were not able to detect SidC_{Llo} in a Western blot analysis (Figure 3.4) nor in an immunofluorescence assay (data not shown) with a polyclonal anti-SidC_{Lpn} antibody [80].

Therefore, a polyclonal anti-SidC_{Llo} antibody using His₆-SidC_{Llo} was produced by a company (SeqLab). The antibody recognized endogenous SidC_{Llo} in *L. longbeachae* wild-type NSW150 as well as SidC_{Llo} produced in *L. pneumophila* JR32. The anti-SidC_{Lpn} antibody only recognized endogenous SidC_{Lpn} and SidC_{Lpn} produced in *L. longbeachae* wild-type. No cross reaction was visible (Figure 3.4) [3].

3. Results

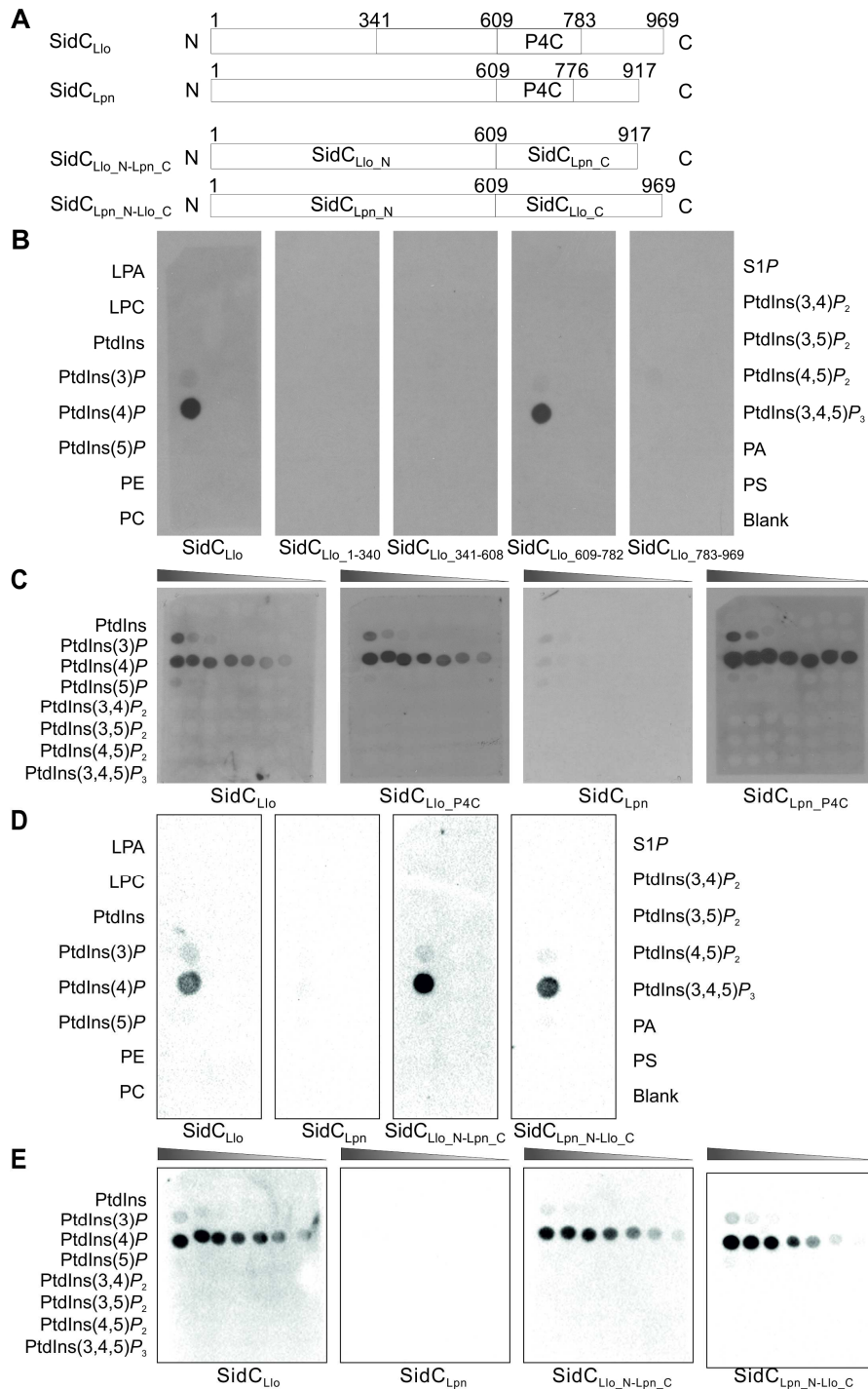


Figure 3.2. SidC_{Llo} binds *in vitro* through a P4C domain to PtdIns(4)P. Fragments of the 111 kDa SidC_{Llo} and the 106 kDa SidC_{Lpn} were fused to a GST-tag (A) [103]. The binding affinities of purified GST-SidC_{Llo} protein, GST-SidC_{Llo} fragments, GST-SidC_{Llo_N-Lpn_C} and GST-SidC_{Lpn_N-Llo_C} (B, D) to PtdIns, PIs or different lipids (100 pmol/spot) were analysed in protein-lipid overlay assays. The binding of the GST-coupled proteins were analysed using an anti-GST antibody. In the left row lysophosphatidic acid (LPA), lysophosphocholine (LPC), phosphatidylinositol (PtdIns), phosphatidylethanolamine (PE) and phosphatidylcholine (PC) are visible. The right row shows sphingosine-1-phosphate (S1P), phosphatidylinositol (PtdIns), phosphatidic acid (PA), phosphatidylserine (PS) and a blank spot (Blank). The binding affinities of GST-SidC_{Llo}, GST-SidC_{Llo_P4C}, GST-SidC_{Lpn}, GST-SidC_{Lpn_P4C}, GST-SidC_{Llo_N-Lpn_C} and GST-SidC_{Lpn_N-Llo_C} were compared using protein-lipid overlay assays with a two-fold serial dilution (1.56–100 pmol/spot) (C, E). In two or three independent experiments similar results were achieved [3].

3. Results

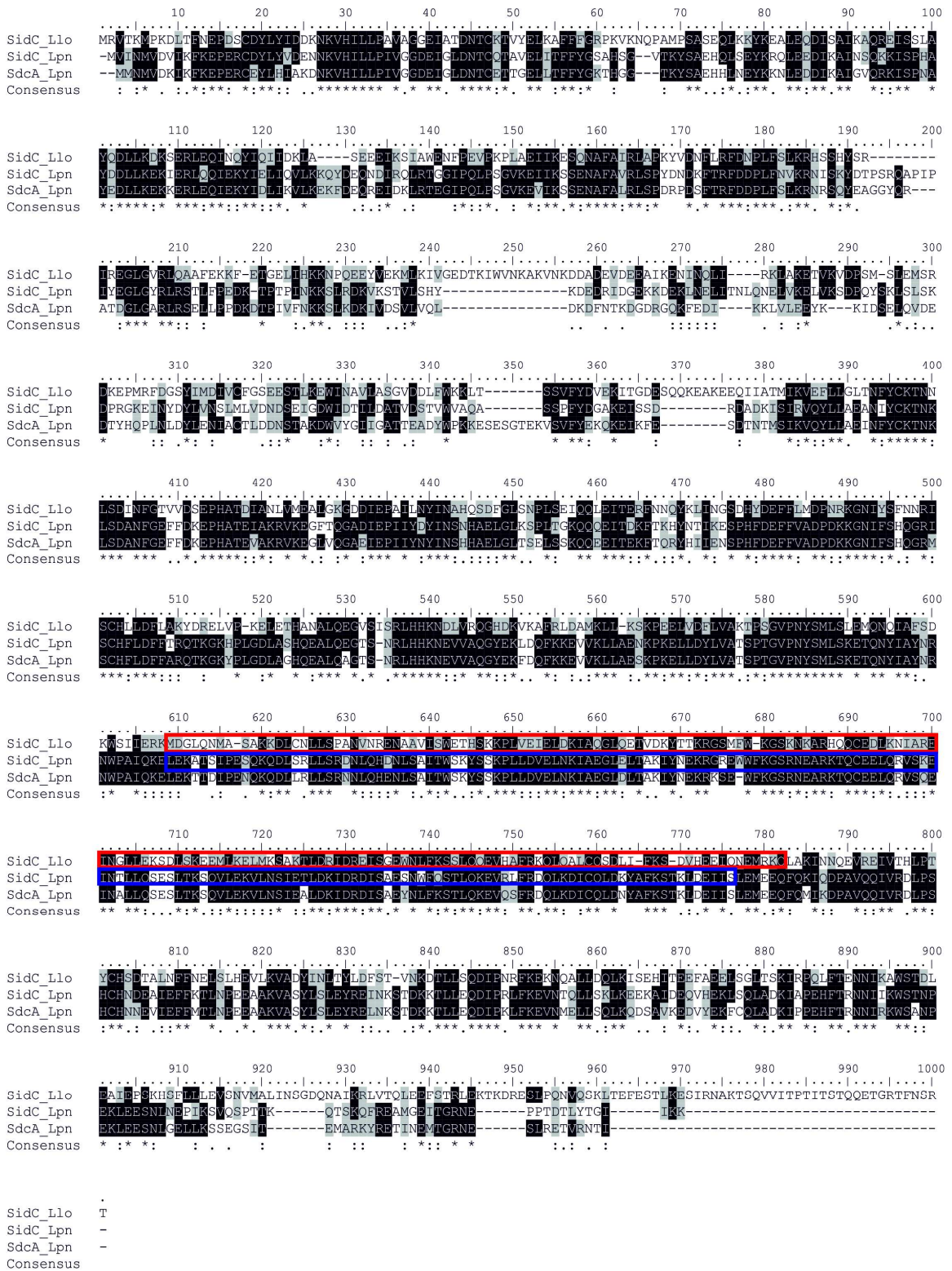


Figure 3.3. Comparison of the primary sequence of SidC_{Llo}, SidC_{Lpn} and SdcA_{Lpn}. SidC_{Llo}, SidC_{Lpn} and SdcA_{Lpn} were aligned using the amino acid sequence and a ClustalOmega algorithm. SidC_{Llo} is 40% identical to SidC_{Lpn} or SdcA_{Lpn}. The P4C domains of SidC_{Llo} (red) and SidC_{Lpn} (blue) share 45% identity. SidC_{Lpn} and SdcA_{Lpn} are 72% identical. Similar (grey) or identical (black) amino acids are labelled. The figure is adapted from a scheme published in [3].

3. Results

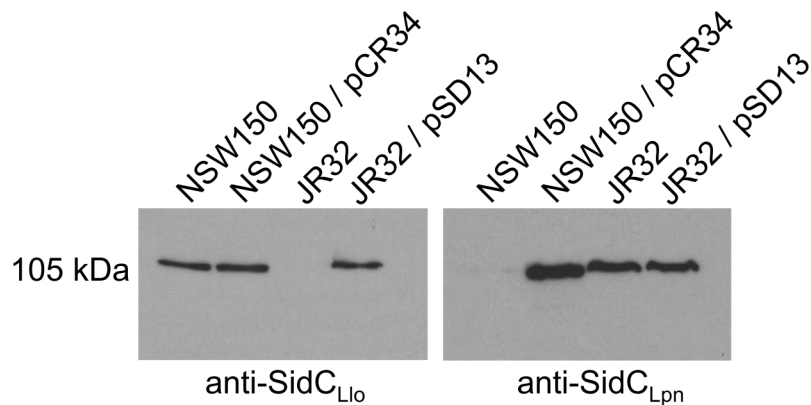


Figure 3.4. Anti-SidC_{Llo} and anti-SidC_{Lpn} antibodies recognize only their cognate proteins. *L. longbeachae* wild-type and *L. pneumophila* wild-type were grown in overnight cultures. M45-SidC_{Llo} (pSD13) or M45-SidC_{Lpn} (pCR34) were transformed and induced in *L. pneumophila* or *L. longbeachae*. The same amount of bacteria was boiled in SDS sample buffer. The proteins were separated by SDS-PAGE and visualized by Western blot using specific polyclonal rabbit anti-SidC_{Llo} and anti-SidC_{Lpn} antibodies. The experiment was repeated three times with the same results [3].

3.1.3 The Icm/Dot substrate SidC_{Llo} localizes to LCVs

To test the Icm/Dot-dependent translocation of SidC_{Llo} an enzyme immunoassay kit (Amersham cAMP Biotrak Enzymeimmunoassay (EIA) System, GE Healthcare Life Sciences) was used. In this assay, the calmodulin-dependent production of cAMP by adenylate cyclase (CyaA) in the host cell cytoplasm is assessed. *L. longbeachae* [30] as well as *L. pneumophila* [48] are able to infect macrophages. Therefore, RAW 264.7 macrophages were infected with *L. longbeachae* or *L. pneumophila* harbouring plasmid-encoded CyaA, CyaA-SidC_{Llo} or CyaA-SidC_{Lpn}. CyaA as well as *dotA* deletion mutants of *L. longbeachae* and *L. pneumophila* were used as negative controls. CyaA was not translocated in all strains. All proteins were not translocated in the *dotA* deletion mutants of both strains. We used CyaA-SidC_{Lpn} as a positive control. SidC_{Lpn} was translocated in *L. pneumophila*, but no translocation was visible in *L. longbeachae*. SidC_{Llo} was neither translocated by *L. longbeachae* nor by *L. pneumophila* (Figure 3.5A). Therefore, the protein production was analyzed. The endogenous SidC_{Lpn} and the ~145 kDa CyaA-SidC_{Lpn} were produced in *L. pneumophila*. The ~151 kDa CyaA-SidC_{Llo} was produced with the expected size in *L. pneumophila*. A small band in the size of SidC_{Llo} alone was also detected. In the *L. longbeachae* samples it seemed as if parts of the CyaA or the whole CyaA were cleaved from SidC_{Llo} or SidC_{Lpn} because the detected bands were between the expected size for the CyaA-coupled proteins and the full-length proteins (Figure 3.5B).

3. Results

Next, a published *L. longbeachae* effector protein was used as a positive control. CyaA-CetLI1 (C-terminal signal for effector translocation of *L. longbeachae* 1) was previously published to be translocated in an Icm/Dot-dependent way in HL-60-derived human macrophages when overexpressed in *L. pneumophila* [58]. Therefore, we transformed CyaA-CetLI1 [58] into *L. longbeachae* and *L. pneumophila*. *DotA* deletion mutants were used as negative controls. Yet, CyaA-CetLI1 was only translocated in *L. pneumophila* wild-type but not in wild-type *L. longbeachae* (Figure 3.5C). Changing the amount of cells and the lysis method used for this assay had no effect on the detection of translocation. Therefore, we decided to use an immunofluorescence approach to analyze if SidC_{Llo} is translocated in an Icm/Dot-dependent manner.

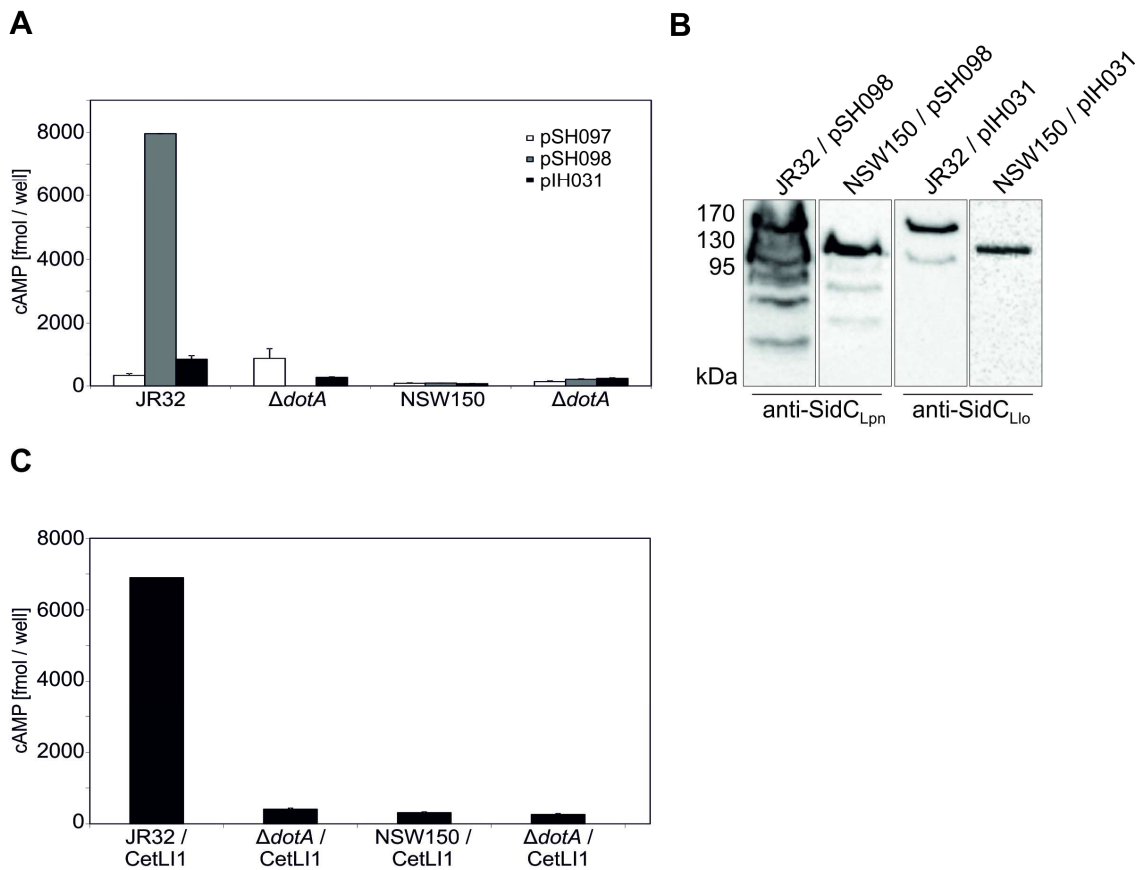


Figure 3.5. Measurement of translocation of SidC_{Llo}. RAW 264.7 macrophages were infected with *L. longbeachae* or *L. pneumophila* wild-type as well as with a *dotA* mutant expressing CyaA (pSH097), CyaA-SidC_{Lpn} (pSH098) or CyaA-SidC_{Llo} (piH031). The translocation of the proteins was measured by the cAMP level. Means and standard deviations were calculated from two independent samples. The experiment has been done once (A). Overnight cultures were boiled, separated by SDS-PAGE and the proteins were visualized by specific anti-SidC antibodies. Between one and three overnight cultures were analyzed per sample (B). The cAMP translocation of CetLI1 in a wild-type or a *dotA* mutant of *L. longbeachae* and *L. pneumophila* was analyzed three times with different lysis methods. Means and standard deviations were calculated from two independent samples (C).

3. Results

RAW 264.7 macrophages were infected with *L. longbeachae* wild-type or a $\Delta dotA$ mutant harbouring a Dsred-producing plasmid or a plasmid coding for Dsred and SidC_{Lpn}. Endogenous SidC_{Llo} and overproduced SidC_{Lpn} were visualized using specific anti-SidC antibodies. An immunofluorescence analysis of the infected macrophages showed a localization of SidC_{Llo} and SidC_{Lpn} on the LCV membrane (Figure 3.6A). 48% of the endogenous SidC_{Llo} and 56% of the overexpressed SidC_{Lpn} co-localized to the LCV membrane. Only less than 1% of the LCVs infected with a *dotA* deletion mutant were positive for SidC_{Llo} or SidC_{Lpn} (Figure 3.6B). Therefore, the translocation of SidC_{Llo} and SidC_{Lpn} to the surface of the *L. longbeachae*-containing vacuole is Icm/Dot-dependent. It seems as if the *L. longbeachae* T4SS translocates both SidC proteins with similar efficiencies.

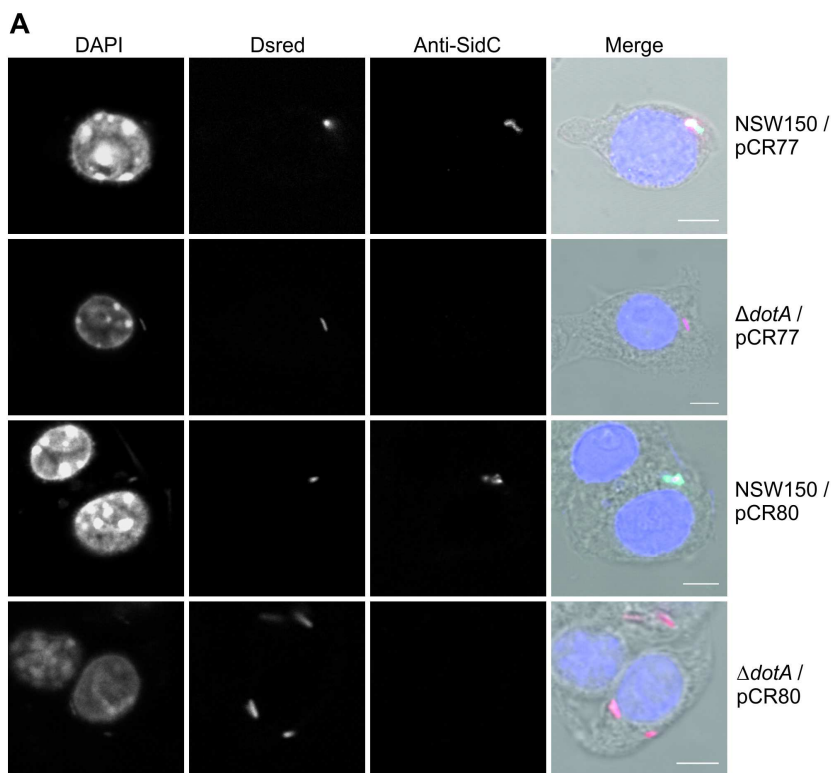
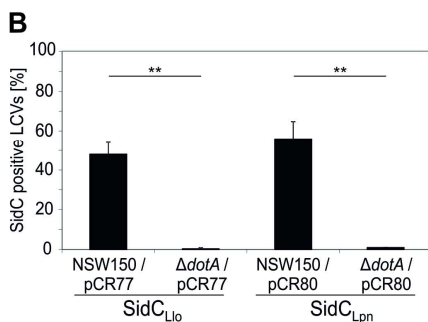


Figure 3.6. SidC_{Llo} is an Icm/Dot-dependent effector protein which localizes to the LCV.

RAW 264.7 macrophages were infected (MOI 50, 1 hour) with wild-type or a *dotA* deletion mutant of *L. longbeachae* harbouring a Dsred-encoding plasmid (pCR77) or a plasmid-encoding Dsred and SidC_{Lpn} (pCR80). The endogenous SidC_{Llo} and the overexpressed SidC_{Lpn} were stained with a specific anti-SidC antibody (light blue). The nucleus was stained with DAPI (dark blue) (bar = 5μm) (A). The SidC_{Llo} and SidC_{Lpn} positive LCVs were counted. The mean and standard deviations were calculated from three independent experiments with 50 LCV each (** p<0.01) (B) [3].



3. Results

3.1.4 The $\Delta sidC_{Llo}$ and $\Delta sidC-sdcA_{Lpn}$ deletion mutants are outcompeted by the wild-type strains in competition assays

The role of SidC_{Llo} on the intracellular replication of *L. longbeachae* in infected amoebae or macrophages was analysed. To this end, a defined *sidC_{Llo}* deletion mutant was used (strain IH02) [3].

We infected *A. castellanii* or RAW 264.7 macrophages with wild-type *L. longbeachae* (NSW150), a *dotA* and a *sidC_{Llo}* deletion strain. *L. longbeachae* wild-type as well as the *sidC_{Llo}* deletion mutant grew equally. Over 3 days of infection both strains grew with similar rates, producing two (Figure 3.7B) or three (Figure 3.7A) orders of magnitude more bacteria. The *L. longbeachae dotA* deletion mutant was not able to grow intracellularly in *A. castellanii* or RAW 264.7 macrophages, as published before (Figure 3.7) [26]. Therefore, SidC_{Llo} is not necessary for the intracellular growth of *L. longbeachae* in *A. castellanii* or RAW 264.7 macrophages.

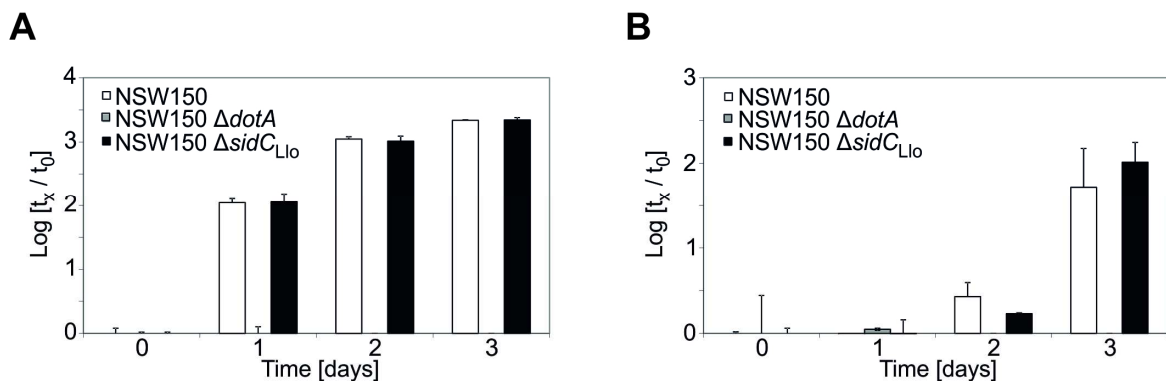


Figure 3.7. *L. longbeachae* lacking *sidC_{Llo}* grows normally in RAW 264.7 macrophages and *A. castellanii*. *A. castellanii* (A) or RAW 264.7 macrophages (B) were infected (MOI 0.1) with *L. longbeachae* wild-type NSW150, a *dotA* or a *sidC_{Llo}* deletion mutant. Supernatants of the infected cells were taken shortly after infection (time point 0) and 1 day, 2 days and 3 days after the infection and plated on CYE plates. The colony forming units (cfus) were counted [3].

In an alternative approach, *A. castellanii* were co-infected with *L. longbeachae* wild-type and the *sidC_{Llo}* deletion mutant, or with *L. pneumophila* and the *sidC-sdcA_{Lpn}* deletion mutant. The *sidC_{Llo}* deletion mutant disappeared in direct competition with its wild-type strain within 24 days (Figure 3.8A). In parallel, the normal growth of both strains alone in *A. castellanii* was confirmed (Figure 3.8C). The *sidC-sdcA_{Lpn}* deletion strain died already within 12 days in direct competition with its wild-type strain (Figure 3.8B). In a single strain infection assay both strains grew normally (Figure 3.8D). Taken together, in direct

3. Results

competition the wild-type strains of *L. longbeachae* and *L. pneumophila* outcompete the corresponding *sidC* mutant strains in *A. castellanii*.

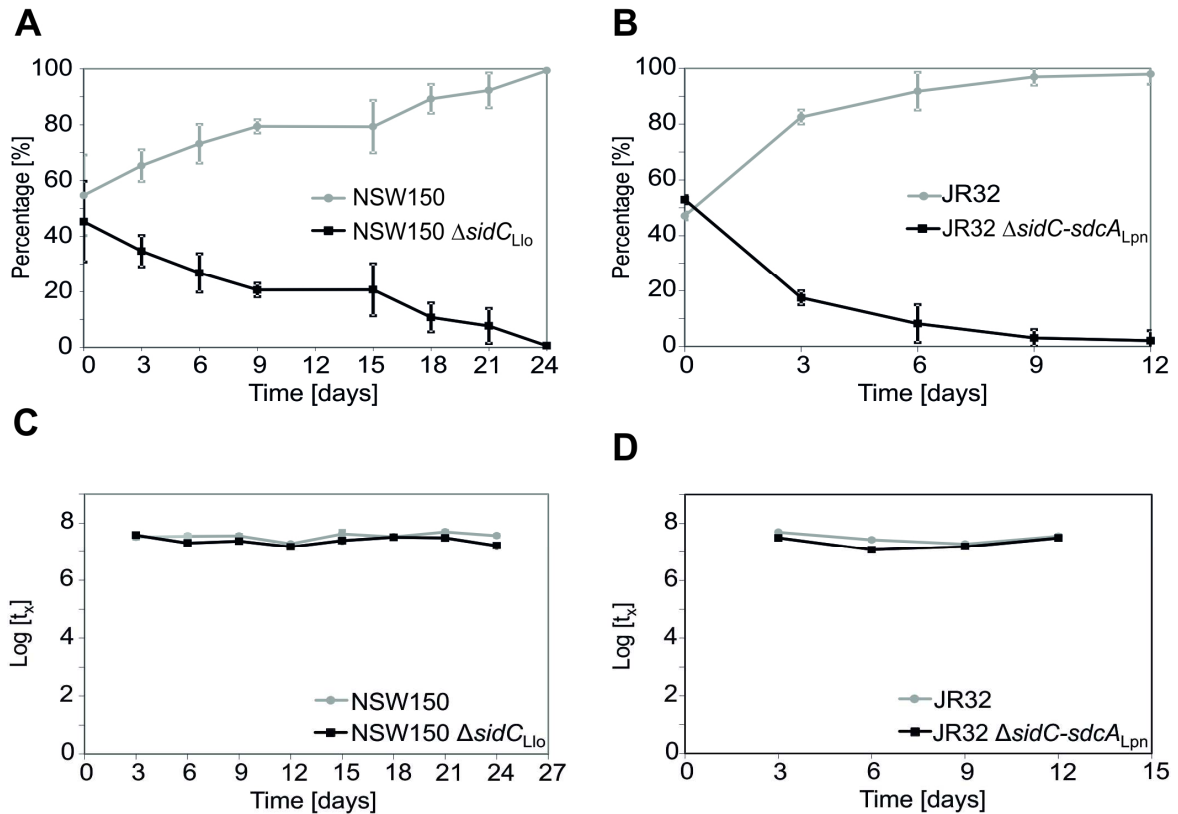


Figure 3.8. *L. longbeachae* and *L. pneumophila* wild-type strains outcompete the Δ sidC_{Llo} and Δ sidC-sdcA_{Lpn} strains. *A. castellanii* were co-infected (MOI 0.01) with *L. longbeachae* wild-type and a Δ sidC_{Llo} deletion mutant (A) or with *L. pneumophila* wild-type and a Δ sidC-sdcA_{Lpn} deletion mutant (B). The infected amoebae and the supernatant was diluted 1:1.000 every third day and a newly seeded layer of amoeba was infected. The colony forming units were counted at the time points indicated. In parallel *A. castellanii* were infected alone with *L. longbeachae* (C) or *L. pneumophila* strains (D). The experiment was done in triplicate. The standard deviations were calculated from three independent infections plated in duplicate [3].

3.1.5 SidC_{Llo} and SidC_{Lpn} promote ER recruitment to the LCV

The ability of *L. longbeachae* to infect *D. discoideum* Ax3 was tested. To this end, we infected the cells with *L. longbeachae* wild-type or a *dotA* deletion mutant. The corresponding strains of *L. pneumophila* were used as a control (Figure 3.9). *L. longbeachae* replicated less efficiently in *D. discoideum* than *L. pneumophila* within 6 days. Both *dotA* deletion mutants were not able to grow intracellularly. *L. longbeachae* is infecting *D. discoideum* but grows slower in *D. discoideum* than *L. pneumophila*.

3. Results

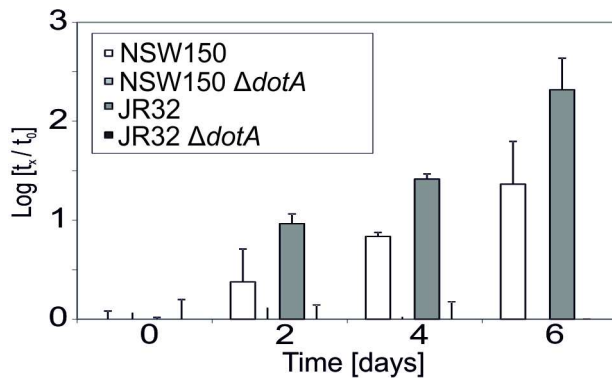


Figure 3.9. Intracellular replication of *L. longbeachae* and *L. pneumophila* in *D. discoideum*. *D. discoideum* Ax3 were infected (MOI 0.01) with *L. longbeachae* or *L. pneumophila* wild-type or a corresponding *dotA* deletion mutant at 25.5°C. The supernatant of the cells was collected every second day and plated on CYE plates. The cfus were counted. The means and standard deviations of infections done in triplicate are shown. The experiment was done three times.

Next, the role of SidC_{LI6} in the ER recruitment to the *L. longbeachae*-containing vacuole was analysed. Calnexin-GFP *D. discoideum* rounded up and detached right after the infection with *L. longbeachae* wild-type. Therefore, the infected cells were lost during the infection and immunofluorescence labelling was difficult.

To analyse this phenomenon in more detail, calnexin-GFP producing *D. discoideum* were infected with *L. longbeachae* wild-type and a *dotA* deletion mutant producing Dsred. The bacteria were spun onto the cells, infected for 1 hour and the cells were fixed without previously washing. After infection with wild-type *L. longbeachae*, many calnexin-GFP *D. discoideum* were lost compared to an infection with a *dotA* deletion mutant of *L. longbeachae*. Therefore, this effect is Icm/Dot-dependent (Figure 3.10).

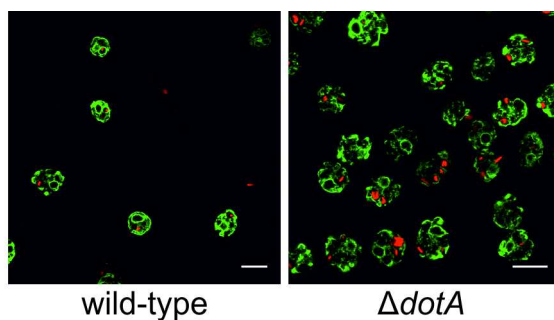


Figure 3.10. *L. longbeachae* wild-type alters the cell adherence of calnexin-GFP producing *D. discoideum*. Calnexin-GFP producing *D. discoideum* (green) were infected (MOI 50) with *L. longbeachae* harbouring a Dsred (red) encoding plasmid for 1 hour. The cells were fixed and analyzed with a confocal microscope. The experiment was done in duplicate (bar = 10 μ m).

The change in *D. discoideum* morphology could be due to a cytotoxic effect of *L. longbeachae*. Therefore, the cytotoxicity of *L. longbeachae* towards *D. discoideum* was tested. *D. discoideum* were infected with *L. longbeachae* and *L. pneumophila* wild-type and a corresponding *dotA* deletion mutant. Cytotoxicity of wild-type *L. longbeachae* or wild-type *L. pneumophila* was low (< 8%) and the *dotA* mutants of *L. longbeachae* and *L. pneumophila* had no cytotoxic effect on *D. discoideum*. The cytotoxic effect of

3. Results

L. longbeachae does not increase with higher MOIs (Figure 3.11). Together, *L. longbeachae* seems to have no cytotoxic effect on *D. discoideum*.

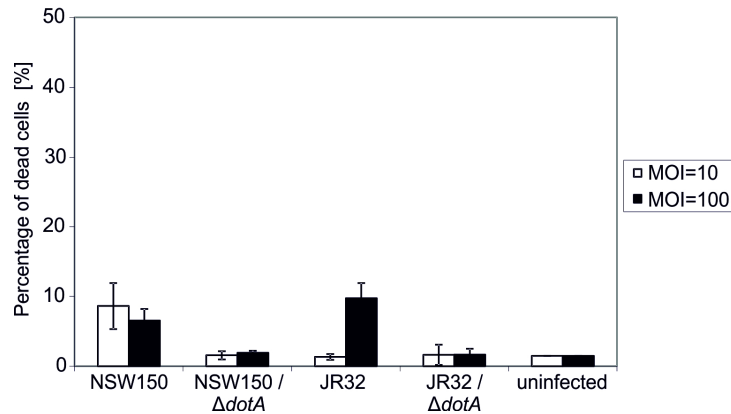


Figure 3.11. *L. longbeachae* shows no cytotoxic effect on *D. discoideum*. *D. discoideum* were infected (MOI 10 and 100) with *L. longbeachae* wild-type and a *dotA* mutant as well as with the corresponding *L. pneumophila* strains for 1 hour. The cells were harvested and the dead cells were stained with propidium iodide. The amount of absorbed propidium iodide was measured with a FACS machine. Uninfected cells were used as a negative control. Mean and standard deviations of three independent experiments are indicated. The experiment was done three times.

Previously published data demonstrated the recruitment of ER to the *L. pneumophila*-containing vacuole in calnexin-GFP producing *D. discoideum* [53, 80, 103, 142]. The ER marker calnexin was recruited to a LCV containing *L. pneumophila* wild-type but not to an *icmT* deletion mutant. Also, the loss of the genes *sidC*_{Lpn} and *sdca*_{Lpn} led to a decreased recruitment of calnexin to the LCV. The effect occurred within 1 hour and remained at least for four hours. The loss of the ER recruitment was complemented by adding plasmid-encoded SidC_{Lpn} or SdcA_{Lpn}, but not with adding the C-terminal part of SidC_{Lpn} [103].

We wanted to test if this effect could be complemented by SidC_{Llo} as well. Therefore, we infected calnexin-GFP producing *D. discoideum* with wild-type, an *icmT* or a *sidC-sdca*_{Lpn} deletion mutant of *L. pneumophila* harbouring the red fluorescent dye Dsred or a plasmid-encoding Dsred and SidC_{Lpn} or SidC_{Llo} (Figure 3.12A). In 72% of the cases calnexin-GFP was recruited to a LCV harbouring wild-type *L. pneumophila*. After an infection with an *icmT* deletion mutant only 1% of the LCVs were calnexin-GFP positive. Also the loss of *sidC*_{Lpn} and *sdca*_{Lpn} led to a decrease in the recruitment of calnexin-GFP to the LCV (19%) (Figure 3.12B) as published before [103]. A complementation of this decreased calnexin recruitment to the LCV was only possible with SidC_{Lpn} as published before (78%) [103] but not with overexpressed SidC_{Llo} (14%). Between one and four hours

3. Results

after the infection the calnexin-GFP recruitment did not alter for a *L. pneumophila sidC-sdcA_{Lpn}* deletion mutant which expressed SidC_{L10} (Figure 3.12C). Noteworthy, these immunofluorescence experiments were performed with formaldehyde-fixed cells.

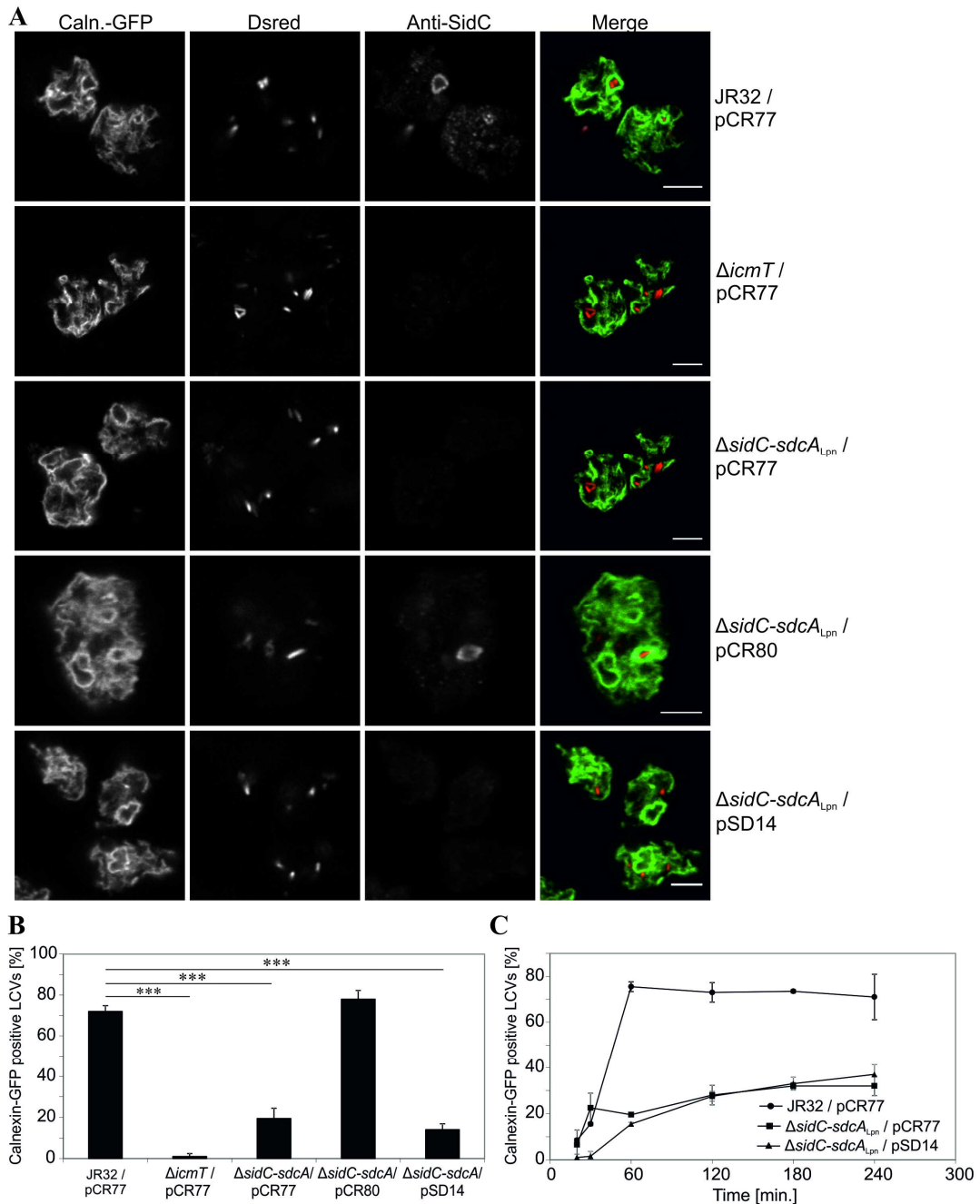


Figure 3.12. The calnexin-GFP recruitment to a LCV harbouring a *sidC-sdcA_{Lpn}* deletion mutant of *L. pneumophila* is not complemented by SidC_{L10}. Calnexin-GFP producing *D. discoideum* were infected (MOI 50) with *L. pneumophila* wild-type, an *icmT* or a *sidC-sdcA_{Lpn}* deletion mutant. The bacteria were harbouring a Dsred (pCR77), a Dsred and SidC_{Lpn} (pCR80) or a Dsred and SidC_{L10} (pSD14) expressing plasmid. The cells were infected for 1 hour, fixed with paraformaldehyde and analysed with a confocal microscope (A) (bar = 5 μ m) (Caln. = calnexin). 100 LCVs were counted in three independent experiments (***) $P < 0.001$) (B). The calnexin-GFP recruitment was analysed over time (C).

3. Results

To test whether the fixation of the cell affects the calnexin-GFP signal, the same set of *L. pneumophila* strains was analysed with living cells (Figure 3.13). The results for *L. pneumophila* wild-type, $\Delta icmT$, $\Delta sidC-sdcA_{Lpn}$ and the complementation strain with SidC_{Lpn} did not alter (Figures 3.12 and 3.13). In contrast, in living cells a complementation of the calnexin recruitment defect of a $\Delta sidC-sdcA_{Lpn}$ strain with SidC_{Llo} was visible (64%) (Figure 3.12). Thus, the fixation process apparently interfered with the signal accumulation. Taken together, the impaired ER recruitment to the *L. pneumophila*-containing vacuole can be complemented by the production of SidC_{Lpn}, SdcA_{Lpn} and SidC_{Llo}.

Finally, we used living *D. discoideum* to analyse the calnexin-GFP recruitment to a *L. longbeachae*-containing vacuole. A pre-test demonstrated that the calnexin-GFP recruitment to the *L. longbeachae* LCV reaches its saturation after 2 hours post infection. Therefore, calnexin-GFP producing *D. discoideum* were infected for 2 hours with wild-type, a *dotA* and a *sidC_{Llo}* deletion mutant harbouring a Dsred-expressing plasmid. For complementation experiments, a *sidC_{Llo}* deletion mutant was used, which harboured a plasmid-encoding for Dsred and SidC_{Llo}, SidC_{Lpn} or SdcA_{Lpn} (Figure 3.14). 82% of the LCVs containing wild-type *L. longbeachae* were calnexin-GFP positive. An infection with a *dotA* deletion mutant produced only 2% calnexin-GFP positive LCVs. This indicates that the recruitment of ER derived vesicles to the *L. longbeachae*-containing vacuole is Icm/Dot-dependent. The deletion of the *sidC_{Llo}* gene led to a decreased calnexin-GFP recruitment to the LCV of around 20%. This effect was complemented by adding plasmid-encoded SidC_{Llo} (80%), SidC_{Lpn} (83%) or SdcA_{Lpn} (74%) (Figure 3.14B).

3. Results

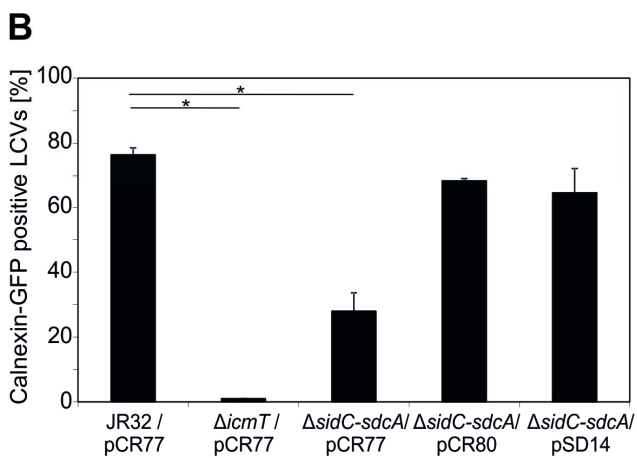
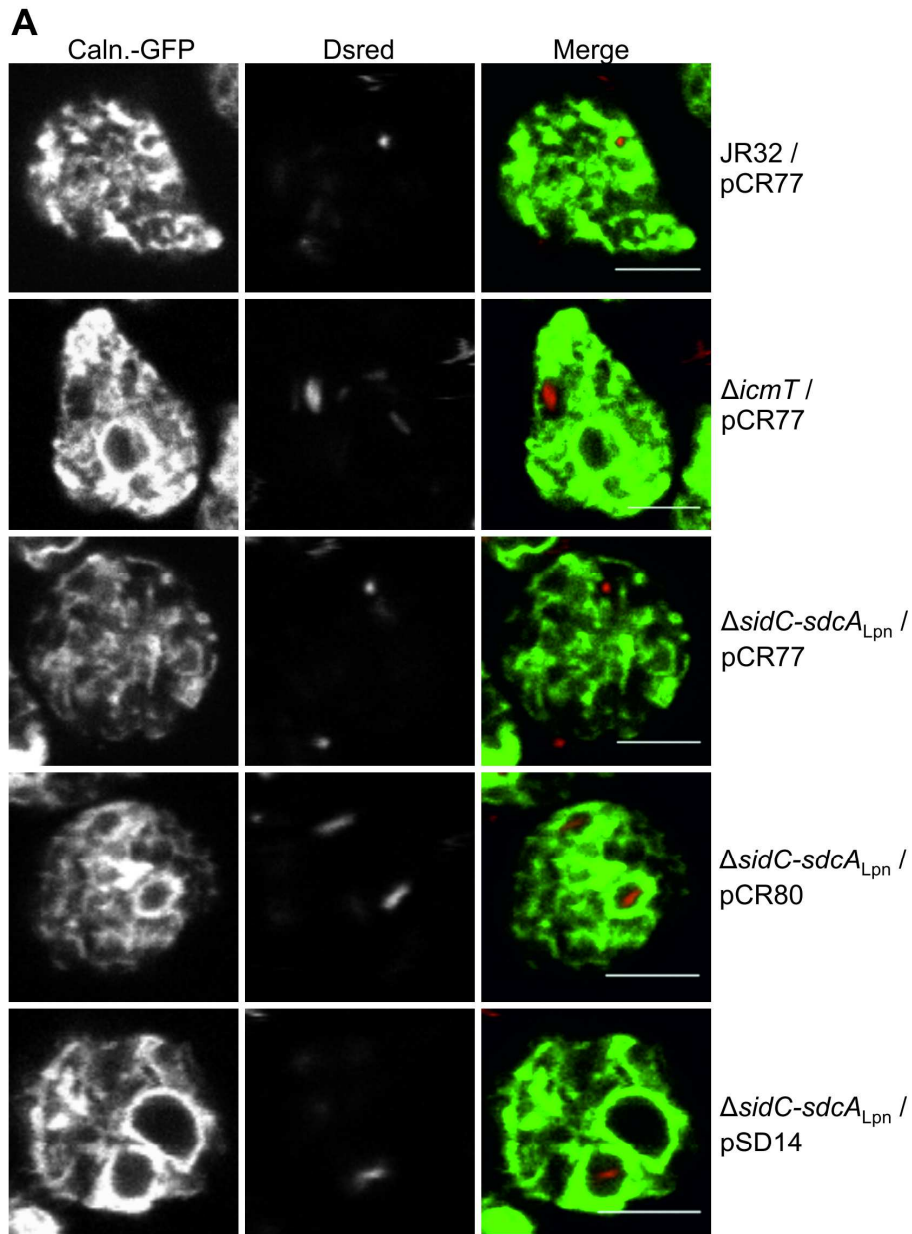


Figure 3.13. The decreased ER recruitment to the *L. pneumophila* $\Delta sidC-sdcA_{Lpn}$ containing vacuole in *D. discoideum* is complemented by SidC_{Llo}. Calnexin-GFP *D. discoideum* were infected (MOI 20, 1 hour) with *L. pneumophila* wild-type, an *icmT* or a *sidC-sdcA_{Lpn}* deletion mutant. The strains harboured a Dsred (pCR77) or a plasmid which produced Dsred and SidC_{Llo} (pSD14) or SidC_{Lpn} (pCR80). Live cells were imaged with a confocal microscope (bar = 5 μ m) (A). The calnexin-GFP signal of 100 *L. longbeachae*-containing vacuoles were counted in two independent experiments (* $P < 0.05$) (B) [3].

3. Results

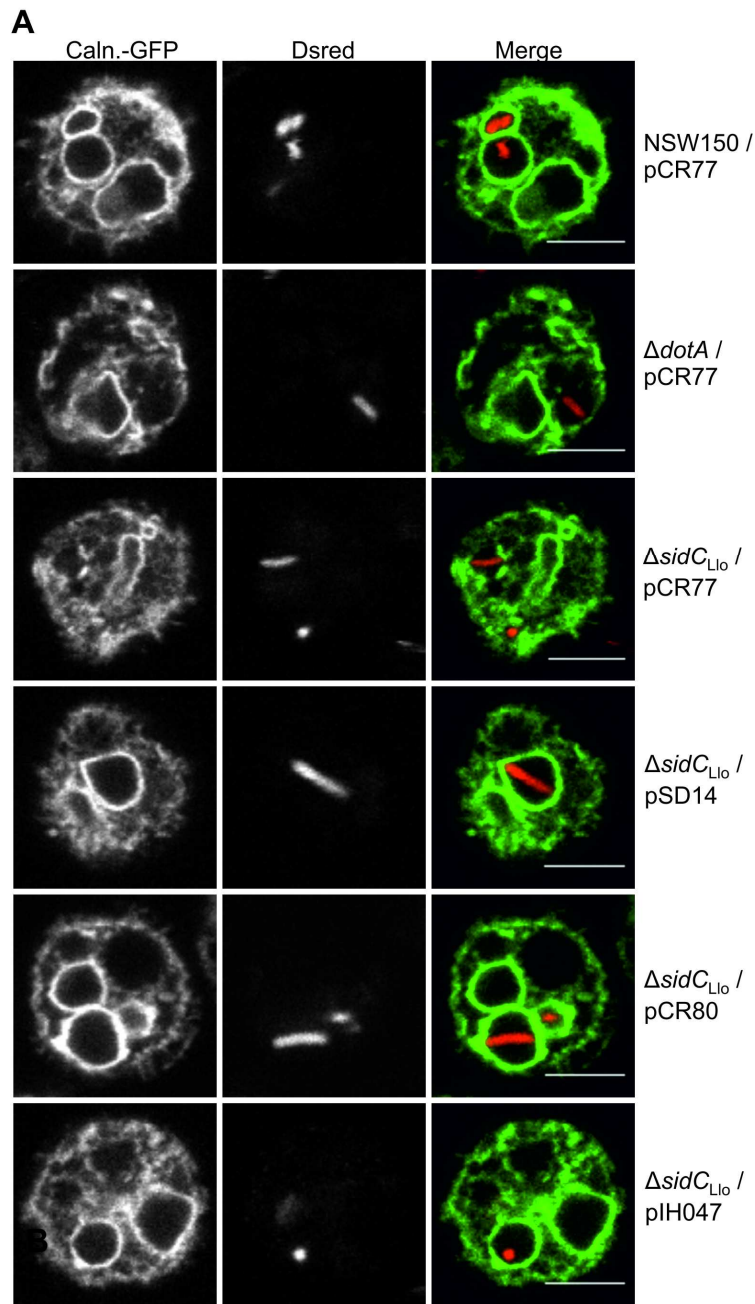
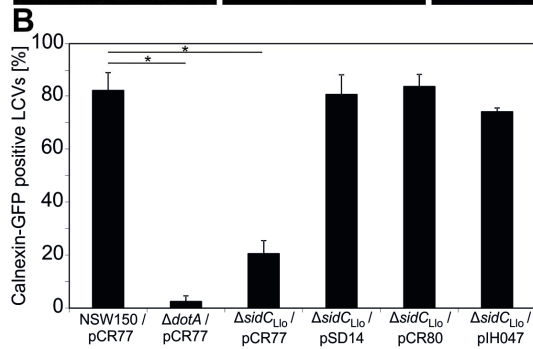


Figure 3.14. *L. longbeachae* Sid_{C_{Llo}} is necessary for the ER recruitment to the LCV.

L. longbeachae wild-type, a *dotA* or a *sidC_{Llo}* deletion mutant harbouring a Dsred expressing plasmid (pCR77) were used to infect (MOI 20) calnexin-GFP producing *D. discoideum* for 2 hours. The *sidC_{Llo}* deletion mutant was complemented with a plasmid encoding for Dsred and Sid_{C_{Llo}} (pSD14), Sid_{C_{Lpn}} (pCR80) or SdcA_{Lpn} (pIH047). The cells were imaged with a confocal microscope (bar = 5 μm) (A). The calnexin-GFP signal of 100 *L. longbeachae*-containing vacuoles were counted in two separate experiments (* *P*<0.05) (B) [3].



3. Results

In summary, we found that the ER recruitment to the LCV of *L. longbeachae* and *L. pneumophila* is Icm/Dot-dependent. The loss of the genes *sidC_{Llo}* as well as *sidC-sdcA_{Lpn}* decreased the ER recruitment to the LCV. These effects can be complemented by adding plasmid-encoded SidC_{Llo}, SidC_{Lpn} as well as SdcA_{Lpn}. Therefore, the function of SidC_{Llo}, SidC_{Lpn} and SdcA_{Lpn} are redundant. Overall, the amount of calnexin-GFP on the LCV is comparable for *L. longbeachae* as well as *L. pneumophila* wild-type strains (Figure 3.13 and 3.14) [103].

3.1.6 SidC_{Llo_P4C} and SidC_{Lpn_P4C} are binding to PtdIns(4)P on the LCV

We were interested if SidC_{Llo_P4C} and SidC_{Lpn_P4C} are localizing to the LCV. Therefore, Calnexin-GFP *D. discoideum* were infected with red fluorescent *L. pneumophila* for 1 hour. The cells were homogenized and incubated with purified GST fusion proteins (Figure 3.15A). Less than 1% of the LCVs incubated with the negative control, GST, were GST positive. 82% of the LCVs were covered with GST-SidC_{Llo_P4C}. A quantification revealed that 88% of the *L. pneumophila*-containing vacuoles were GST-SidC_{Lpn_P4C} positive. For the positive control GST-PH_{FAPP1} 77% of the LCVs were GST-PH_{FAPP1} positive (Fig. 3.15B). Similar results were published previously for GST-PH_{FAPP1} [80]. Therefore, GST-SidC_{Llo_P4C} binds to LCVs to a similar extent as GST-SidC_{Lpn_P4C} and GST-PH_{FAPP1}. These findings indicate that both P4C domains can be used as PtdIns(4)P binding probes for *L. longbeachae* or *L. pneumophila* in all biological experiments.

3. Results

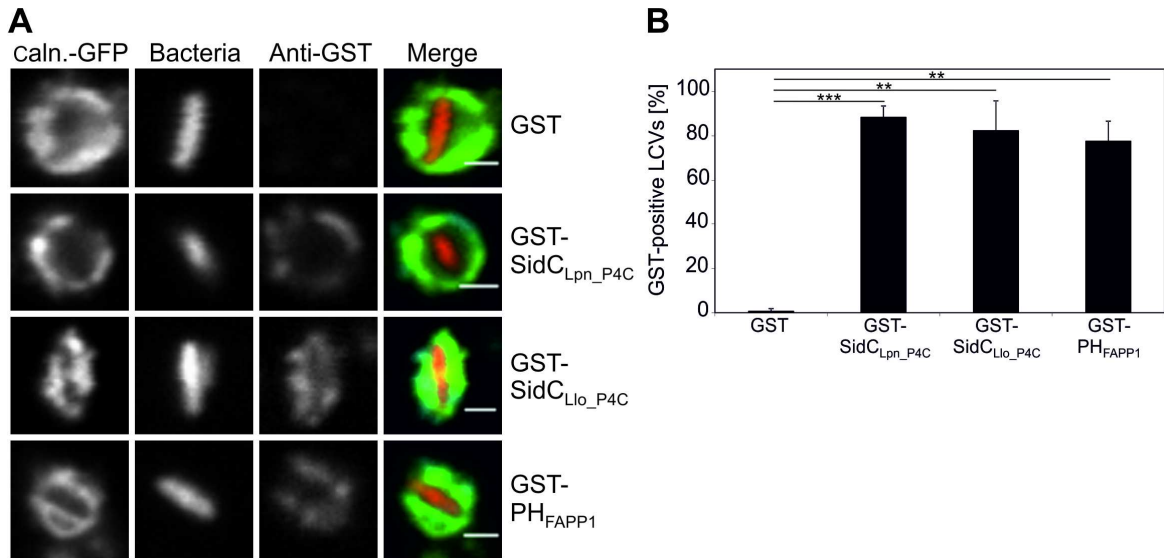


Figure 3.15. SidC_{Llo_P4C} and SidC_{Lpn_P4C} binds through PtdIns(4)P to the LCV. Calnexin-GFP producing *D. discoideum* were infected with red fluorescent *L. pneumophila* (MOI 100, 1h). The cells were homogenised, fixed and the samples were incubated with GST-tagged proteins. An anti-GST antibody was used. Images were taken with a confocal microscope (bar = 1 μ m) (A). Means and standard deviations from three independent experiments are shown, in which 100 LCVs each were counted (** P<0.01, *** P<0.001) (B) [3].

3.2. Purification of LCVs from *L. longbeachae*

A protocol for the isolation of *L. pneumophila*-containing vacuoles from infected *D. discoideum* was previously published [143]. In this protocol calnexin-GFP producing *D. discoideum* were infected with Dsred expressing *L. pneumophila*. A cell-free homogenate was incubated with an anti-SidC_{Lpn} antibody followed by a secondary antibody, which was coupled to magnetic beads. The homogenate was run through a magnetic separator (Figure 3.16), followed by a density centrifugation step [143].

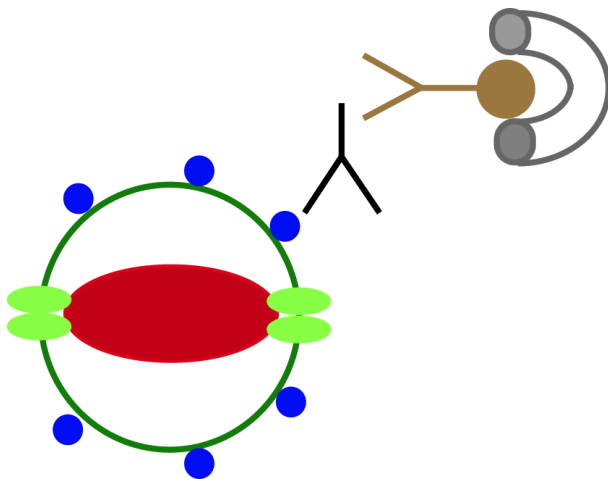


Figure 3.16. Purification of *L. pneumophila*-containing vacuoles. Cells were infected with Dsred expressing *L. pneumophila* (red). SidC_{Lpn} (blue) was translocated through the Icm/Dot T4SS (light green) to the surface of the LCV (dark green). The LCVs were incubated with an anti-SidC_{Lpn} antibody (black) followed by a secondary antibody coupled with a magnetic bead (brown). The LCVs were isolated over a magnet (gray). The scheme is based on the model previously published [1, 2].

3. Results

Liquid chromatography coupled to tandem mass spectrometry (MS/MS) was done with purified LCVs of *L. pneumophila* and over 560 host proteins of *D. discoideum* were identified including lipid phosphatases and kinases [143]. A purification method was established to purify LCVs from infected RAW 264.7 macrophages. The protocol was similar to the protocol used for *D. discoideum* [2]. Mass spectrometry analysis identified over 1150 host proteins on the LCVs of macrophages including members of the Rab family [2].

These protocols were used as a starting point for the purification of *L. longbeachae*-containing vacuoles from *D. discoideum* or RAW 264.7 macrophages. To this end, SidC_{Lpn} was overexpressed in *L. longbeachae* and an anti-SidC_{Lpn} antibody was used for the purification. With the newly raised SidC_{Llo} antibody a purification with the endogenous SidC_{Llo} and the corresponding SidC_{Llo} antibody was tried as well. The goal was to obtain enough purified LCVs from both cell lines to perform a proteome analysis of the *L. longbeachae*-containing vacuole.

3.2.1 Purification of *L. longbeachae*-containing vacuoles from *D. discoideum* with an anti-SidC_{Lpn} antibody

For proteomic analysis purified *L. longbeachae* LCVs were needed. At the beginning of this work no specific SidC_{Llo} antibody or any other *L. longbeachae* specific antibody was available which detects a marker of the *L. longbeachae*-containing vacuole.

We showed that the anti-SidC_{Lpn} antibody [80] does not recognize endogenous SidC_{Llo} on the *L. longbeachae*-containing vacuole in *D. discoideum*, but after overexpression of SidC_{Lpn} in *L. longbeachae*, the antibody recognized SidC_{Lpn} on the LCV (Figure 3.17). Therefore, we decided to use a *L. longbeachae* strain harbouring a plasmid coding for Dsred and SidC_{Lpn} for the LCV purification.

3. Results

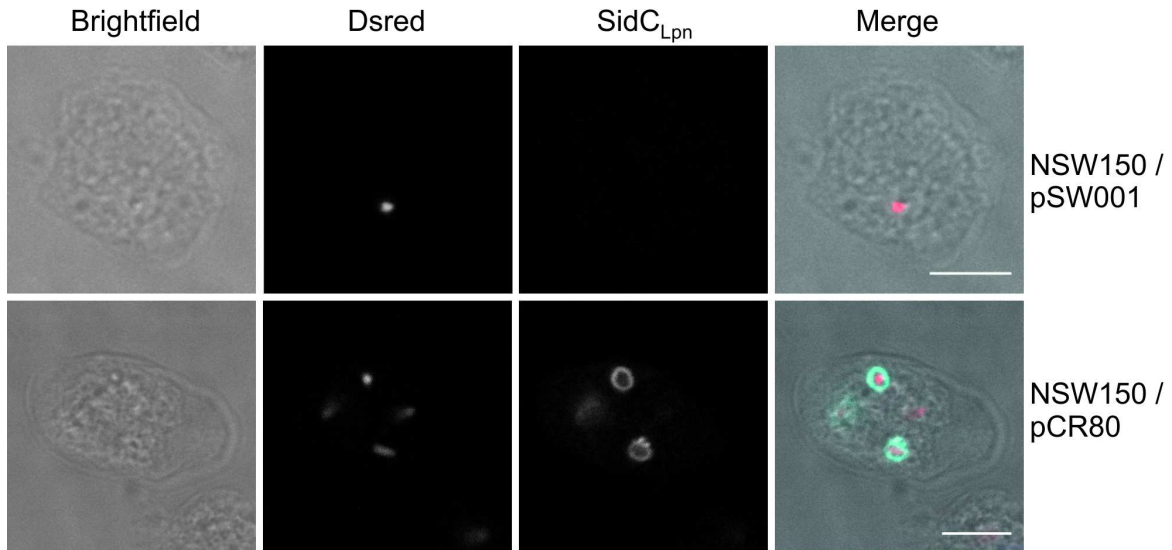


Figure 3.17. Overexpressed SidC_{Lpn} is covering a *L. longbeachae*-containing vacuole in infected *D. discoideum*. *D. discoideum* were infected (MOI 50) with wild-type *L. longbeachae* harbouring a Dsred encoding plasmid (pSW001) or a plasmid-encoding Dsred and SidC_{Lpn} (pCR80) for one hour. The cells were fixed and stained with an anti-SidC_{Lpn} antibody followed by an anti-rabbit IgG (Cy5) secondary antibody (bar = 5 μ m). The experiment was performed twice.

As a positive control *D. discoideum* producing calnexin-GFP were infected with Dsred expressing *L. pneumophila* (pSW001) (Figure 3.18). Many calnexin-GFP positive LCVs were visible in the homogenate and in the pellet. Bacteria which had not infected the cells were not binding to the column and were appearing in the flow through sample. The LCVs were collected in the eluate sample. After the Histodenz gradient most of the LCVs were found in fraction 4 and some LCVs in fraction 3 (Figure 3.18).

D. discoideum Ax3 or calnexin-GFP producing *D. discoideum* were infected with *L. longbeachae* producing Dsred and SidC_{Lpn} (pCR80) (Figure 3.19). After infection with *L. longbeachae* producing Dsred and SidC_{Lpn} the cells detached right after the infection (Figure 3.10). Since many cells were lost during the washing step of the infected cells, the washing step was omitted in further experiments. The infected cells were homogenized and the binding to the column was mediated through an anti-SidC_{Lpn} antibody followed by the secondary MACS anti-rabbit antibody. LCVs were visible in the homogenate and in the pellet sample. After adding the sample to the MACS column it took in most of the experiments much longer for the sample to flow through the column than we have seen before for the *L. pneumophila* samples. The flow through contained free bacteria (Figure 3.19). In the eluate LCVs were found. After the separation step through the Histodenz gradient some LCVs were found in fraction 3, 4 and 5. The major amount of LCVs was

3. Results

found in fraction 4 (Figure 3.19) which is comparable with the distribution of LCVs in the Histodenz gradient of *L. pneumophila* [2, 54, 140, 141].

Throughout this work the yield of isolated LCVs was too small for further proteomic analysis. This problem was not solved by omitting the first washing step of the cells or through increasing the MOI. Also, a lot of cell debris were left in fraction 4 (Figure 3.19).

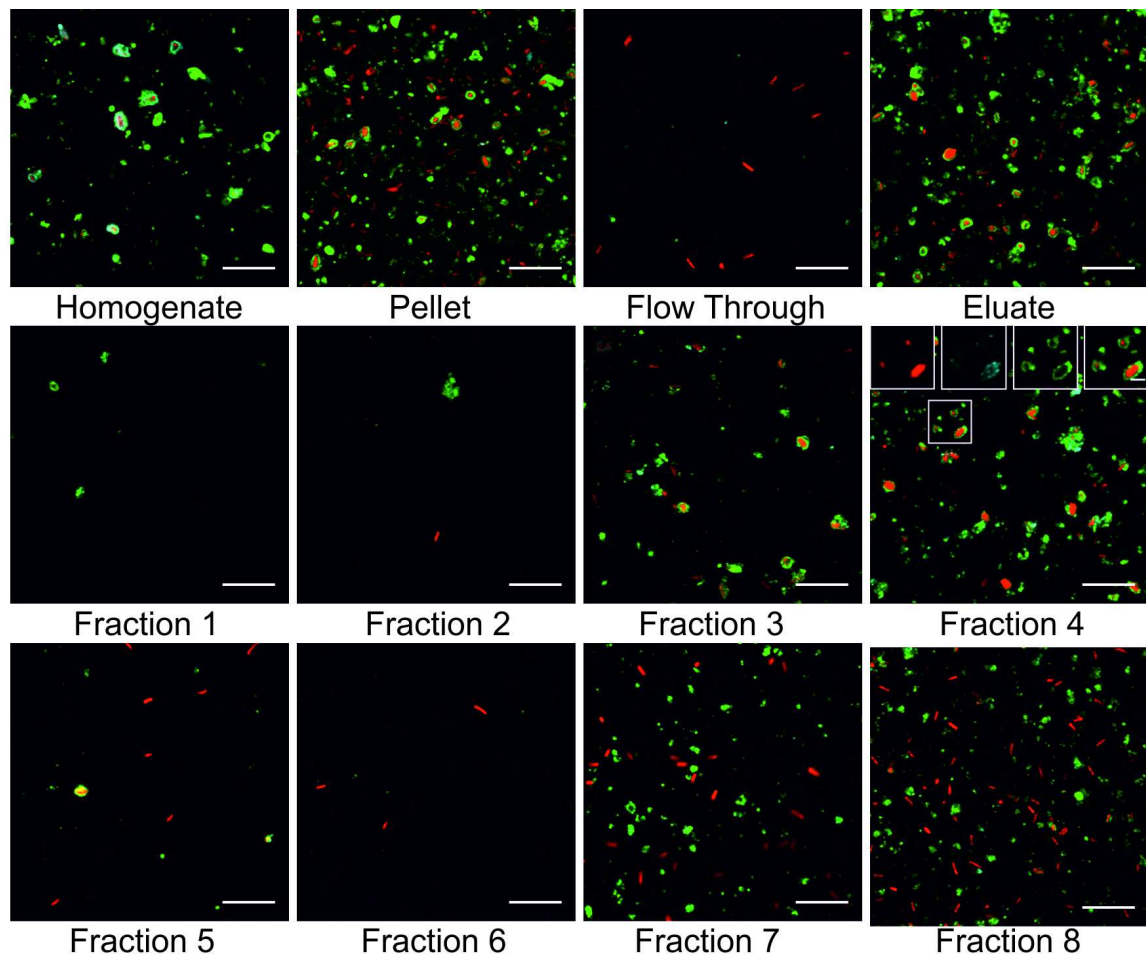


Figure 3.18. Purification of *L. pneumophila*-containing vacuoles from *D. discoideum*. Calnexin-GFP producing *D. discoideum* Ax3 (green) were infected (MOI 50, 1h) with *L. pneumophila* harbouring Dsred (red) on a plasmid (pSW001) at 25°C. The infected cells were homogenized (homogenate), centrifuged (pellet) and incubated with an anti-SidC_{Lpn} antibody followed by a MACS anti-rabbit antibody. The cell suspension was added to the column (flow through) and was eluted with HB-buffer (eluate). The eluate was added on a Histodenz gradient, centrifuged and eight fractions were analyzed starting from the bottom of the column (fraction 1 to 8). SidC_{Lpn} was stained with an anti-SidC_{Lpn} antibody (blue). The bar in the large pictures denote 10 µm and in the smaller picture 2 µm. The experiment has been done with calnexin-GFP producing or unlabeled *D. discoideum* Ax3 three times.

3. Results

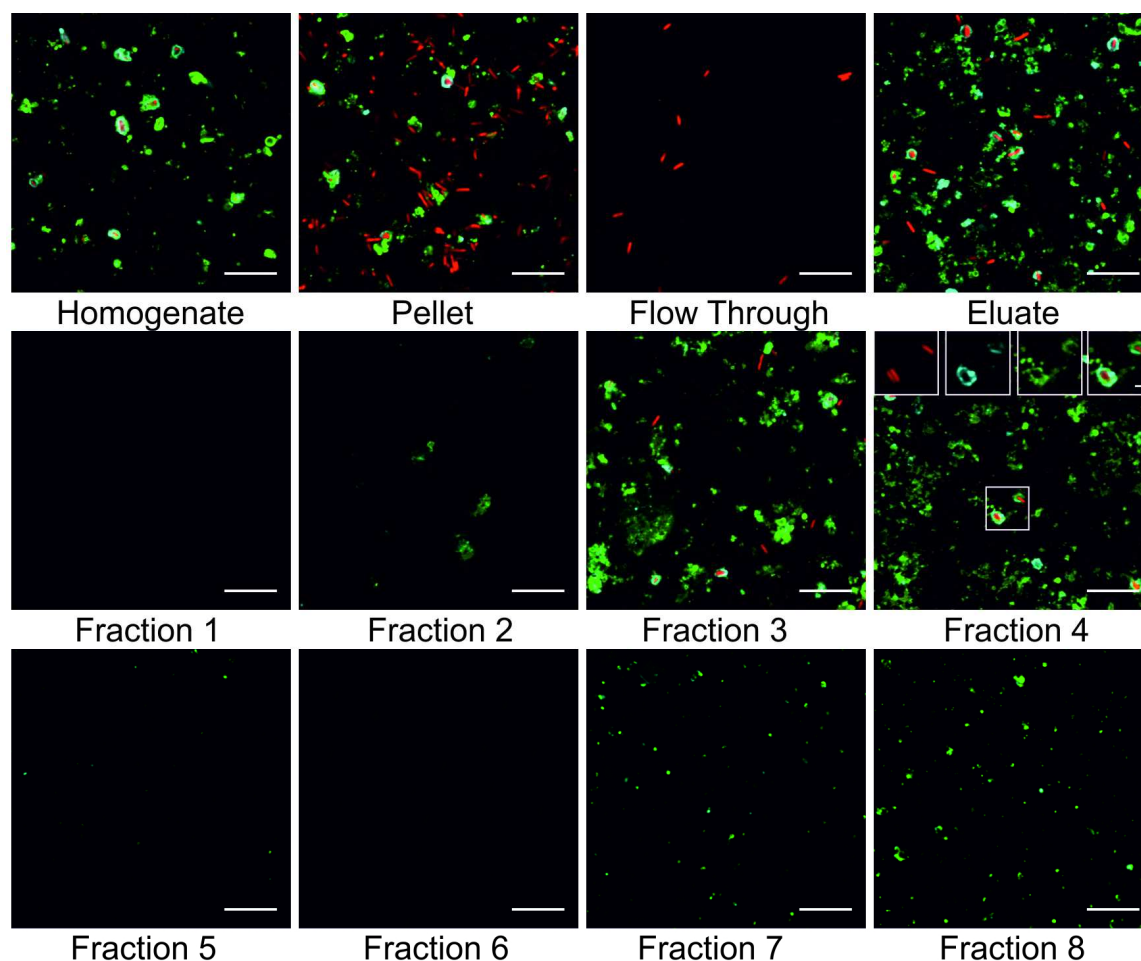


Figure 3.19. Purification of *L. longbeachae*-containing vacuoles from calnexin-GFP producing *D. discoideum*. Calnexin-GFP producing *D. discoideum* Ax3 (green) were infected (MOI 50, 1h) with *L. longbeachae* harbouring Dsred (red) and SidC_{Lpn} on a plasmid (pCR80) at 25°C. A homogenate was prepared and the cell suspension was centrifuged (pellet). The cell solution was incubated with an anti-SidC_{Lpn} antibody followed by a MACS anti-rabbit antibody. The LCVs were separated from free bacteria with a column (flow through and eluate). A further separation step was done with a Histodenz gradient (fraction 1 to 8). All samples were centrifuged on coverslips coated with poly-L-lysine. The overexpressed SidC_{Lpn} was stained with an anti-SidC_{Lpn} antibody (blue). The bar of the big pictures denote 10 µm and of the smaller picture 2 µm. The experiment was done twice with wild-type *D. discoideum* Ax3 or calnexin-GFP producing *D. discoideum*.

3.2.2 Purification of *L. longbeachae*-containing vacuoles from RAW 264.7 macrophages

After realizing that the purification of a *L. longbeachae*-containing vacuole from *D. discoideum* does not seem to be possible without extensive alterations of the protocol we decided to try to isolate the LCVs from RAW 264.7 macrophages.

3. Results

3.2.2.1 Purification of *L. longbeachae*-containing vacuoles from RAW 264.7 macrophages with an anti-SidC_{Lpn} antibody

To this end, we infected RAW 264.7 macrophages with *L. longbeachae* harbouring a plasmid encoding Dsred and SidC_{Lpn}. Again as a control experiment RAW 264.7 macrophages were infected with Dsred expressing *L. pneumophila* (Figure 3.20). *L. pneumophila*-containing vacuoles covered by SidC_{Lpn} were visible in the homogenate and the amount of LCVs was enriched in the pellet. In the flow through no LCVs were visible. Small amounts of LCVs were detected in the eluate and in fraction 4 (Figure 3.20).

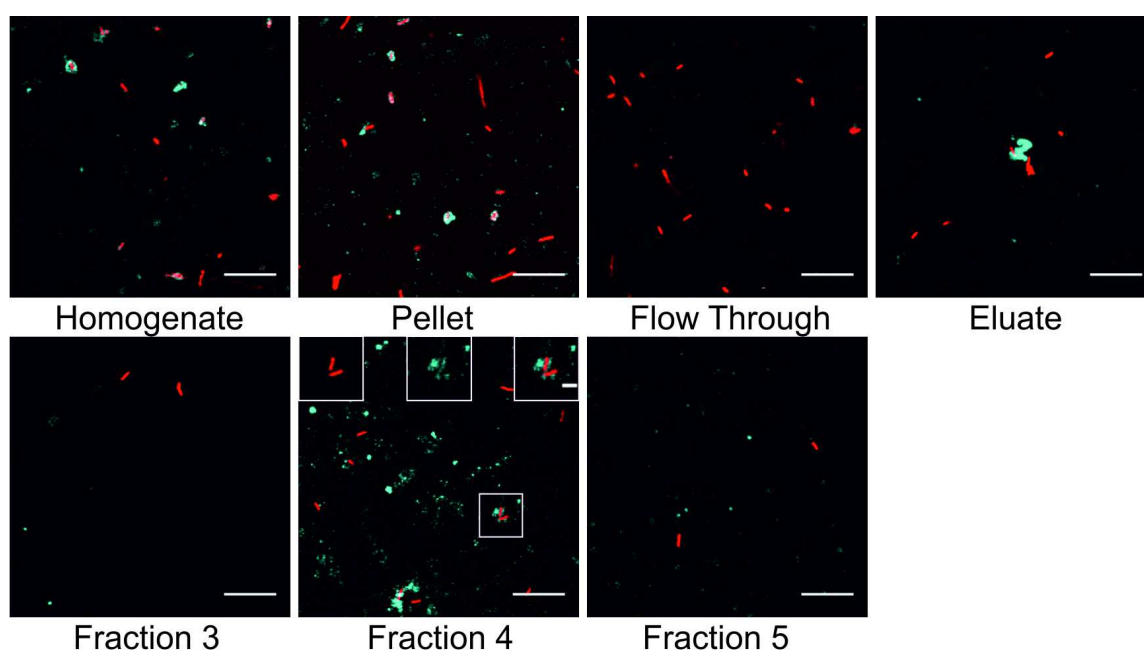


Figure 3.20. Purification of *L. pneumophila*-containing vacuoles from RAW 264.7 macrophages. Dsred expressing *L. pneumophila* (pSW001) (red) were used to infect RAW 264.7 macrophages (MOI 50) for 1 hour at 37°C with 5% CO₂. The cells were homogenized. The cell suspension was concentrated by centrifugation and was resuspended in a smaller volume of buffer (pellet). An anti-SidC_{Lpn} antibody followed by a MACS anti-rabbit antibody was used to incubate the cell suspension. This suspension was applied to the column (flow through) and was eluted with HB-buffer (eluate). A further separation step was performed with a Histodenz gradient. Eight fractions were taken from the gradient starting from the bottom of the column (fraction 1 to 8). The samples were fixed on coverslips and the endogenous SidC_{Lpn} was stained with an anti-SidC_{Lpn} antibody. The bar of the big pictures denote 10 µm and of the smaller picture 2 µm. The experiment was done two times.

After infecting RAW 264.7 macrophages with *L. longbeachae* harbouring a Dsred- and SidC_{Lpn}-encoding plasmid the amount of LCVs in the homogenate and the pellet were comparable with the amount of LCVs in the *L. pneumophila* control (Figures 3.20 and 3.21). Again we observed that the sample applied to the column took much longer to rinse through the column than the *L. pneumophila* samples did before. In the flow through

3. Results

bacteria were visible and in the eluate few LCVs were found. Most of the bacteria appeared in fraction four and five whereas the LCVs were located in fraction four. However, only few *L. longbeachae*-containing vacuoles were observed (Figure 3.21).

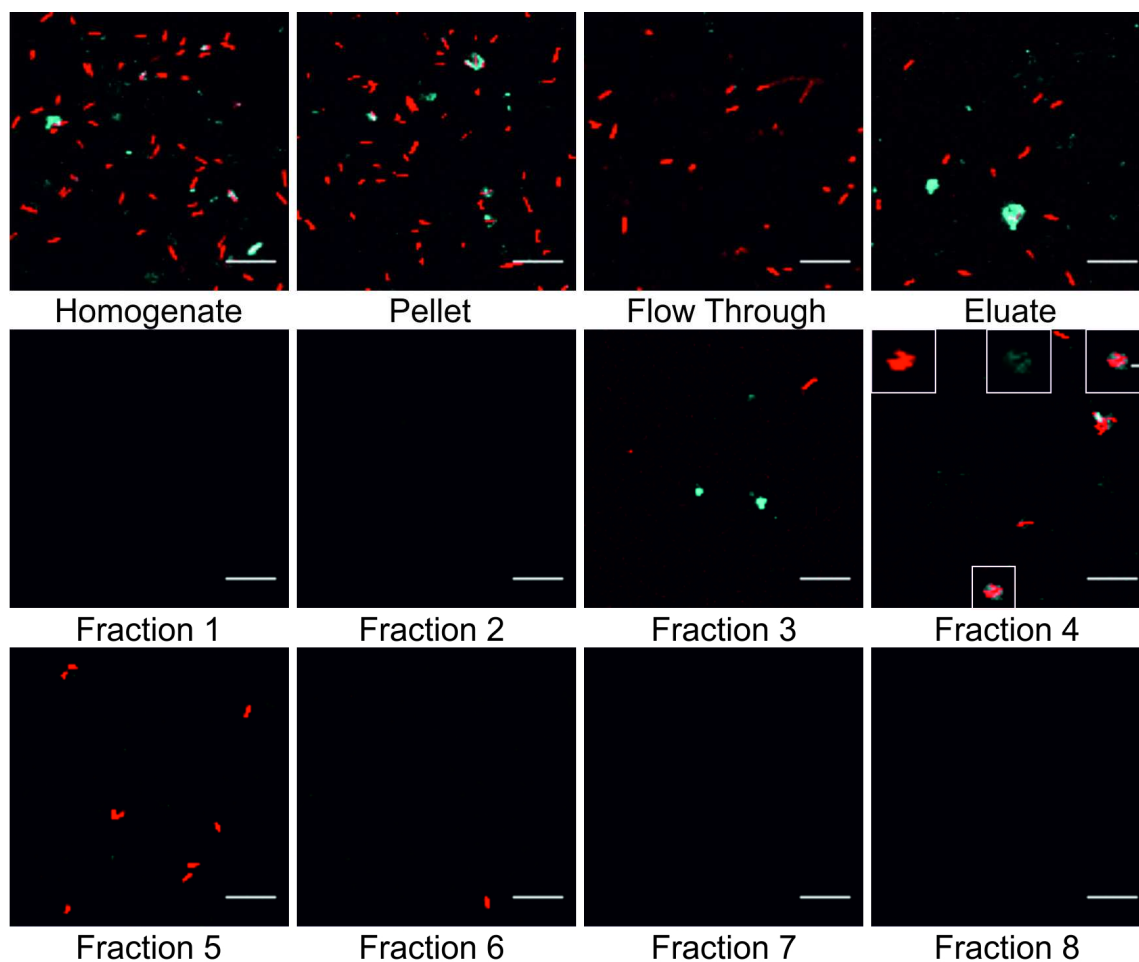


Figure 3.21. Purification of *L. longbeachae*-containing vacuoles from 264.7 macrophages with an anti-SidC_{Lpn} antibody. RAW 264.7 macrophages were infected (MOI 50, 1h) with *L. longbeachae* harbouring plasmid-encoded Dsred and SidC_{Lpn} (pCR80) at 37°C with 5% CO₂. After homogenization the cells were centrifuged (pellet). The cell suspension was incubated with an anti-SidC_{Lpn} antibody followed by a MACS anti-rabbit antibody. The cell suspension was run through a column (flow through). The bound sample was eluted with HB-buffer (eluate). The eluate was separated with a Histodenz gradient. An analysis of eight fractions starting from the bottom of the column (fraction 1 to 8) was performed (bar = 10 µm). After fixing the samples on coverslips the samples were stained with an anti-SidC_{Lpn} antibody. The bar of the big pictures denote 10 µm and of the smaller picture 2 µm. The experiment was done four times.

3.2.2.2 Purification of *L. longbeachae*-containing vacuoles from RAW 264.7 macrophages with an anti-SidC_{Llo} antibody

After generating the new anti-SidC_{Llo} antibody (section 2.2.10) a purification of *L. longbeachae*-containing vacuoles from infected RAW 264.7 macrophages was tried

3. Results

using wild-type *L. longbeachae* harbouring a Dsred producing plasmid. The previously published protocol for the LCV purification from RAW 264.7 macrophages [2] was not changed, other than using the anti-SidC_{L10} antibody instead of the anti-SidC_{Lpn} antibody.

Compared to a LCV isolation from RAW 264.7 macrophages infected with *L. pneumophila* using a SidC_{Lpn} specific antibody (Figure 3.20), the amount of bacteria and also the amount of LCVs in the homogenate and pellet were low. This did not change with increasing MOI. In the flow through bacteria were visible. Unfortunately, only bacteria without a SidC_{L10} staining were found in the eluate. Subsequently, the bacteria were found in fraction three and four. Taken together, it seems that the purification of a *L. longbeachae*-containing vacuole with endogenous SidC_{L10} is not possible with this protocol (Figure 3.22).

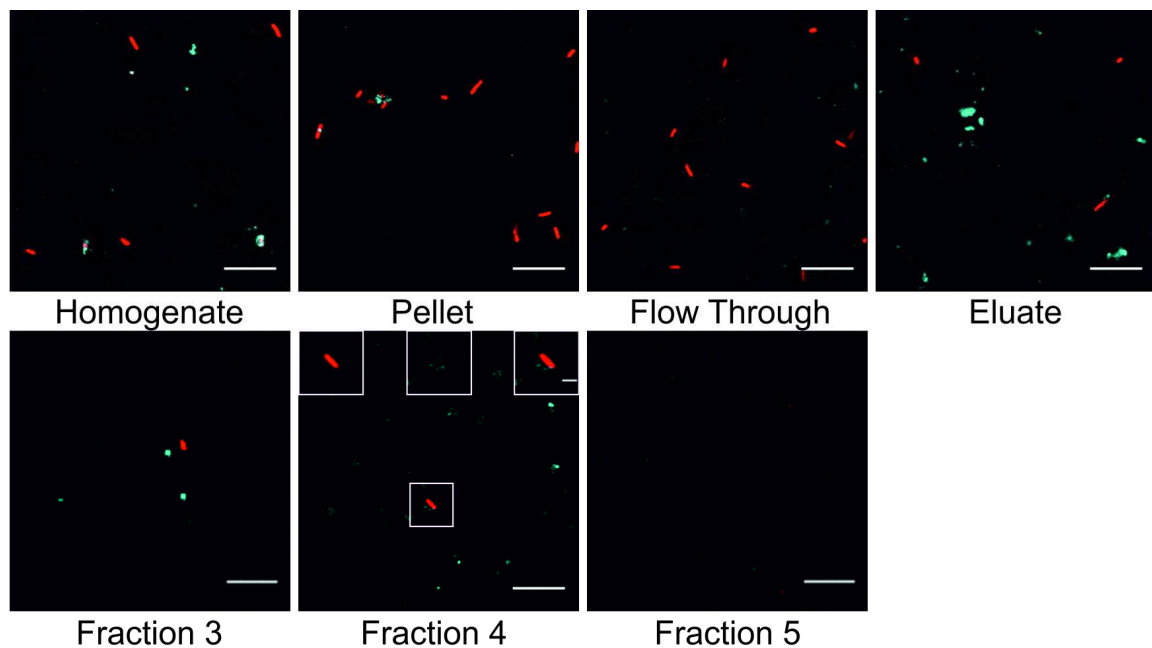


Figure 3.22. Purification of *L. longbeachae*-containing vacuoles from RAW 264.7 macrophages with an anti-SidC_{L10} antibody. The cells were infected (MOI 10, 1h) with *L. longbeachae* harbouring a Dsred-encoding plasmid (pSW001) at 37°C with 5% CO₂. The infected cells were homogenized and the cell suspension was centrifuged (pellet). The cell suspension was incubated with an anti-SidC_{L10} antibody followed by a MACS anti-rabbit antibody. The sample was added to a MACS column and the flow through was collected (flow through). The sample bound to the MACS column was eluted with HB-buffer. A Histodenz gradient was used to further separate the eluate into eight fractions. The fractions were collected starting from the bottom of the column (fraction 1 to 8). The samples were fixed on coverslips coated with poly-L-lysine and stained with an anti-SidC_{L10} antibody. The bar of the big pictures denote 10 µm and of the smaller picture 2 µm. The experiment was done two times with different MOIs.

4. Discussions

4.1 The *L. longbeachae* Icm/Dot substrate SidC_{Llo}

L. longbeachae and *L. pneumophila* are the causative agents of the Legionnaire's disease. *L. pneumophila* is well characterized regarding ecological habitat, transmission, physiology and effector proteins. In contrast, only little is known about *L. longbeachae*. The aim of this part of the PhD thesis was to analyze the first effector protein, SidC_{Llo}, of *L. longbeachae*. To this end, biochemical and genetic analysis were used. In an unbiased phosphoinositide-pulldown *L. longbeachae* lysate was incubated with PtdIns or different PIs. SidC_{Llo} coupled to agarose beads was found to be the major PtdIns(4)*P* binding protein of *L. longbeachae*. No other effector protein was found, which bound to PtdIns or any PI lipid [3]. In the case of *L. pneumophila* among over 300 known effector proteins [56, 57] many are binding in an Icm/Dot-dependent manner to PI lipids. The Rab1 GEF/AMPyase SidM (also known as DrrA) [45, 56, 81, 104, 144], SidC_{Lpn} and its paralogous protein SdcA_{Lpn} [80, 103] are binding to PtdIns(4)*P*, and the retromer interactor RidL [91] is known to bind to PtdIns(3)*P*. In the analogous experiment using *L. pneumophila* lysate, SidM and not SidC_{Lpn} was previously found to bind with high affinity to PtdIns(4)*P* [81, 145]. It was previously shown that the amino acids 340 to 647 of SidM, which contain the GEF domain and the P4M domain, had a higher binding affinity to PtdIns(4)*P* ($K_D = 30$ nM) [104] than SidC_{Lpn} has ($K_D = 243$ nM) [3]. The low binding affinity of SidC_{Lpn} to PtdIns(4)*P* could be the reason why SidC_{Lpn} was not even detected in the absence of SidM [81]. SidC_{Llo}, however, had a K_D of 71 nM and thus a 3.4 fold higher binding affinity to PtdIns(4)*P* than SidC_{Lpn} as measured by isothermal calorimetry measurement (ITC) [3]. Therefore, this assay does not seem to detect binding partners with a low affinity to PtdIns or the different PIs. Other *L. longbeachae* proteins could also form complexes with PtdIns or PI binding proteins of *L. longbeachae* and thus prohibit the pulldown. Chaperones like DnaK could be possible interaction partners.

The P4C domain of SidC_{Llo} was found in an assay using "PIP-strips" to localize to the amino acid region 609 to 769 (Figure 3.2B) [3]. This region is analogous to the P4C domain of SidC_{Lpn} which is localized in the amino acid region 609 to 776 [103]. The binding affinity of SidC_{Llo} to PtdIns(4)*P* was also in this case much higher than the affinity of SidC_{Lpn} to PtdIns(4)*P* analyzed with "PIP-arrays" (Figure 3.2C) [3]. This result was

4. Discussions

supported by the ITC measurement mentioned before [3]. SidC_{Lpn_P4C} is binding stronger to PtdIns(4)*P* than SidC_{Llo_P4C} (Figure 3.2C) [3]. It could be that amino acids outside the SidC_{Llo_P4C} domain support the binding and are missing in this assay. Unfortunately, due to an insolubility of the P4C domains of the proteins at the high concentrations needed for the ITC measurements it was not possible to further quantify the binding affinities of the two P4C domains. The influences of the N-terminal domains of SidC_{Llo} and SidC_{Lpn} on the P4C domain of *L. pneumophila* and *L. longbeachae* were tested using PIP-strips and -arrays. The chimera proteins showed nearly the same binding affinity towards PtdIns(4)*P* like the corresponding P4C domains (Figures 3.2C, D and E). This result can be due to a missing effect of the N-terminal part of SidC_{Llo} or SidC_{Lpn} on the binding affinity of the P4C domains of *L. pneumophila* or *L. longbeachae* to PtdIns(4)*P* or due to a miss folding of the protein. Therefore we cannot say, if the N-terminal domain of SidC_{Llo} and SidC_{Lpn} has an effect on the binding affinity of the P4C domains of SidC_{Lpn} and SidC_{Llo} to PtdIns(4)*P*. Certainly the P4C domains of *L. longbeachae* and *L. pneumophila* are the major PtdIns(4)*P* binding part of SidC_{Llo} and SidC_{Lpn}. It was shown that despite of their different binding affinity to PtdIns(4)*P*, SidC_{Llo} and SidC_{Lpn} share similar secondary structure compositions [3], whereas the sequence identity of these two proteins is only 40% (Figure 3.3) [3]. Also the P4C domains of SidC_{Llo} and SidC_{Lpn} consist only of 45% of the same amino acids (Figure 3.3)[3]. Therefore, the difference in the sequences could be a reason for the differences in the binding affinity. An amino acid exchanges in the P4C domain of SidC_{Llo} and SidC_{Lpn} might play a role in the different binding affinities to PtdIns(4)*P*. The Icm/Dot-dependent translocation of SidC_{Llo} was analyzed using plasmid-encoded CyaA-SidC_{Llo} transformed into wild-type and a *dotA* deletion mutant of *L. longbeachae* and *L. pneumophila*. Unfortunately, the only Icm/Dot-dependent translocation was shown for the positive control CyaA-SidC_{Lpn} translocated from *L. pneumophila* wild-type but not from the *dotA* deletion mutant (Figure 3.5A). In a Western blot analysis using specific anti-SidC antibodies it was obvious that only *L. pneumophila* but not *L. longbeachae* is producing CyaA-SidC_{Lpn} and CyaA-SidC_{Llo} (Figure 3.5B). No CyaA specific antibody was available. Therefore, it was not possible to show whether the CyaA-tag of CyaA-SidC_{Lpn} and CyaA-SidC_{Llo} produced in *L. longbeachae* was cut off, or if the fusion proteins are produced at all. Even a change in the duration of the induction did not change the results seen in the Western blot analysis (data not shown). In a further attempt a plasmid with the

4. Discussions

L. longbeachae effector protein CetLI1 coupled to CyaA was obtained from the group of Gil Segal to test if a translocation of a *L. longbeachae* effector protein could be shown at all. CetLI1 was published to be translocated when overexpressed in *L. pneumophila* [58]. After transformation of the CyaA-CetLI1-producing plasmid into wild-type and a *dotA* deletion mutant of *L. longbeachae* and *L. pneumophila*, a cAMP assay was performed. In repeated attempts using different lysis methods, the protein CetLI1 was only translocated by *L. pneumophila* wild-type but not by *L. longbeachae* wild-type (Figure 3.5C). This ruled out that the change of the cell line from HL-60-derived human macrophages used from the group of Gil Segal [58] to RAW 264.7 macrophages used in this experiment could be the reason for the failure to observe translocation in the case of *L. longbeachae* wild-type. Maybe the capsule of *L. longbeachae* prevents the detection of translocation in this assay. In another attempt the new SidC_{L10} antibody was used in an immunofluorescence assay using RAW 264.7 macrophages to verify if SidC_{L10} is translocated in an Icm/Dot-dependent manner. Around 50% of the LCVs harbouring wild-type *L. longbeachae* were positive for endogenous SidC_{L10} whereas the translocation of SidC_{Lpn} was slightly more efficient. This could be due to the higher amount of SidC_{Lpn} produced compared to the endogenously produced SidC_{L10}. Nearly no SidC_{L10} or SidC_{Lpn} localization was visible on a LCV harbouring the *dotA* deletion mutant of *L. longbeachae* (Figure 3.6). Therefore SidC_{L10} is translocated in an Icm/Dot-dependent manner.

In the next step the role of SidC_{L10} in the intracellular replication of *L. longbeachae* in RAW 264.7 macrophages and *A. castellanii* was characterized more closely. To this end, a *sidC_{L10}* deletion strain [3] was used. The infection rates were similar for the wild-type and the *sidC_{L10}* deletion strain, whereas the *dotA* deletion mutant did not grow (Figure 3.7) [3]. The wild-type strain of *L. longbeachae* outcompeted the *sidC_{L10}* deletion strain in a direct competition assay within 24 days of *A. castellanii* infection (Figure 3.8A). Both strains grew equally alone in *A. castellanii* (Figure 3.8C). In the case of a wild-type *L. pneumophila* strain compared to a *sidC-sdcA_{Lpn}* deletion mutant the wild-type won the competition within 12 days (Figure 3.8B). Again both strains grew equally alone in *A. castellanii* (Figure 3.8D) [3]. Therefore, SidC_{L10} seems to be less important for the infection of *A. castellanii* than SidC_{Lpn} and SdcA_{Lpn}. The reason remains unclear. A similar competition defect was previously observed for the Icm/Dot-translocated protein LegG1, a Ran GTPase activating effector [84, 146].

4. Discussions

We analyzed the effect of SidC_{L10} in the ER recruitment to the LCV in *D. discoideum* infected with *L. longbeachae*. The cells rounded up right after the infection and were lost during the washing steps of the immunofluorescence labeling. In a direct comparison between a wild-type and a *dotA* deletion mutant of *L. longbeachae* it was shown that the effect was Icm/Dot-dependent (Figure 3.10). A cytotoxic effect of *L. longbeachae* on *D. discoideum* could be ruled out (Figure 3.11). The cell surface seems to get modified and therefore the cell is not able to attach to the surface any longer. Effector proteins are known for *L. pneumophila*, which modulate the cytoskeleton. For example the Icm/Dot-dependent *L. pneumophila* effector protein LegG1 activates the small GTPase Ran and promotes the migration of *D. discoideum* [146, 147]. LegG1 is missing in the genome of *L. longbeachae* [26]. Other Icm/Dot-dependent effector proteins of *L. longbeachae* could interfere with the cytoskeleton. A lack of these effector proteins could result in a cell which rounds up.

Calnexin recruitment to the LCV in infected *D. discoideum* was impaired due to the loss of the *L. pneumophila* genes *sidC*_{Lpn} and *sdcA*_{Lpn}. The decreased calnexin recruitment can be complemented by overexpressing SidC_{Lpn} or SdcA_{Lpn} [103]. Calnexin-GFP *D. discoideum* were infected with a *L. pneumophila sidC-sdcA*_{Lpn} deletion strain harbouring a plasmid encoding for SidC_{L10} and the cells were fixed with paraformaldehyde. Only few LCVs were covered with calnexin-GFP (Figures 3.12A and B). This result did not alter in an infection from one till four hours (Figure 3.12C).

In a next step, life cell imaging was used to assay the ER recruitment with *L. pneumophila* infected *D. discoideum* (Figure 3.13). Using this approach a complementation of the loss of the calnexin recruitment to the LCV in cells infected with *L. pneumophila* lacking the *sidC-sdcA*_{Lpn} genes with SidC_{L10} was observed (Figure 3.13) [3]. Therefore, the fixation of the cells seemed to affect the calnexin-GFP signal on the LCV. Why this influenced only the calnexin-GFP recruitment in the complementation assay with SidC_{L10} remains unclear. Afterward we analyzed the ER recruitment with *L. longbeachae* infected *D. discoideum* with life cell imaging (Figure 3.14). LCVs harbouring wild-type *L. longbeachae* were calnexin-GFP positive. The *dotA* and *sidC*_{L10} genes were necessary for the calnexin recruitment to the LCV infected with *L. longbeachae*. A complementation of the loss of the calnexin recruitment to the LCV was possible through

4. Discussions

overexpression of SidC_{Lio}, SidC_{Lpn} and SdcA_{Lpn} (Figure 3.14) [3]. Despite of a sequence identity of only 40% both SidC effectors proteins seem to be functionally redundant.

The PH_{FAPP1} domain binds through PtdIns(4)*P* to the LCV [80]. Also SidC_{Lio_P4C} and SidC_{Lpn_P4C} bind to the *L. pneumophila*-containing vacuole with nearly the same efficiency as the PH_{FAPP1} domain [3]. Therefore, SidC_{Lio_P4C} and SidC_{Lpn_P4C} can be used as LCV markers (Figure 3.15).

The results of this study pave the way for further analysis of the role of SidC_{Lio} in the ER recruitment to LCVs. Also, the first antibody against a *L. longbeachae* effector is now available to characterize the *L. longbeachae*-containing vacuole more closely.

4.2 Purification of LCVs from *L. longbeachae*

At the onset of this project no antibody was available which recognized any known *L. longbeachae* effector protein covering the LCV. Yet, the translocation of SidC_{Lpn} to the *L. longbeachae*-containing vacuole was observed in infected *D. discoideum* cells, and SidC_{Lpn} covered the whole LCV (Figure 3.17). Hence a purification of a *L. longbeachae*-containing vacuole was tried using *L. longbeachae* harbouring a plasmid coding for a Dsred protein and SidC_{Lpn} (Figure 3.19). LCV purification with *L. pneumophila* producing Dsred was done as a control (Figure 3.18). The previously published protocols were used for the LCV purification [2, 54, 140, 141]. Many cells were lost during the washing step due to the fact that the *D. discoideum* cells detached from the flask within minutes after adding *L. longbeachae*. Therefore, a protocol without washing was used in further experiments (Figure 3.19). An enrichment of the LCVs in the eluate was visible and the amount of LCVs was comparable to the amount of LCVs obtained in the control experiment with *L. pneumophila* wild-type. A Histodenz gradient was used to get rid of extracellular bacteria and cell debris. Unfortunately, the amount of LCVs decreased significantly and much cell debris remained. Nevertheless most of the LCVs were found in fraction 4 (Figure 3.19). The amount and purity of the LCVs was not enough for a proteome analysis of *L. longbeachae*-containing vacuoles. The purification step with the Histodenz gradient seems not to be optimal for the purification of *L. longbeachae*-containing vacuoles. An alternative purification step should be tried. Therefore, other gradients like “OptiPrepTM Density Gradient Medium” (Sigma) could be tried.

4. Discussions

A purification of *L. longbeachae*-containing vacuoles from infected RAW 264.7 macrophages was tried. Again a purification of *L. pneumophila*-containing vacuoles was performed as a positive control (Figure 3.20). After infection of the RAW 264.7 macrophages with *L. longbeachae* harbouring a plasmid coding for Dsred and SidC_{Lpn} the cells did not detach from the flask like *D. discoideum*. Few LCVs were found in the eluate and in fraction 4. A separation of the LCVs from extracellular bacteria and cell debris was obtained but the number of LCVs visible in fraction 4 was much too low for a proteomic analysis (Figure 3.21).

During this work a SidC_{Llo} antibody was raised. Therefore, a purification of *L. longbeachae*-containing vacuoles from RAW 264.7 macrophages using endogenous SidC_{Llo} and the corresponding antibody was tried. Unfortunately, the yield of LCVs was from the beginning much lower than in the experiments with overexpressed SidC_{Lpn} (Figures 3.20 and 3.22). The few LCVs were lost during the enrichment process in the cell suspension and upon running the sample through the MACS column. Therefore, only extracellular bacteria were found in fraction 3 and 4 (Figure 3.22). We have noticed that the sample took much longer to rinse through the column than the *L. pneumophila* samples. Maybe the column was clogged and the LCVs were retained by the column. The reason for this remains unclear.

In all preparations SidC_{Lpn} or SidC_{Llo} rarely cover the LCV completely. If SidC_{Lpn} was overexpressed the amount of SidC_{Lpn} translocated to the LCV membrane was much higher than the amount of SidC_{Llo} which is produced endogenously. Therefore, recognition of LCVs in the samples and binding of the LCVs to the MACS column was enhanced. As a consequence, the purification of *L. longbeachae*-containing vacuoles from RAW 264.7 macrophages could be more efficient with a strain overexpressing SidC_{Lpn} than with the endogenous produced SidC_{Llo} (Figures 3.20 till 3.22). Also an increased cell number could be tried. However, further cellular analysis of the influence of SidC_{Lpn} on the protein composition of *L. longbeachae*-containing vacuoles need to be done, if a *L. longbeachae* strain harbouring Dsred and SidC_{Lpn} is used to obtain LCVs for a proteomic analysis. Alternatively, other *L. longbeachae* effector proteins which cover the LCV completely and an antibody against this protein could be used. Thus, the amount of purified LCVs harbouring *L. longbeachae* might be increased.

5. General conclusions and outlook

In my Ph.D. thesis I have analyzed the first Icm/Dot-dependent effector protein of *L. longbeachae*, SidC_{Llo}. SidC_{Llo} binds with a distinct P4C domain to PtdIns(4)*P* located on the LCV. This P4C domain can be used as a LCV marker in immunofluorescence assays. The binding affinity of SidC_{Llo} to PtdIns(4)*P* is much higher compared to SidC_{Lpn}. Just as SidC_{Lpn} SidC_{Llo} is also important for ER recruitment to the LCV, and therefore, plays a pivotal role in the pathogen-host interaction. Interestingly, this effect could be complemented by adding plasmid-encoded SidC_{Llo} or SidC_{Lpn} in reciprocal assays. Both proteins seem to improve the intracellular replication of *L. longbeachae* and *L. pneumophila* in infected *A. castellanii*. Despite of a small sequence identity and the difference in the binding affinities to PtdIns(4)*P* both proteins seem to play similar roles in the intracellular replication of *L. longbeachae*.

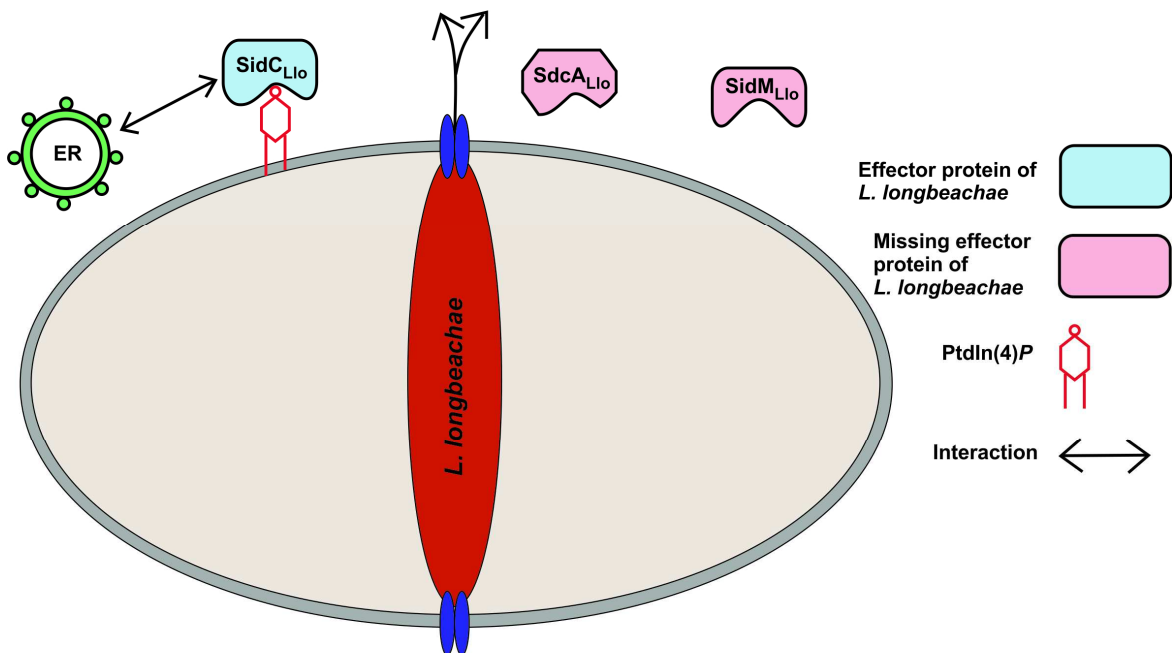


Figure 4.1. The Icm/Dot-dependent effector protein SidC_{Llo} is binding through PtdIns(4)*P* to *L. longbeachae*-containing vacuoles and interacts with the ER. SidC_{Llo} is translocated by the Icm/Dot T4SS into the host cell cytoplasm and binds through PtdIns(4)*P* to the *L. longbeachae*-containing vacuole. The effector protein SidC_{Llo} interacts with the ER [3]. SidM and SdcA are missing in the genome of *L. longbeachae* [26].

We started to isolate *L. longbeachae*-containing vacuoles from *D. discoideum* or RAW 264.7 macrophages with protocols previously published [2, 54, 140, 141]. To this end, we

5. General conclusions and outlook

overexpressed SidC_{Lpn} in *L. longbeachae* and used an anti-SidC_{Lpn} antibody for the purification. The isolation from LCVs from *D. discoideum* worked much better than the isolation from RAW 264.7 macrophages. We raised the first known antibody against a *L. longbeachae* effector protein, which recognizes only SidC_{Llo} but not SidC_{Lpn}. This antibody was used to isolate *L. longbeachae*-containing vacuoles from infected RAW 264.7 macrophages. Unfortunately, this attempt failed. Further investigations need to be done to optimize the existing protocols for a purification of *L. longbeachae*-containing vacuoles. Thus, it should be possible to isolate *L. longbeachae*-containing vacuoles at least from infected *D. discoideum* in an appropriate yield and purity to analyse their proteome.

6. List of abbreviations

6. List of abbreviations

Amp	ampicillin
AMPylation	adenosine mono-phosphorylation
APS	ammonium persulphate
ARF	ADP ribosylation factor
AYE	ACES yeast extract
BSA	bovine serum albumin
Caln	calnexin
Cam	chloramphenicol
CetLI	C-terminal signal for effector translocation of <i>L. longbeachae</i>
cfu	colony forming units
CYE	charcoal yeast extract
DAG	diacylglycerol
Dd5P4	<i>Dictyostelium discoideum</i> 5-phosphatase 4
DFA	direct fluorescent antibody
dot	defective in organelle trafficking
EDTA	ethylenediaminetetraacetate
EEA1	early endosomal antigen 1
EGTA	ethyleneglycol-bis(aminoethylether)-N, N, N', N'-tetra acetic acid
ER	endoplasmic reticulum
FAPP1	phosphatidylinositol (4) phosphate adaptor protein 1
G418	geneticin sulphate
GAP	GTPase-activating protein
GDI	guanine nucleotide dissociation inhibitor
GDF	GDI displacement factor
GEF	guanine nucleotide exchange factor

6. List of abbreviations

icm	intracellular multiplication
IPTG	isopropyl- β -D-thiogalactopyranoside
ITC	isothermal titration calorimetry
Kan	kanamycin
K _D	dissociation equilibrium constant
kDa	kilo Dalton
LAMP1	lysosomal associated membran glycoprotein 1
LB	Luria-Bertani
LCMS	liquid chromatography-mass spectrometry
LCV	<i>Legionella</i> -containing vacuole
LidA	lowered viability in the presence of <i>dotA</i>
LPA	lysophosphatidic acid
LPC	lysophosphocholine
MALDI-TOF	matrix-assisted laser desorption/ionization-time of flight
MOI	multiplicity of infection
MOPS	3-(N-morpholino)propane sulfonic acid
MVB	multivesicular bodies
OCRL1	oculocerebrorenal syndrome of Lowe 1
OD ₆₀₀	optical density at 600nm
P4C	<u>P</u> tdIns(4) <u>P</u> -binding of Sid <u>C</u>
P4M	<u>P</u> tdIns(4) <u>P</u> -binding of Sid <u>M</u> /DrrA
PA	phosphatidic acid
PBS	phosphate-buffered saline
PC	phosphatidylcholine
PE	phosphatidylethanolamine
PFA	paraformaldehyde
PH	pleckstrin homology

6. List of abbreviations

PI	phosphoinositide
PI3K	phosphatidylinositol 3-kinase
PI4KIII β	PtdIns 4-kinase III β
PMSF	phenylmethylsulfonylfluoride
PS	phosphatidylserine
psi	pound-force per square inch
PtdIns	phosphatidylinositol
PtdIns(4) <i>P</i>	phosphatidylinositol(4)phosphate
RalF	recruitment of Arf to <i>Legionella</i> phagosome
rER	rough endoplasmic reticulum
RT	room temperature
S1P	sphingosine-1-phosphate
SDS	sodium dodecyl sulfate
Sg1	serogroup 1
SidC	substrate of Icm/Dot transporter
SorC	Sörensen phosphate buffer
T4SS	type IV secretion system
TEMED	N, N, N', N' tetramethylethyldiamine
TBS	TRIS buffered saline
TCEP	TRIS(2-carboxyethyl)phosphine
TROV	Texas red ovalbumin

7. Index of figures

Figure 1.1. <i>L. pneumophila</i> replicates in phagocytes.	5
Figure 1.2. The role of SidC _{Lpn} and SdcA _{Lpn} on a <i>L. pneumophila</i> -containing vacuole.	11
Figure 1.3. The role of SidC _{Llo} on a <i>L. longbeachae</i> -containing vacuole.	12
Figure 1.4. Effector proteins compete with SidM for Rab1 on the <i>L. pneumophila</i> -containing vacuole.	14
Figure 3.1. SidC _{Llo} is the major PtdIns(4) <i>P</i> binding protein of <i>L. longbeachae</i>	50
Figure 3.2. SidC _{Llo} binds <i>in vitro</i> through a P4C domain to PtdIns(4) <i>P</i>	53
Figure 3.3. Comparison of the primary sequence of SidC _{Llo} , SidC _{Lpn} and SdcA _{Lpn}	54
Figure 3.4. Anti-SidC _{Llo} and anti-SidC _{Lpn} antibodies recognize only their cognate proteins.	55
Figure 3.5. Measurement of translocation of SidC _{Llo}	56
Figure 3.6. SidC _{Llo} is an Icm/Dot-dependent effector protein which localizes to the LCV.	57
Figure 3.7. <i>L. longbeachae</i> lacking <i>sidC</i> _{Llo} grows normally in RAW 264.7 macrophages and <i>A. castellanii</i>	58
Figure 3.8. <i>L. longbeachae</i> and <i>L. pneumophila</i> wild-type strains outcompete the Δ <i>sidC</i> _{Llo} and Δ <i>sidC-sdcA</i> _{Lpn} strains.	59
Figure 3.9. Intracellular replication of <i>L. longbeachae</i> and <i>L. pneumophila</i> in <i>D. discoideum</i>	60
Figure 3.10. <i>L. longbeachae</i> wild-type alters the cell adherence of calnexin-GFP producing <i>D. discoideum</i>	60
Figure 3.11. <i>L. longbeachae</i> shows no cytotoxic effect on <i>D. discoideum</i>	61
Figure 3.12. The calnexin-GFP recruitment to a LCV harbouring a <i>sidC-sdcA</i> _{Lpn} deletion mutant of <i>L. pneumophila</i> is not complemented by SidC _{Llo}	62
Figure 3.13. The decreased ER recruitment to the <i>L. pneumophila</i> Δ <i>sidC-sdcA</i> _{Lpn} containing vacuole in <i>D. discoideum</i> is complemented by SidC _{Llo}	64
Figure 3.14. <i>L. longbeachae</i> SidC _{Llo} is necessary for the ER recruitment to the LCV.	65
Figure 3.15. SidC _{Llo_P4C} and SidC _{Lpn_P4C} binds through PtdIns(4) <i>P</i> to the LCV.	67

7. Index of figures

Figure 3.16. Purification of <i>L. pneumophila</i> -containing vacuoles.	67
Figure 3.17. Overexpressed SidC _{Lpn} is covering a <i>L. longbeachae</i> -containing vacuole in infected <i>D. discoideum</i>	69
Figure 3.18. Purification of <i>L. pneumophila</i> -containing vacuoles from <i>D. discoideum</i>	70
Figure 3.19. Purification of <i>L. longbeachae</i> -containing vacuoles from calnexin-GFP producing <i>D. discoideum</i>	71
Figure 3.20. Purification of <i>L. pneumophila</i> -containing vacuoles from RAW 264.7 macrophages.	72
Figure 3.21. Purification of <i>L. longbeachae</i> -containing vacuoles from 264.7 macrophages with an anti-SidC _{Lpn} antibody.	73
Figure 3.22. Purification of <i>L. longbeachae</i> -containing vacuoles from RAW 264.7 macrophages with an anti-SidC _{Llo} antibody.	74
Figure 4.1. The Icm/Dot-dependent effector protein SidC _{Llo} is binding through PtdIns(4) <i>P</i> to <i>L. longbeachae</i> -containing vacuoles and interacts with the ER.	81

8. Index of tables

Table 2.1. Bacterial strains*.....	16
Table 2.2. Eukaryotic cell lines*.....	17
Table 2.3. Plasmids*.....	17
Table 2.4. Oligonucleotides [3].....	18
Table 2.5. Lab equipments.....	20
Table 2.6. Charcoal yeast extract agar (CYE) [17]*.....	22
Table 2.7. ACES yeast extract medium (AYE) [17]*.....	23
Table 2.8. Antibiotics.....	25
Table 2.9. TFB1*, **.....	26
Table 2.10. TFB2 *, **.....	26
Table 2.11. HL5-medium [135]*, **.....	27
Table 2.12. Freezing medium.....	28
Table 2.13. PYG medium*, **.....	28
Table 2.14. Freezing medium.....	29
Table 2.15. Freezing medium.....	30
Table 2.16. 50x TAE buffer*.....	32
Table 2.17. 5x SDS sample buffer*.....	32
Table 2.18. SDS gel.....	33
Table 2.19. 10x running buffer*.....	33
Table 2.20. Coomassie staining and destaining solutions*.....	34
Table 2.21. Impregnating solution*.....	34
Table 2.22. Developing solution*.....	35
Table 2.23. 10x transfer blotting buffer.....	35
Table 2.24. 10x phosphate buffered saline (PBS)*.....	36
Table 2.25. 10x TRIS buffered saline (TBS).....	36

8. Index of tables

Table 2.26. Primary antibodies.....	36
Table 2.27. Secondary antibodies.....	37
Table 2.28. Lysis buffer*.....	38
Table 2.29. Washing puffer*.....	38
Table 2.30. Elution buffer*.....	38
Table 2.31. Dialysis buffer.....	39
Table 2.32. Elution buffer*.....	40
Table 2.33. Washing solution.....	41
Table 2.34. Sörensens phosphate buffer (SorC) [137]*, **.....	42
Table 2.35. Primary antibodies.....	43
Table 2.36. Secondary antibodies.....	43
Table 2.37. MB medium [138]*, **.....	44
Table 2.38. Ac buffer*.....	45
Table 2.39. HB buffer*.....	47

9. Acknowledgement

I would like to thank my supervisor Prof. Hubert Hilbi for giving me the opportunity to work on this fascinating project. With ideas for the progress of my Ph.D. thesis and technical support he helped me through arising difficulties throughout the project.

His huge research network enabled us to gain access to a *L. longbeachae* wild-type and the corresponding *dotA* deletion mutant provided by Prof. Carmen Buchrieser from the Pasteur Institute in France. I would also like to thank Prof. Carmen Buchrieser for her help.

Through the network of Prof. Hubert Hilbi we were also able to gain access to biophysical techniques provided by Prof. Aymelt Itzen and his Ph.D. student Adam Cichy from the Technische Universität in Munich. Thank you both for providing the ITC and CD measurement data. I want to thank Dr. Mandy Hannemann from the Technische Universität in Munich for cloning the GST-SidC_{L10_1-608-Lpn_609-917} plasmid.

Our whole research group in Munich has helped me with a lot of inspiring discussions and technical help. Especially I want to thank Dr. Ina Haneburger which constructed the *sidC*_{L10} deletion mutant, helped me with the genetic difficulties of *L. longbeachae* and was involved in my publication [3].

10. References

1. Hoffmann, C., et al., *Functional analysis of novel Rab GTPases identified in the proteome of purified Legionella-containing vacuoles from macrophages*. Cell Microbiol, 2013.
2. Hoffmann, C., I. Finsel, and H. Hilbi, *Pathogen vacuole purification from legionella-infected amoeba and macrophages*. Methods Mol Biol, 2013. **954**: p. 309-21.
3. Dolinsky, S., Haneburger, I., Cichy, A., Hannemann, H., Itzen, I., Hilbi, H., *The Legionella longbeachae Icm/Dot substrate SidC selectively binds PtdIns(4)P with nanomolar affinity and promotes pathogen vacuole-ER interactions*. Infect Immun, 2014 (in revision).
4. Mampel, J., et al., *Biofilm formation of Legionella pneumophila in complex medium under static and dynamic flow conditions*. In N. P. Cianciotto et al. (eds.), *Legionella: State of the art 30 years after its recognition*. ASM Press, Washington, D.C. , 2006. **pp**: p. 398-402.
5. Fields, B.S., R.F. Benson, and R.E. Besser, *Legionella and Legionnaires' disease: 25 years of investigation*. Clin Microbiol Rev, 2002. **15**(3): p. 506-26.
6. Steele, T.W., J. Lanser, and N. Sangster, *Isolation of Legionella longbeachae serogroup I from potting mixes*. Appl Environ Microbiol, 1990. **56**(1): p. 49-53.
7. Newton, H.J., et al., *Molecular pathogenesis of infections caused by Legionella pneumophila*. Clin Microbiol Rev, 2010. **23**(2): p. 274-98.
8. Gomez-Valero, L., et al., *Comparative and functional genomics of legionella identified eukaryotic like proteins as key players in host-pathogen interactions*. Front Microbiol, 2011. **2**: p. 208.
9. McKinney, R.M., et al., *Legionella longbeachae species nova, another etiologic agent of human pneumonia*. Ann Intern Med, 1981. **94**(6): p. 739-43.
10. Bibb, W.F., et al., *Recognition of a second serogroup of Legionella longbeachae*. J Clin Microbiol, 1981. **14**(6): p. 674-7.
11. Tsai, T.F., et al., *Legionnaires' disease: clinical features of the epidemic in Philadelphia*. Ann Intern Med, 1979. **90**(4): p. 509-17.

10. References

12. Boshuizen, H.C., et al., *Subclinical Legionella infection in workers near the source of a large outbreak of Legionnaires disease*. J Infect Dis, 2001. **184**(4): p. 515-8.
13. Macfarlane, J.T., et al., *Comparative radiographic features of community acquired Legionnaires' disease, pneumococcal pneumonia, mycoplasma pneumonia, and psittacosis*. Thorax, 1984. **39**(1): p. 28-33.
14. Benin, A.L., et al., *An outbreak of travel-associated Legionnaires disease and Pontiac fever: the need for enhanced surveillance of travel-associated legionellosis in the United States*. J Infect Dis, 2002. **185**(2): p. 237-43.
15. Yu, V.L., et al., *Distribution of Legionella species and serogroups isolated by culture in patients with sporadic community-acquired legionellosis: an international collaborative survey*. J Infect Dis, 2002. **186**(1): p. 127-8.
16. Feeley, J.C., et al., *Primary isolation media for Legionnaires disease bacterium*. J Clin Microbiol, 1978. **8**(3): p. 320-5.
17. Feeley, J.C., et al., *Charcoal-yeast extract agar: primary isolation medium for Legionella pneumophila*. J Clin Microbiol, 1979. **10**(4): p. 437-41.
18. Edelstein, P.H. and M.A. Edelstein, *Evaluation of the Merifluor-Legionella immunofluorescent reagent for identifying and detecting 21 Legionella species*. J Clin Microbiol, 1989. **27**(11): p. 2455-8.
19. Gosting, L.H., et al., *Identification of a species-specific antigen in Legionella pneumophila by a monoclonal antibody*. J Clin Microbiol, 1984. **20**(6): p. 1031-5.
20. Flournoy, D.J., et al., *False positive Legionella pneumophila direct immunofluorescent monoclonal antibody test caused by Bacillus cereus spores*. Diagn Microbiol Infect Dis, 1988. **9**(2): p. 123-5.
21. Rogers, J., et al., *Influence of temperature and plumbing material selection on biofilm formation and growth of Legionella pneumophila in a model potable water system containing complex microbial flora*. Appl Environ Microbiol, 1994. **60**(5): p. 1585-92.
22. Rowbotham, T.J., *Preliminary report on the pathogenicity of Legionella pneumophila for freshwater and soil amoebae*. J Clin Pathol, 1980. **33**(12): p. 1179-83.

10. References

23. Hilbi, H., et al., *Update on Legionnaires' disease: pathogenesis, epidemiology, detection and control*. Mol Microbiol, 2010. **76**(1): p. 1-11.
24. Hoffmann, C., C.F. Harrison, and H. Hilbi, *The natural alternative: protozoa as cellular models for Legionella infection*. Cell Microbiol, 2014. **16**(1): p. 15-26.
25. Lau, H.Y. and N.J. Ashbolt, *The role of biofilms and protozoa in Legionella pathogenesis: implications for drinking water*. J Appl Microbiol, 2009. **107**(2): p. 368-78.
26. Cazalet, C., et al., *Analysis of the Legionella longbeachae genome and transcriptome uncovers unique strategies to cause Legionnaires' disease*. PLoS Genet, 2010. **6**(2): p. e1000851.
27. Horwitz, M.A., and S.C. Silverstein., *Legionnaires' disease bacterium (Legionella pneumophila) multiplies intracellularly in human monocytes*. J Clin Invest, 1980. **66**: p. 441-450.
28. Solomon, J.M., et al., *Intracellular growth of Legionella pneumophila in Dictyostelium discoideum, a system for genetic analysis of host-pathogen interactions*. Infect Immun, 2000. **68**(5): p. 2939-47.
29. Hagele, S., et al., *Dictyostelium discoideum: a new host model system for intracellular pathogens of the genus Legionella*. Cell Microbiol, 2000. **2**(2): p. 165-71.
30. Asare, R. and Y. Abu Kwaik, *Early trafficking and intracellular replication of Legionella longbeachaea within an ER-derived late endosome-like phagosome*. Cell Microbiol, 2007. **9**(6): p. 1571-87.
31. Fields, B.S., *The molecular ecology of legionellae*. Trends Microbiol, 1996. **4**(7): p. 286-90.
32. Cirillo, J.D., S. Falkow, and L.S. Tompkins, *Growth of Legionella pneumophila in Acanthamoeba castellanii enhances invasion*. Infect Immun, 1994. **62**(8): p. 3254-61.
33. Gobin, I., et al., *Experimental Legionella longbeachae infection in intratracheally inoculated mice*. J Med Microbiol, 2009. **58**(Pt 6): p. 723-30.

10. References

34. Molofsky, A.B., et al., *Cytosolic recognition of flagellin by mouse macrophages restricts Legionella pneumophila infection*. J Exp Med, 2006. **203**(4): p. 1093-104.
35. Ren, T., et al., *Flagellin-deficient Legionella mutants evade caspase-1- and Naip5-mediated macrophage immunity*. PLoS Pathog, 2006. **2**(3): p. e18.
36. Wright, E.K., et al., *Naip5 affects host susceptibility to the intracellular pathogen Legionella pneumophila*. Curr Biol, 2003. **13**(1): p. 27-36.
37. Lamkanfi, M., et al., *The Nod-like receptor family member Naip5/Birc1e restricts Legionella pneumophila growth independently of caspase-1 activation*. J Immunol, 2007. **178**(12): p. 8022-7.
38. Lightfield, K.L., et al., *Critical function for Naip5 in inflammasome activation by a conserved carboxy-terminal domain of flagellin*. Nat Immunol, 2008. **9**(10): p. 1171-8.
39. Byrne, B. and M.S. Swanson, *Expression of Legionella pneumophila virulence traits in response to growth conditions*. Infect Immun, 1998. **66**(7): p. 3029-34.
40. Watarai, M., et al., *Legionella pneumophila is internalized by a macropinocytotic uptake pathway controlled by the Dot/Icm system and the mouse lgn1 locus*. J Exp Med, 2001. **194**(8): p. 1081-1096.
41. Hilbi, H., G. Segal, and H.A. Shuman, *Icm/Dot-dependent upregulation of phagocytosis by Legionella pneumophila*. Mol Microbiol, 2001. **42**(3): p. 603-17.
42. Horwitz, M.A., *Phagocytosis of the Legionnaires' disease bacterium (Legionella pneumophila) occurs by a novel mechanism: engulfment with a pseudopod coil*. Cell, 1984. **36**: p. 27-33.
43. Bozue, J.A. and W. Johnson, *Interaction of Legionella pneumophila with Acanthamoeba castellanii: uptake by coiling phagocytosis and inhibition of phagosome-lysosome fusion*. Infect Immun, 1996. **64**(2): p. 668-673.
44. Peracino, B., A. Balest, and S. Bozzaro, *Phosphoinositides differentially regulate bacterial uptake and Nramp1-induced resistance to Legionella infection in Dictyostelium*. J Cell Sci, 2010. **123**(Pt 23): p. 4039-51.
45. Hilbi, H. and A. Haas, *Secretive bacterial pathogens and the secretory pathway*. Traffic, 2012. **13**(9): p. 1187-97.

10. References

46. Simonsen, A., et al., *EEA1 links PI(3)K function to Rab5 regulation of endosome fusion*. Nature, 1998. **394**(6692): p. 494-8.
47. Isberg, R.R., T.J. O'Connor, and M. Heidtman, *The Legionella pneumophila replication vacuole: making a cosy niche inside host cells*. Nat Rev Microbiol, 2009. **7**(1): p. 13-24.
48. Horwitz, M.A., *Formation of a novel phagosome by the Legionnaires' disease bacterium (Legionella pneumophila) in human monocytes*. J Exp Med, 1983. **158**(4): p. 1319-31.
49. Cirillo, J.D., et al., *Intracellular growth in Acanthamoeba castellanii affects monocyte entry mechanisms and enhances virulence of Legionella pneumophila*. Infect Immun, 1999. **67**(9): p. 4427-4434.
50. Hilbi, H., S. Weber, and I. Finsel, *Anchors for effectors: subversion of phosphoinositide lipids by legionella*. Front Microbiol, 2011. **2**: p. 91.
51. Shevchuk, O., et al., *Proteomic analysis of Legionella-containing phagosomes isolated from Dictyostelium*. Int J Med Microbiol, 2009. **299**(7): p. 489-508.
52. Li, Z., J.M. Solomon, and R.R. Isberg, *Dictyostelium discoideum strains lacking the RtoA protein are defective for maturation of the Legionella pneumophila replication vacuole*. Cell Microbiol, 2005. **7**(3): p. 431-42.
53. Lu, H. and M. Clarke, *Dynamic properties of Legionella-containing phagosomes in Dictyostelium amoebae*. Cell Microbiol, 2005. **7**(7): p. 995-1007.
54. Urwyler, S., et al., *Proteome analysis of Legionella vacuoles purified by magnetic immunoseparation reveals secretory and endosomal GTPases*. Traffic, 2009. **10**(1): p. 76-87.
55. Brüggemann, H., et al., *Virulence strategies for infecting phagocytes deduced from the in vivo transcriptional program of Legionella pneumophila*. Cell Microbiol, 2006. **8**(8): p. 1228-40.
56. Hubber, A. and C.R. Roy, *Modulation of host cell function by Legionella pneumophila type IV effectors*. Annu Rev Cell Dev Biol, 2010. **26**: p. 261-83.
57. Zhu, W., et al., *Comprehensive identification of protein substrates of the Dot/Icm type IV transporter of Legionella pneumophila*. PLoS One, 2011. **6**(3): p. e17638.

10. References

58. Lifshitz, Z., et al., *Computational modeling and experimental validation of the Legionella and Coxiella virulence-related type-IVB secretion signal*. Proc Natl Acad Sci U S A, 2013. **110**(8): p. E707-15.
59. Urwyler, S., E. Brombacher, and H. Hilbi, *Endosomal and secretory markers of the Legionella-containing vacuole*. Commun Integr Biol, 2009. **2**(2): p. 107-9.
60. Molmeret, M., et al., *Disruption of the phagosomal membrane and egress of Legionella pneumophila into the cytoplasm during the last stages of intracellular infection of macrophages and Acanthamoeba polyphaga*. Infect Immun, 2004. **72**(7): p. 4040-51.
61. Molmeret, M., et al., *Temporal and spatial trigger of post-exponential virulence-associated regulatory cascades by Legionella pneumophila after bacterial escape into the host cell cytosol*. Environ Microbiol, 2010. **12**(3): p. 704-15.
62. Molmeret, M., et al., *icmT is essential for pore formation-mediated egress of Legionella pneumophila from mammalian and protozoan cells*. Infect Immun, 2002. **70**(1): p. 69-78.
63. Alli, O.A., et al., *Temporal pore formation-mediated egress from macrophages and alveolar epithelial cells by Legionella pneumophila*. Infect Immun, 2000. **68**(11): p. 6431-40.
64. Molmeret, M., et al., *The C-terminus of IcmT is essential for pore formation and for intracellular trafficking of Legionella pneumophila within Acanthamoeba polyphaga*. Mol Microbiol, 2002. **43**(5): p. 1139-50.
65. Bouyer, S., et al., *Long-term survival of Legionella pneumophila associated with Acanthamoeba castellanii vesicles*. Environ Microbiol, 2007. **9**(5): p. 1341-4.
66. Asare, R., et al., *Genetic susceptibility and caspase activation in mouse and human macrophages are distinct for Legionella longbeachae and L. pneumophila*. Infect Immun, 2007. **75**(4): p. 1933-45.
67. Newton, H.J., et al., *Sell repeat protein LpnE is a Legionella pneumophila virulence determinant that influences vacuolar trafficking*. Infect Immun, 2007. **75**(12): p. 5575-85.

10. References

68. Fortier, A., et al., *Birc1e/Naip5 rapidly antagonizes modulation of phagosome maturation by Legionella pneumophila*. Cell Microbiol, 2007. **9**(4): p. 910-23.
69. Hilbi, H., *Modulation of phosphoinositide metabolism by pathogenic bacteria*. Cell Microbiol, 2006. **8**(11): p. 1697-706.
70. Rossier, O. and N.P. Cianciotto, *Type II protein secretion is a subset of the PilD-dependent processes that facilitate intracellular infection by Legionella pneumophila*. Infect Immun, 2001. **69**(4): p. 2092-8.
71. Cianciotto, N.P., *Many substrates and functions of type II secretion: lessons learned from Legionella pneumophila*. Future Microbiol, 2009. **4**(7): p. 797-805.
72. Vincent, C.D., et al., *Identification of the core transmembrane complex of the Legionella Dot/Icm type IV secretion system*. Mol Microbiol, 2006. **62**(5): p. 1278-91.
73. Qiu, J. and Z.Q. Luo, *Effector Translocation by the Legionella Dot/Icm Type IV Secretion System*. Curr Top Microbiol Immunol, 2013. **376**: p. 103-15.
74. Berger, K.H. and R.R. Isberg, *Two distinct defects in intracellular growth complemented by a single genetic locus in Legionella pneumophila*. Mol Microbiol, 1993. **7**(1): p. 7-19.
75. Brand, B.C., A.B. Sadosky, and H.A. Shuman, *The Legionella pneumophila icm locus: a set of genes required for intracellular multiplication in human macrophages*. Mol Microbiol, 1994. **14**(4): p. 797-808.
76. Segal, G. and H.A. Shuman, *Characterization of a new region required for macrophage killing by Legionella pneumophila*. Infect Immun, 1997. **65**(12): p. 5057-5066.
77. Swanson, M.S. and R.R. Isberg, *Identification of Legionella pneumophila mutants that have aberrant intracellular fates*. Infect Immun, 1996. **64**(7): p. 2585-2594.
78. Vogel, J.P., et al., *Conjugative transfer by the virulence system of Legionella pneumophila*. Science, 1998. **279**(5352): p. 873-6.
79. Komano, T., et al., *The transfer region of IncII plasmid R64: similarities between R64 tra and legionella icm/dot genes*. Mol Microbiol, 2000. **35**(6): p. 1348-59.

10. References

80. Weber, S.S., et al., *Legionella pneumophila exploits PI(4)P to anchor secreted effector proteins to the replicative vacuole*. PLoS Pathog, 2006. **2**(5): p. e46.
81. Brombacher, E., et al., *Rab1 guanine nucleotide exchange factor SidM is a major phosphatidylinositol 4-phosphate-binding effector protein of Legionella pneumophila*. J Biol Chem, 2009. **284**(8): p. 4846-56.
82. Chen, J., et al., *Legionella effectors that promote nonlytic release from protozoa*. Science, 2004. **303**(5662): p. 1358-61.
83. Conover, G.M., et al., *The Legionella pneumophila LidA protein: a translocated substrate of the Dot/Icm system associated with maintenance of bacterial integrity*. Mol Microbiol, 2003. **48**(2): p. 305-21.
84. Luo, Z.Q. and R.R. Isberg, *Multiple substrates of the Legionella pneumophila Dot/Icm system identified by interbacterial protein transfer*. Proc Natl Acad Sci U S A, 2004. **101**(3): p. 841-6.
85. Luo, Z.Q., *Striking a balance: modulation of host cell death pathways by legionella pneumophila*. Front Microbiol, 2011. **2**: p. 36.
86. O'Connor, T.J., et al., *Minimization of the Legionella pneumophila genome reveals chromosomal regions involved in host range expansion*. Proc Natl Acad Sci U S A, 2011. **108**(36): p. 14733-40.
87. Nagai, H., et al., *A bacterial guanine nucleotide exchange factor activates ARF on Legionella phagosomes*. Science, 2002. **295**(5555): p. 679-82.
88. Nagai, H., et al., *A C-terminal translocation signal required for Dot/Icm-dependent delivery of the Legionella RalF protein to host cells*. Proc Natl Acad Sci U S A, 2005. **102**(3): p. 826-31.
89. Xu, L., et al., *Inhibition of host vacuolar H⁺-ATPase activity by a Legionella pneumophila effector*. PLoS Pathog, 2010. **6**(3): p. e1000822.
90. Choy, A., et al., *The Legionella effector RavZ inhibits host autophagy through irreversible Atg8 deconjugation*. Science, 2012. **338**(6110): p. 1072-6.
91. Finsel, I., et al., *The Legionella Effector RidL Inhibits Retrograde Trafficking to Promote Intracellular Replication*. Cell Host Microbe, 2013. **14**(1): p. 38-50.

10. References

92. Haneburger, I. and H. Hilbi, *Phosphoinositide lipids and the legionella pathogen vacuole*. *Curr Top Microbiol Immunol*, 2013. **376**: p. 155-73.
93. Pizarro-Cerda, J. and P. Cossart, *Subversion of phosphoinositide metabolism by intracellular bacterial pathogens*. *Nat Cell Biol*, 2004. **6**(11): p. 1026-33.
94. Weber, S.S., C. Ragaz, and H. Hilbi, *Pathogen trafficking pathways and host phosphoinositide metabolism*. *Mol Microbiol*, 2009. **71**(6): p. 1341-52.
95. Di Paolo, G. and P. De Camilli, *Phosphoinositides in cell regulation and membrane dynamics*. *Nature*, 2006. **443**(7112): p. 651-7.
96. De Matteis, M.A. and A. Godi, *PI-losing membrane traffic*. *Nat Cell Biol*, 2004. **6**(6): p. 487-92.
97. Behnia, R. and S. Munro, *Organelle identity and the signposts for membrane traffic*. *Nature*, 2005. **438**(7068): p. 597-604.
98. Blumental-Perry, A., et al., *Phosphatidylinositol 4-phosphate formation at ER exit sites regulates ER export*. *Dev Cell*, 2006. **11**(5): p. 671-82.
99. Wang, D.S. and G. Shaw, *The association of the C-terminal region of beta I sigma II spectrin to brain membranes is mediated by a PH domain, does not require membrane proteins, and coincides with a inositol-1,4,5 triphosphate binding site*. *Biochem Biophys Res Commun*, 1995. **217**(2): p. 608-15.
100. Lemmon, M.A., *Membrane recognition by phospholipid-binding domains*. *Nat Rev Mol Cell Biol*, 2008. **9**(2): p. 99-111.
101. Weber, S.S., C. Ragaz, and H. Hilbi, *The inositol polyphosphate 5-phosphatase OCRL1 restricts intracellular growth of Legionella, localizes to the replicative vacuole and binds to the bacterial effector LpnE*. *Cell Microbiol*, 2009. **11**(3): p. 442-60.
102. Hsu, F., et al., *Structural basis for substrate recognition by a unique Legionella phosphoinositide phosphatase*. *Proc Natl Acad Sci U S A*, 2012. **109**(34): p. 13567-72.
103. Ragaz, C., et al., *The Legionella pneumophila phosphatidylinositol-4 phosphate-binding type IV substrate SidC recruits endoplasmic reticulum vesicles to a replication-permissive vacuole*. *Cell Microbiol*, 2008. **10**(12): p. 2416-33.

10. References

104. Schoebel, S., et al., *High-affinity binding of phosphatidylinositol 4-phosphate by Legionella pneumophila DrrA*. EMBO Rep, 2010. **11**(8): p. 598-604.
105. Huang, L., et al., *The E Block motif is associated with Legionella pneumophila translocated substrates*. Cell Microbiol, 2011. **13**(2): p. 227-45.
106. Weber, S., M. Wagner, and H. Hilbi, *Live-cell imaging of phosphoinositide dynamics and membrane architecture during Legionella infection*. MBio, 2013. **5**(1): p. e00839-13.
107. Bardill, J.P., J.L. Miller, and J.P. Vogel, *IcmS-dependent translocation of SdeA into macrophages by the Legionella pneumophila type IV secretion system*. Mol Microbiol, 2005. **56**(1): p. 90-103.
108. Ninio, S., et al., *The Legionella IcmS-IcmW protein complex is important for Dot/Icm-mediated protein translocation*. Mol Microbiol, 2005. **55**(3): p. 912-26.
109. Horenkamp, F.A., et al., *Legionella pneumophila Subversion of Host Vesicular Transport by SidC Effector Proteins*. Traffic, 2014.
110. Alix, E., et al., *The capping domain in RalF regulates effector functions*. PLoS Pathog, 2012. **8**(11): p. e1003012.
111. Ingmundson, A., et al., *Legionella pneumophila proteins that regulate Rab1 membrane cycling*. Nature, 2007. **450**(7168): p. 365-9.
112. Murata, T., et al., *The Legionella pneumophila effector protein DrrA is a Rab1 guanine nucleotide-exchange factor*. Nat Cell Biol, 2006. **8**(9): p. 971-7.
113. Machner, M.P. and R.R. Isberg, *Targeting of host Rab GTPase function by the intravacuolar pathogen Legionella pneumophila*. Dev Cell, 2006. **11**(1): p. 47-56.
114. Jaffe, A.B. and A. Hall, *Rho GTPases: biochemistry and biology*. Annu Rev Cell Dev Biol, 2005. **21**: p. 247-69.
115. Machner, M.P. and R.R. Isberg, *A bifunctional bacterial protein links GDI displacement to Rab1 activation*. Science, 2007. **318**(5852): p. 974-7.
116. Hardiman, C.A. and C.R. Roy, *AMPylation is critical for Rab1 localization to vacuoles containing Legionella pneumophila*. MBio, 2014. **5**(1): p. e01035-13.
117. Suh, H.Y., et al., *Structural insights into the dual nucleotide exchange and GDI displacement activity of SidM/DrrA*. EMBO J, 2010. **29**(2): p. 496-504.

10. References

118. Zhu, Y., et al., *Structural mechanism of host Rab1 activation by the bifunctional Legionella type IV effector SidM/DrrA*. Proc Natl Acad Sci U S A, 2010. **107**(10): p. 4699-704.
119. Muller, M.P., et al., *The Legionella effector protein DrrA AMPylates the membrane traffic regulator Rab1b*. Science, 2010. **329**(5994): p. 946-9.
120. Mukherjee, S., et al., *Modulation of Rab GTPase function by a protein phosphocholine transferase*. Nature, 2011. **477**(7362): p. 103-6.
121. Derre, I. and R.R. Isberg, *LidA, a translocated substrate of the Legionella pneumophila type IV secretion system, interferes with the early secretory pathway*. Infect Immun, 2005. **73**(7): p. 4370-80.
122. Neunuebel, M.R., et al., *Legionella pneumophila LidA affects nucleotide binding and activity of the host GTPase Rab1*. J Bacteriol, 2012. **194**(6): p. 1389-400.
123. Neunuebel, M.R. and M.P. Machner, *The taming of a Rab GTPase by Legionella pneumophila*. Small GTPases, 2012. **3**(1): p. 28-33.
124. Chen, Y., et al., *Structural basis for Rab1 de-AMPylation by the Legionella pneumophila effector SidD*. PLoS Pathog, 2013. **9**(5): p. e1003382.
125. Oesterlin, L.K., R.S. Goody, and A. Itzen, *Posttranslational modifications of Rab proteins cause effective displacement of GDP dissociation inhibitor*. Proc Natl Acad Sci U S A, 2012. **109**(15): p. 5621-6.
126. Tan, Y., R.J. Arnold, and Z.Q. Luo, *Legionella pneumophila regulates the small GTPase Rab1 activity by reversible phosphorylcholation*. Proc Natl Acad Sci U S A, 2011. **108**(52): p. 21212-7.
127. Sadosky, A.B., L.A. Wiater, and H.A. Shuman, *Identification of Legionella pneumophila genes required for growth within and killing of human macrophages*. Infect Immun, 1993. **61**(12): p. 5361-73.
128. Segal, G. and H.A. Shuman, *Intracellular multiplication and human macrophage killing by Legionella pneumophila are inhibited by conjugal components of IncQ plasmid RSF1010*. Mol Microbiol, 1998. **30**(1): p. 197-208.
129. Muller-Taubenberger, A., et al., *Calreticulin and calnexin in the endoplasmic reticulum are important for phagocytosis*. Embo J, 2001. **20**(23): p. 6772-82.

10. References

130. Dowler, S., et al., *Identification of pleckstrin-homology-domain-containing proteins with novel phosphoinositide-binding specificities*. *Biochem J*, 2000. **351**(Pt 1): p. 19-31.
131. Godi, A., et al., *FAPPs control Golgi-to-cell-surface membrane traffic by binding to ARF and PtdIns(4)P*. *Nat Cell Biol*, 2004. **6**(5): p. 393-404.
132. Mampel, J., et al., *Planktonic replication is essential for biofilm formation by Legionella pneumophila in a complex medium under static and dynamic flow conditions*. *Appl Environ Microbiol*, 2006. **72**(4): p. 2885-95.
133. Chen, D.Q., S.S. Huang, and Y.J. Lu, *Efficient transformation of Legionella pneumophila by high-voltage electroporation*. *Microbiol Res*, 2006. **161**(3): p. 246-51.
134. Otto, G.P., et al., *Macroautophagy is dispensable for intracellular replication of Legionella pneumophila in Dictyostelium discoideum*. *Mol Microbiol*, 2004. **51**(1): p. 63-72.
135. Watts, D.J. and J.M. Ashworth, *Growth of myxameobae of the cellular slime mould Dictyostelium discoideum in axenic culture*. *Biochem J*, 1970. **119**(2): p. 171-4.
136. Dowler, S., G. Kular, and D.R. Alessi, *Protein lipid overlay assay*. *Sci STKE*, 2002. **2002**(129): p. pl6.
137. Malchow, D., et al., *Membrane-bound cyclic AMP phosphodiesterase in chemotactically responding cells of Dictyostelium discoideum*. *Eur J Biochem*, 1972. **28**(1): p. 136-42.
138. Solomon, J.M. and R.R. Isberg, *Growth of Legionella pneumophila in Dictyostelium discoideum: a novel system for genetic analysis of host-pathogen interactions*. *Trends Microbiol*, 2000. **8**(10): p. 478-80.
139. Kessler, A., et al., *The Legionella pneumophila orphan sensor kinase LqsT regulates competence and pathogen-host interactions as a component of the LAI-1 circuit*. *Environ Microbiol*, 2013. **15**(2): p. 646-62.
140. Hoffmann, C., I. Finsel, and H. Hilbi, *Purification of pathogen vacuoles from Legionella-infected phagocytes*. *J Vis Exp*, 2012(64).

10. References

141. Finsel, I., C. Hoffmann, and H. Hilbi, *Immunomagnetic purification of fluorescent Legionella-containing vacuoles*. *Methods Mol Biol*, 2013. **983**: p. 431-43.
142. Weber, S., S. Dolinsky, and H. Hilbi, *Interactions of legionella effector proteins with host phosphoinositide lipids*. *Methods Mol Biol*, 2013. **954**: p. 367-80.
143. Urwyler, S., et al., *Isolation of Legionella-containing vacuoles by immuno-magnetic separation*. *Curr Protoc Cell Biol*, 2010. **Chapter 3**: p. Unit 3 34.
144. Itzen, A. and R.S. Goody, *Covalent coercion by Legionella pneumophila*. *Cell Host Microbe*, 2011. **10**(2): p. 89-91.
145. Schoebel, S., et al., *RabGDI displacement by DrrA from Legionella is a consequence of its guanine nucleotide exchange activity*. *Mol Cell*, 2009. **36**(6): p. 1060-72.
146. Rothmeier, E., et al., *Activation of Ran GTPase by a Legionella effector promotes microtubule polymerization, pathogen vacuole motility and infection*. *PLoS Pathog*, 2013. **9**(9): p. e1003598.
147. Simon, S., et al., *Icm/Dot-dependent inhibition of phagocyte migration by Legionella is antagonized by a translocated Ran GTPase activator*. *Cell Microbiol*, 2014.